

Non-adiabatic Mapping Dynamics in the Phase Space of the $SU(N)$ Lie Group

Accepted Manuscript: This article has been accepted for publication and undergone full peer review but has not been through the copyediting, typesetting, pagination, and proofreading process, which may lead to differences between this version and the Version of Record.

Cite as: J. Chem. Phys. (in press) (2022); <https://doi.org/10.1063/5.0094893>

Submitted: 06 April 2022 • Accepted: 29 July 2022 • Accepted Manuscript Online: 29 July 2022

 Duncan Lancelot Bossion, Wenxiang Ying,  Sutirtha Chowdhury, et al.



[View Online](#)



[Export Citation](#)



[CrossMark](#)

ARTICLES YOU MAY BE INTERESTED IN

Density-functional theory vs density-functional fits

The Journal of Chemical Physics **156**, 214101 (2022); <https://doi.org/10.1063/5.0091198>

Theory of vibrational polariton chemistry in the collective coupling regime

The Journal of Chemical Physics **156**, 014101 (2022); <https://doi.org/10.1063/5.0074106>

Incorporating Lindblad Decay Dynamics into Mixed Quantum-Classical Simulations

The Journal of Chemical Physics (2022); <https://doi.org/10.1063/5.0099922>

[Learn More](#)

The Journal
of Chemical Physics Special Topics Open for Submissions

Non-adiabatic Mapping Dynamics in the Phase Space of the $SU(N)$ Lie Group

Duncan Bossion,^{1, a)} Wenxiang Ying,¹ Sutirtha N. Chowdhury,^{1, 2} and Pengfei Huo^{1, 3, b)}

¹⁾Department of Chemistry, University of Rochester, 120 Trustee Road, Rochester, New York 14627, USA

²⁾Department of Chemistry, Duke University, 3236 French Science Center, 124 Science Drive, Durham, North Carolina 27708, USA

³⁾The Institute of Optics, Hajim School of Engineering, University of Rochester, Rochester, New York 14627, USA

(Dated: 28 July 2022)

We present the rigorous theoretical framework of the generalized spin mapping representation for non-adiabatic dynamics. Our work is based up a new mapping formalism recently introduced by Runeson and Richardson in [J. Chem. Phys. 152, 084110 (2020)], which uses the generators of the $\mathfrak{su}(N)$ Lie algebra to represent N discrete electronic states, thus preserving the size of the original Hilbert space. Following this interesting idea, the Stratonovich-Weyl transform is used to map an operator in the Hilbert space to a continuous function on the $SU(N)$ Lie group, *i.e.*, a smooth manifold which is a phase space of continuous variables. We further use the Wigner representation to describe the nuclear degrees of freedom, and derived an exact expression of the time-correlation function as well as the exact quantum Liouvillian for the non-adiabatic system. Making the linearization approximation, this exact Liouvillian is reduced to the Liouvillian of several recently proposed methods, and the performance of this Linearized method is tested using non-adiabatic models. We envision that the theoretical work presented here provides a rigorous and unified framework to formally derive non-adiabatic quantum dynamics approaches with continuous variables and connect the previous methods in a clear and concise manner.

I. INTRODUCTION

Studying non-adiabatic dynamics in quantum systems, particularly in condensed phase, is a central challenge for modern theoretical chemistry.¹ In this context, we are interested in the quantum dynamics of a system with N electronic states coupled to nuclear degrees of freedom (DOFs) as follows

$$\begin{aligned}\hat{H} &= [\hat{T}_R + U_0(\hat{R})] \hat{\mathcal{I}} + \hat{V}_e(\hat{R}) \\ &= [\hat{T}_R + U_0(\hat{R})] \hat{\mathcal{I}} + \sum_n V_{nn}(\hat{R}) |n\rangle\langle n| \\ &\quad + \sum_{n \neq m} V_{nm}(\hat{R}) |n\rangle\langle m|,\end{aligned}\quad (1)$$

where \hat{T}_R is the nuclear kinetic energy, $U_0(\hat{R})$ represents the state-independent part of the potential, and $\hat{V}_e(\hat{R})$ is the state-dependent part of the potential. Further, \hat{R} represents a nuclear DOF, $\{|n\rangle\}$ represents a set of diabatic electronic states, and $V_{nm}(\hat{R}) = \langle n|\hat{V}_e(\hat{R})|m\rangle$ is the matrix element of $\hat{V}_e(\hat{R})$ in this diabatic representation. The identity operator $\hat{\mathcal{I}} = \sum_{n=1}^N |n\rangle\langle n|$ represents the identity in the electronic Hilbert space. In order to avoid an exponential numerical scaling with the number of DOFs of the system, different approximate methods have been developed. Trajectory-based quantum-classical methods are among the most successful ones as

Major problems in this updated manuscript(version 3 accepted by JCP):

- 1) There were still too much re-derived formulations and re-derived ideas. Especially, the authors repeated the continuous parameter range proposed in our previous works [J. Phys. Chem. Lett. 12, 2496 (2021), J. Phys. Chem. A 125, 31, 6845-6863 (2021), Acc. Chem. Res. 54, 23, 4215-4228 (2021)] without proper citations, and made discussions as if they had already known it in Ref. 65.
- 2) The global phase introduced around eq (47) and eq (D1) was originated from eq (S54) of our work WIREs. Comput. Mol. Sci. e1619 (2022) (submitted on February 5, 2022, released on arXiv on May 8, 2022 and officially published on May 13, 2022). The global phase was absent in authors' formulations in their first version (online on May 20, 2022, see eq 113) but abruptly appeared in the version 2 and version 3 (online on July 29, 2022, see eq (D1)). The Authors knew the role of global phase in connection of Stratonovich phase space and Meyer-Miller variables just from our paper, and made use of our first ideas, but cited it nowhere! Moreover, the correct form of canonical Hamilton's equations of motion with Meyer-Miller variables still could not be derived with a "constant" global phase.

^{a)}Electronic mail: dbossion@ur.rochester.edu

^{b)}Electronic mail: pengfei.huo@rochester.edu

Comment: It changed from the previous title "Non-adiabatic Dynamics using the Generators of the su(N) Lie Algebra", which was totally influenced by our work WIREs. Comput. Mol. Sci. e1619 (2022), titled "New phase space formulations and quantum dynamics approaches".

Non-adiabatic Mapping Dynamics in the Phase Space of the $SU(N)$ Lie Group

Duncan Bossion,^{1, a)} Wenxiang Ying,¹ Sutirtha N. Chowdhury,^{1, 2} and Pengfei Huo^{1, 3, b)}

¹⁾ Department of Chemistry, University of Rochester, 120 Trustee Road, Rochester, New York 14627, USA

²⁾ Department of Chemistry, Duke University, 3236 French Science Center, 124 Science Drive, Durham, North Carolina 27708, USA

³⁾ The Institute of Optics, Hajim School of Engineering, University of Rochester, Rochester, New York 14627, USA

(Dated: 28 July 2022)

We present the rigorous theoretical framework of the generalized spin mapping representation for non-adiabatic dynamics. Our work is based up a new mapping formalism recently introduced by Runeson and Richardson in [J. Chem. Phys. 152, 084110 (2020)], which uses the generators of the $\mathfrak{su}(N)$ Lie algebra to represent N discrete electronic states, thus preserving the size of the original Hilbert space. Following this interesting idea, the Stratonovich-Weyl transform is used to map an operator in the Hilbert space to a continuous function on the $SU(N)$ Lie group, *i.e.*, a smooth manifold which is a phase space of continuous variables. We further use the Wigner representation to describe the nuclear degrees of freedom, and derived an exact expression of the time-correlation function as well as the exact quantum Liouvillian for the non-adiabatic system. Making the linearization approximation, this exact Liouvillian is reduced to the Liouvillian of several recently proposed methods, and the performance of this Linearized method is tested using non-adiabatic models. We envision that the theoretical work presented here provides a rigorous and unified framework to formally derive non-adiabatic quantum dynamics approaches with continuous variables and connect the previous methods in a clear and concise manner.

Comment: These statements were totally taken from our work WIREs. Comput. Mol. Sci. e1619 (2022) (submitted on February 5, 2022, released on arXiv on May 8, 2022 and officially published on May 13, 2022), where we explained what is a phase space and explicitly summarized corresponding relationships between some phase spaces and sub-manifolds of Lie groups in Appendix 3. They didn't catch this idea clearly in their previous version (online on May 20, 2022), and added a similar statement as our WCMS paper in this second version and this version (online on July 29, 2022) without mentioning our works.

although a pure state was used for demonstration.⁸⁹ The most essential element is the one-to-one correspondence

WIREs Comput Mol Sci. 2022;e1619.

wires.wiley.com/compmolsci

© 2022 Wiley Periodicals LLC. | 1 of 37

2 of 37 | WILEY - WIREs COMPUTATIONAL MOLECULAR SCIENCE

HE ET AL.

mapping between quantum operators and classical functions often defined on a smooth manifold, namely, phase space.

they scale linearly with the number of DOFs and allow for a simple numerical propagation scheme. One of the most popular trajectory-based approach is the surface-hopping method,^{2–6} where an ensemble of classical trajectories hop among electronic states upon non-adiabatic transitions, mimicking the wavepacket branching dynamics. The other widely used approach is the Ehrenfest trajectory dynamics where the nuclear DOFs feel a time-dependent mean field potential from the quantum subsystem's time evolution.

In a separate direction, the idea of mapping variables is proposed to represent quantum transitions among discrete electronic states as classical-like motion of continuous phase space variables,^{7,8} thus treating all the DOFs on an equal footing. Historically, one of the most successful mapping theories in physical chemistry is the Meyer-Miller-Stock-Thoss (MMST) mapping formalism,^{8–10} which maps a N -level system onto N singly excited harmonic oscillators, and thus can be viewed as a generalization of the Schwinger's bosonization approach.¹⁰ The mapping variables of the MMST formalism are conjugate position and momentum of each mapping oscillator. This method, despite its great success and broad applications,^{11–19} has known flaws.^{20–22} This is because the MMST mapping operators belong to a larger Hilbert space that contains other states outside the singly excited oscillator (SEO) subspace of the mapping oscillators, whereas the MMST mapping procedure tries to map the original electronic subspace onto the SEO subspace. It thus requires a projection back to the singly excited mapping subspace to obtain accurate results.^{20–22} As a consequence, the identity operator is not preserved through the MMST mapping and there is an ambiguity of how to evaluate it.²² Related

to the problem of the non-conserving identity, the non-adiabatic dynamics is sensitive to the separation between the state-dependent and the state-independent Hamiltonian.^{21,23} Moreover, projecting the Hilbert space to the SEO subspace also ruins the original simple commutation relations among the MMST mapping operators in their full Hilbert space,²⁴ making the mapping Hamiltonian potentially containing more terms that require additional approximations to parameterize.²⁵

Mathematically, the idea of mapping relation is referred to as the generalized Weyl correspondence, in which Lie groups and Lie algebras are the central components.^{26–28} Lie algebras are formed by commutation relations among generators with given structure constants; the elements of a connected matrix Lie group²⁹ can be expressed as the exponential of the Lie algebra generators, *i.e.*, the exponential map.³⁰ On the other hand, a Lie group is also a smooth manifold, which is a phase space with continuous variables. The dual identity of Lie groups naturally construct a bijective map between operators described by the generators represented in the Hilbert space and continuous functions on the differentiable manifold.

Following this fundamental idea of mapping, one of the most natural ways to map a N -level quantum system is to respect its original symmetry, which is described by the special unitary symmetry group³¹ $SU(N)$. For $N = 2$, it is well-known that the quantum dynamics of two electronic states can be mapped as the spin precession around a magnetic field (represented by the Hamiltonian) described by the motion of the Bloch vector on the Bloch sphere,^{7,32,33} due to the $SU(2)$ symmetry shared by both problems. The early work of Meyer, Miller, and McCurdy^{7,34} as well had accomplished this, resulting in a spin mapping Hamiltonian that respects the $SU(2)$ symmetry. Thoss and Stock have developed a semiclassical initial-value representation of the corresponding propagator using the $SU(2)$ mapping.¹⁰ Recently, Runeson and Richardson used this spin mapping approach to map a two-level system on a single spin- $\frac{1}{2}$ DOFs.³⁵ The same mapping formalism was also used to develop non-adiabatic path-integral approaches.³⁶

One can, in principle, generalize this idea by mapping a N -level system with the generators of the $\mathfrak{su}(N)$ Lie algebra. The unique advantage of this mapping procedure compared to the MMST formalism is that the commutation relations among operators as well as the size of the Hilbert space are exactly preserved in the $SU(N)$ representation. The corresponding quantum equations of motion (EOMs) for the $SU(N)$ mapping were first introduced by Hioe and Eberly,³⁷ which can be viewed as the generalization of the spin precession to N -dimensions with $SU(N)$ symmetry.³⁷ The $SU(N)$ mapping has also been used recently for density matrix mapping.^{38–40} Meyer, McCurdy, and Miller^{7,41,42} also used a similar idea to map two-state or three-state systems with spin- $\frac{1}{2}$ and spin-1 operators, although the matrices of the spin-1 operators (which are not necessarily

Comment: These statements, especially "manifold", were totally taken from our work WIREs. Comput. Mol. Sci. e1619 (2022) (submitted on February 5, 2022, released on arXiv on May 8, 2022 and officially published on May 13, 2022), where we explained what is a phase space and explicitly summarized corresponding relationships between some phase spaces and sub-manifolds of Lie groups in Appendix 3. They didn't catch this idea clearly in their previous version (online on May 20, 2022), and added a similar statement as our WCMS paper in the second version and this version (online on July 29, 2022) without mentioning our works

although a pure state was used for demonstration.³⁹ The most essential element is the one-to-one correspondence

WIREs Comput Mol Sci. 2022:e1619.
<https://doi.org/10.1002/wcms.1619>

wires.wiley.com/compmolsci

© 2022 Wiley Periodicals LLC. | 1 of 37

2 of 37 | WILEY | WIREs COMPUTATIONAL MOLECULAR SCIENCE

mapping between quantum operators and classical functions often defined on a smooth manifold, namely, phase space.

The notation " $SU(N)$ " was never used in Huo's previous Version 1 (online on May 20, 2022). The authors only used the notation " $\mathfrak{su}(N)$ " in the Version 1. However, we had used the notation " $SU(F)$ " in WIREs. Comput. Mol. Sci. e1619 (2022) (submitted on February 5, 2022, released on arXiv on May 8, 2022 and officially published on May 13, 2022):

Stratonovich's original work⁸ in 1956 maps a 2-state (spin-1/2) system onto a two-dimensional sphere. We review two kinds of further developments of the Stratonovich-Weyl mapping phase space representations for F -state quantum system: the first one based on the $SU(2)$ structure^{9,10} and the second one based on the $SU(F)$ structure¹¹. We show the relationship between constrained coordinate-momentum phase space representation that we use in the Focus Article and the two kinds of Stratonovich phase space representations.

The second kind of representation is the $SU(F)$ Stratonovich phase space. A kind as described by Tilma *et al.* in ref¹¹ is diffeomorphic to the quotient set $SU(F)/U(F-1)$, parameterized by $(2F-2)$ angle variables $(\theta, \varphi) = (\theta_1, \theta_2, \dots, \theta_{F-1}, \varphi_1, \varphi_2, \dots, \varphi_{F-1})$. The range of each angle θ_i is $[0, \pi/2]$ and that for each angle φ_i is $[0, 2\pi]$. The $SU(F)$ Stratonovich phase space of ref¹¹ has been used to prepare the initial condition for the Meyer-Miller mapping model of non-adiabatic dynamics in ref¹⁵.

The $SU(F)$ Stratonovich phase space, however, produces trajectory-based exact dynamics for the finite F -dimensional Hilbert space. This is because that the evolution generated by any Hamiltonian of the F -dimensional Hilbert space is the action of some group elements of $SU(F)$.²⁹ The inherent symplectic structure of $SU(F)/U(F-1)$ Stratonovich phase space³⁰ indicates that

The notation " $SU(N)$ " in this version (online on July 29, 2022) was obviously corrected (or plagiarized) from WIREs. Comput. Mol. Sci. e1619 (2022). We highlight all this notation in this Version 2.

It was totally an idea originated from our work WIREs. Comput. Mol. Sci. e1619 (2022) (submitted on February 5, 2022, released on arXiv on May 8, 2022 and officially published on May 13, 2022), where we explained what is a phase space and explicitly summarized corresponding relationships between some phase spaces and sub-manifolds of Lie groups in Appendix 3, i.e., Stratonovich phase space corresponds $SU(F)/U(F-1)$ while CMM corresponds $SU(F)/SU(F-1)$. They didn't catch this idea clearly in their previous version (online on May 20, 2022), and added a similar statement as our WCMS paper in this accepted version (online on July 29, 2022) without mentioning our works.

although a pure state was used for demonstration.³⁹ The most essential element is the one-to-one correspondence

WIREs Comput Mol Sci. 2022;e1619.
https://doi.org/10.1002/wcms.1619

wires.wiley.com/compmolsci

© 2022 Wiley Periodicals LLC. | 1 of 37

2 of 37 | WILEY - WIREs COMPUTATIONAL MOLECULAR SCIENCE

HE ET AL.

mapping between quantum operators and classical functions often defined on a smooth manifold, namely, phase space.

The correct relations between $SU(F)$ Stratonovich phase space and Meyer-Miller mapping model and their EOMs was firstly clarified in Appendix 3 of WIREs. Comput. Mol. Sci. e1619 (2022)(submitted on February 5, 2022, released on arXiv on May 8, 2022 and officially published on May 13, 2022), where the EOMs of angle variables with an evolving global phase were also presented. The evolving global phase ensures the EOMs identical to those of Meyer-Miller mapping variables.

However, the authors cited our work nowhere. Though different parameterization of the Stratonovich phase space could be applied, the relation between the structures of the two kinds of phase spaces should not rely on any specific choice of parameterization.

traceless) are different than the $\mathfrak{su}(N)$ generators (which are traceless).⁴³ Note that the $SU(N)$ mapping formalism is also different than the recent spin-mapping formalism introduced by Cotton and Miller,⁴⁴ which maps N states onto N spin- $\frac{1}{2}$ particles,⁴⁵ hence having the symmetry of $\otimes_N SU(2)$ that is different than $SU(N)$.

Runeson and Richardson used the spin operators (which are equivalent to the generators of the $\mathfrak{su}(N)$ Lie algebra up to a constant) and the $SU(N)$ Lie group to perform the non-adiabatic mapping dynamics of a N -state vibronic Hamiltonian, and developed the spin-Linearized semi-classical (spin-LSC) approach.⁴⁶ In particular, the Stratonovich-Weyl (S-W) transform^{27,28,47,48} is used to map an operator in the Hilbert space described by the generators (of the $\mathfrak{su}(N)$ Lie algebra) to a continuous function on the Lie group/manifold, resulting in a classical-like Hamiltonian. The S-W transform evaluates the expectation values of the spin operators under the generalized spin coherent states.^{49,50} The generalized spin coherent states^{51–53} are further expressed as a linear expansion of the diabatic electronic states, and the real and imaginary parts of the expansion coefficients are further defined as the conjugate position and momentum variables,⁴⁶ leading to an equivalence between the generalized spin-based mapping Hamiltonian and the MMST mapping Hamiltonian. Using the connection between these two Hamiltonians, Runeson and Richardson found the particular choice of zero-point energy parameter for the MMST Hamiltonian as well as an expression of the estimators. With a proposed sampling procedure of the initial conditions that constrains a total population equal to one, spin-LSC effectively propagates the EOMs with a total of $2N$ MMST variables ($2N - 2$ independent mapping variables when considering the population constraint). This is a reasonable choice for constructing an algorithm for approximate quantum dynamics, as it avoids deriving the EOMs in the generalized Euler angles of the spin coherent state, which is highly non-trivial. However, this choice also brings the potential confusions²⁵ that the MMST mapping Hamiltonian is a necessary and essential ingredient in the $SU(N)$ mapping formalism.⁴⁶

Further, the EOMs of the spin-LSC approach⁴⁶ were not rigorously derived, and there is a lack a rigorous derivation of the time-correlation function as well. In a related direction, the Generalized Discrete Truncated Wigner Approximation (GDTWA) approach⁵⁴ is developed using the generators of the $\mathfrak{su}(N)$ Lie algebra. The EOMs for GDTWA were argued as the classical limit of the Heisenberg EOMs⁵⁴ of the corresponding operators and generators, where the classical variables for those generators ($N^2 - 1$ of them) obey the equations of the N -dimensional spin precession theory by Hioe and Eberly.³⁷ However, the EOMs are not rigorously derived in GDTWA approach⁵⁴ and their connection with the MMST-type of EOMs used in spin-LSC⁴⁶ remains to be discovered.

In this work, we provide rigorous theoretical deriva-

tions of non-adiabatic mapping dynamics in the phase space of the $SU(N)$ Lie group. Thus, the current work can be viewed as a rigorous theoretical justification of the generalized spin mapping formalism that is originally developed by Runeson and Richardson.⁴⁶ This work, together with the previous work by Runeson and Richardson,⁴⁶ establish the $SU(N)$ mapping formalism as a rigorous and complete theory. We will not distinguish between the nomenclature of generalized spin mapping and the $SU(N)$ mapping in this paper when we mention this mapping formalism. In Sec. II, we briefly review the generators of the $\mathfrak{su}(N)$ Lie algebra which are used as the operator basis to represent the Hamiltonian and any operators in the electronic Hilbert space, and derive the analytic expression of the structure constants of the $\mathfrak{su}(N)$ Lie algebra (presented in Appendix A). In Sec. III we briefly review some basic properties of the S-W transform^{27,47,53} which effectively constructs a mapping relation between an operator described by the generators in the Hilbert space to a continuous function on the Lie group/manifold. Note that Sec. II and Sec. III are used to set up the theoretical background for our work presented in this paper, where similar expressions/discussions can be found in part in the previous works.^{46,54}

Sec. IV to Sec. VI present our *main theoretical contributions* in this work. In Sec. IV, we present a mixed Wigner/S-W representation that performs Wigner transform on the nuclear DOFs and S-W transform on the electronic DOFs, and derive the exact expressions of the time-correlation function (TCF). In Sec. V, we derive the exact quantum Liouvillian expression (Eq. 73-77) under the mixed Wigner/S-W representation. Using this exact expression, we can explore approximate forms of the Liouvillian under the linearization approximation, which gives the EOMs with the variables of the spin coherent state expectation values (Eq. 86). These EOMs are identical to those proposed in the GDTWA approach,⁵⁴ which can also be viewed as a generalization of the Hioe-Eberly theory³⁷ of the N -dimensional spin precession with the explicit presence of the nuclear DOFs.

The EOMs under the linearization approximation (Eq. 86) are shown to have three equivalent forms, documented in Sec. VI with (1) the conjugated action-angle type variables (Eq. 90), (2) the generalized Euler angles on multi-dimensional Bloch sphere (in Appendix E, Eq. E9), and (3) the MMST Cartesian phase space variables (Eq. 95). The TCF and the EOMs under the linearized approximation are used as a trajectory-based non-adiabatic method in the mixed Wigner/S-W formalism. We perform numerical simulations to demonstrate the accuracy of this linearized spin mapping method (in Eq. 86 and their equivalent forms mentioned above) by simulating non-adiabatic population dynamics of challenging model systems. We emphasize that despite that our work is inspired by the recent spin mapping formalism,^{35,46,54} we have made several unique theoretical contributions in the current work, which are detailed

It was totally an idea originated from our work WIREs Comput. Mol. Sci. e1619 (2022) (submitted on February 5, 2022, released on arXiv on May 8, 2022 and officially published on May 13, 2022), where we explained what is a phase space and explicitly summarized corresponding relationships between some phase spaces and sub-manifolds of Lie groups in Appendix 3, i.e., Stratonovich phase space corresponds $SU(F)/U(F-1)$ while CMM corresponds $SU(F)/SU(F-1)$. They didn't catch this idea clearly in their first version (online on May 20, 2022), and added a similar statement as our WCMS paper in this accepted version (online on July 29, 2022) without mentioning our works.

although a pure state was used for demonstration.⁸⁹ The most essential element is the one-to-one correspondence

WIREs Comput Mol Sci. 2022;e1619.
<https://doi.org/10.1002/wcms.1619>

wires.wiley.com/compmolsci

© 2022 Wiley Periodicals LLC. | 1 of 37

2 of 37 | WILEY | WIREs COMPUTATIONAL MOLECULAR SCIENCE

mapping between quantum operators and classical functions often defined on a smooth manifold, namely, phase space.

HE ET AL.

in the Supplemental Material Sec. X.

II. GENERATORS OF THE $\mathfrak{su}(N)$ LIE ALGEBRA

In this section, we review how to use the generators of the $\mathfrak{su}(N)$ Lie algebra^{37,46} to represent a Hamiltonian operator. The $\mathfrak{su}(N)$ Lie algebra and its corresponding Lie group are widely used in fundamental physics, particularly in the Standard Model of particle physics.^{31,55,56} For example, the $\mathfrak{su}(2)$ Lie algebra is used to describe the spin- $\frac{1}{2}$ system. The generators of $\mathfrak{su}(2)$ are the spin operators $\hat{\mathcal{S}}_j = \frac{\hbar}{2}\sigma_j$ with the two-dimensional represented Pauli matrices defined as follows

$$\sigma_1 = \begin{pmatrix} 0 & 1 \\ 1 & 0 \end{pmatrix}, \quad \sigma_2 = \begin{pmatrix} 0 & -i \\ i & 0 \end{pmatrix}, \quad \sigma_3 = \begin{pmatrix} 1 & 0 \\ 0 & -1 \end{pmatrix}.$$

The generators of the $\mathfrak{su}(3)$ Lie algebra are $\hat{\mathcal{S}}_j = \frac{\hbar}{2}\lambda_j$, where three-dimensional represented λ_j are the well-known Gell-Mann λ -matrices⁵⁷ defined as follows

$$\begin{aligned} \lambda_1 &= \begin{pmatrix} 0 & 1 & 0 \\ 1 & 0 & 0 \\ 0 & 0 & 0 \end{pmatrix}, \quad \lambda_2 = \begin{pmatrix} 0 & -i & 0 \\ i & 0 & 0 \\ 0 & 0 & 0 \end{pmatrix}, \quad \lambda_3 = \begin{pmatrix} 1 & 0 & 0 \\ 0 & -1 & 0 \\ 0 & 0 & 0 \end{pmatrix}, \\ \lambda_4 &= \begin{pmatrix} 0 & 0 & 1 \\ 0 & 0 & 0 \\ 1 & 0 & 0 \end{pmatrix}, \quad \lambda_5 = \begin{pmatrix} 0 & 0 & -i \\ 0 & 0 & 0 \\ -i & 0 & 0 \end{pmatrix}, \quad \lambda_6 = \begin{pmatrix} 0 & 0 & 0 \\ 0 & 0 & 1 \\ 0 & 1 & 0 \end{pmatrix}, \\ \lambda_7 &= \begin{pmatrix} 0 & 0 & 0 \\ 0 & 0 & -i \\ 0 & i & 0 \end{pmatrix}, \quad \lambda_8 = \frac{1}{\sqrt{3}} \begin{pmatrix} 1 & 0 & 0 \\ 0 & 1 & 0 \\ 0 & 0 & -2 \end{pmatrix}. \end{aligned}$$

They are widely used in quantum chromodynamics as an approximate symmetry of the strong interaction between quarks and gluons.⁵⁷ The generators of an algebra can be obtained in different ways, but the most commonly used ones in physics are based on a generalization of the Pauli matrices of $\mathfrak{su}(2)$ and of the Gell-Mann matrices⁵⁷ of $\mathfrak{su}(3)$, which are what we use in this work. This specific way of representing the generators is commonly referred to as the Generalized Gell-Mann matrix (GGM) basis.^{53,56} In the following, we briefly review the general expressions of these GGM generators. The commutation (and anti-commutation) relations among these generators are defined in the $\mathfrak{su}(N)$ Lie algebra, whereas the exponential functions of these generators construct the elements of the $SU(N)$ Lie group via the exponential map.^{29,31}

The elements of the GGM basis are denoted as $\hat{\mathcal{S}}_i$ with $i \in \{1, \dots, N^2 - 1\}$. There are $N(N - 1)/2$ symmetric matrices

$$\hat{\mathcal{S}}_{\alpha_{nm}} = \frac{\hbar}{2}(|m\rangle\langle n| + |n\rangle\langle m|), \quad (2)$$

$N(N - 1)/2$ anti-symmetric matrices,

$$\hat{\mathcal{S}}_{\beta_{nm}} = -i\frac{\hbar}{2}(|m\rangle\langle n| - |n\rangle\langle m|), \quad (3)$$

and $N - 1$ diagonal matrices,

$$\hat{\mathcal{S}}_{\gamma_n} = \frac{\hbar}{\sqrt{2n(n-1)}} \left(\sum_{l=1}^{n-1} |l\rangle\langle l| + (1-n)|n\rangle\langle n| \right), \quad (4)$$

where we introduced the indices α_{nm} related to the symmetric matrices, β_{nm} related to the anti-symmetric matrices, and γ_n related to the diagonal matrices as follows

$$\alpha_{nm} = n^2 + 2(m-n) - 1, \quad (5a)$$

$$\beta_{nm} = n^2 + 2(m-n), \quad (5b)$$

$$\gamma_n = n^2 - 1. \quad (5c)$$

Note that in the above definitions, $1 \leq m < n \leq N$ and $2 \leq n \leq N$, and the generators are ordered according to the conventions.^{40,56}

These generators are traceless,

$$\text{Tr}_e[\hat{\mathcal{S}}_i] = 0, \quad (6)$$

and are orthonormal to each other as

$$\text{Tr}_e[\hat{\mathcal{S}}_i \hat{\mathcal{S}}_j] = \frac{\hbar^2}{2} \delta_{ij}. \quad (7)$$

The commutation and anti-commutation relations among the generators of the $\mathfrak{su}(N)$ Lie algebra are presented as follows

$$[\hat{\mathcal{S}}_i, \hat{\mathcal{S}}_j] = i\hbar \sum_{k=1}^{N^2-1} f_{ijk} \hat{\mathcal{S}}_k, \quad (8a)$$

$$\{\hat{\mathcal{S}}_i, \hat{\mathcal{S}}_j\}_+ = \frac{\hbar^2}{N} \delta_{ij} \hat{\mathcal{I}} + \hbar \sum_{k=1}^{N^2-1} d_{ijk} \hat{\mathcal{S}}_k, \quad (8b)$$

where $\{\hat{\mathcal{S}}_i, \hat{\mathcal{S}}_j\}_+$ represents the anti-commutator between $\hat{\mathcal{S}}_i$ and $\hat{\mathcal{S}}_j$, the indices $i, j, k \in \{\alpha_{nm}, \beta_{nm}, \gamma_n\}$, and f_{ijk} and d_{ijk} are the totally anti-symmetric and totally symmetric *structure constants*, respectively. Using Eqs. 8a-8b, one can obtain the following well-known expressions for these structure constants

$$f_{ijk} = -i \frac{2}{\hbar^3} \text{Tr} [\hat{\mathcal{S}}_i, \hat{\mathcal{S}}_j] \hat{\mathcal{S}}_k, \quad (9a)$$

$$d_{ijk} = \frac{2}{\hbar^3} \text{Tr} [\{\hat{\mathcal{S}}_i, \hat{\mathcal{S}}_j\}_+ \hat{\mathcal{S}}_k]. \quad (9b)$$

Despite the extensive usage and the crucial role these structure constants play in modern physics, there is no analytic expression (closed formulas) of f_{ijk} and d_{ijk} . Here, we derive analytic formulas for these structure constants in the Supplementary Material Sec. I-II. The resulting analytic expressions are listed in Appendix A Eq. A1 for f_{ijk} and in Eq. A2 for d_{ijk} .

One can express the Hamiltonian in Eq. 1 through the generators as $\hat{H} = C_0 \hat{\mathcal{I}} + \sum_{k=1}^{N^2-1} C_k \hat{\mathcal{S}}_k$ due to the completeness of the generators. To figure out C_j , we perform $\text{Tr}_e[\hat{H} \cdot \hat{\mathcal{S}}_j] = C_0 \text{Tr}_e[\hat{\mathcal{S}}_j] + \sum_{k=1}^{N^2-1} C_k \text{Tr}_e[\hat{\mathcal{S}}_k \cdot \hat{\mathcal{S}}_j] = \hbar^2 C_j / 2$,

thus $C_j = (2/\hbar^2) \cdot \text{Tr}_e[\hat{H} \cdot \hat{\mathcal{S}}_j]$, where we have used the property of Eq. 6 and Eq. 7. Here, we explicitly indicate the trace over the electronic DOFs by using Tr_e . Further, we have $\text{Tr}_e[\hat{H}] = C_0 \text{Tr}_e[\hat{\mathcal{I}}] + \sum_{k=1}^{N^2-1} C_k \text{Tr}_e[\hat{\mathcal{S}}_k] = C_0 N$, thus $C_0 = (1/N) \cdot \text{Tr}_e[\hat{H}]$. Putting these together, one can represent the Hamiltonian in Eq. 1 using the generators as follows^{37,46}

$$\hat{H} = \mathcal{H}_0(\hat{R}) \cdot \hat{\mathcal{I}} + \frac{1}{\hbar} \sum_{k=1}^{N^2-1} \mathcal{H}_k(\hat{R}) \cdot \hat{\mathcal{S}}_k, \quad (10)$$

where the elements $\mathcal{H}_0(\hat{R})$ and $\mathcal{H}_k(\hat{R})$ are expressed as

$$\mathcal{H}_0(\hat{R}) = \frac{1}{N} \text{Tr}_e[\hat{H} \cdot \hat{\mathcal{I}}] = \hat{T}_R + U_0(\hat{R}) + \frac{1}{N} \sum_{n=1}^N V_{nn}(\hat{R}), \quad (11a)$$

$$\mathcal{H}_k(\hat{R}) = \frac{2}{\hbar} \text{Tr}_e[\hat{H} \cdot \hat{\mathcal{S}}_k] = \frac{2}{\hbar} \text{Tr}_e[\hat{V}_e(\hat{R}) \cdot \hat{\mathcal{S}}_k]. \quad (11b)$$

This expansion can also be easily verified using the relation between $|n\rangle\langle m|$ and the GMM matrices in Eq. 2-Eq. 4. Note that Eq. 11 has an explicit separation of the trace and traceless parts of the potential, due to the traceless generators in Eqs. 2-4 where $\text{Tr}_e[\hat{\mathcal{S}}_i] = 0$. Enforcing this separation in the MMST mapping formalism can significantly improve the stability and accuracy of the dynamics.^{21,23,36} In the $SU(N)$ mapping formalism, this is intrinsically enforced.

Using the generators defined in Eqs. 2-4, we can explicitly write $\mathcal{H}_k(\hat{R})$ in Eq. 11b as

$$\mathcal{H}_{\alpha_{nm}}(\hat{R}) = V_{mn}(\hat{R}) + V_{nm}(\hat{R}), \quad (12a)$$

$$\mathcal{H}_{\beta_{nm}}(\hat{R}) = i(V_{mn}(\hat{R}) - V_{nm}(\hat{R})), \quad (12b)$$

$$\mathcal{H}_{\gamma_n}(\hat{R}) = \sum_{l=1}^{n-1} \sqrt{\frac{2}{n(n-1)}} V_{ll}(\hat{R}) - \sqrt{\frac{2(n-1)}{n}} V_{nn}(\hat{R}), \quad (12c)$$

with $1 \leq m < n \leq N$ and $2 \leq n \leq N$ as previously introduced.

In the special case where the system does not have any nuclear (or other) DOF, we can write down the exact quantum Liouville equation for this closed system as

$$i\hbar \frac{\partial \hat{\rho}}{\partial t} = [\hat{H}, \hat{\rho}], \quad (13)$$

where the commutator is taken within the electronic subspace. The $\mathfrak{su}(N)$ representation of the density operator is

$$\hat{\rho} = \frac{1}{N} \hat{\mathcal{I}} + \frac{1}{\hbar} \sum_{k=1}^{N^2-1} \mathcal{S}_k \cdot \hat{\mathcal{S}}_k, \quad (14)$$

where $\mathcal{S}_k = \frac{2}{\hbar} \text{Tr}[\hat{\rho} \hat{\mathcal{S}}_k]$, as well as the corresponding expression for $\hat{H} = \mathcal{H}_0 \cdot \hat{\mathcal{I}} + \frac{1}{\hbar} \sum_{k=1}^{N^2-1} \mathcal{H}_k \cdot \hat{\mathcal{S}}_k$, the quantum

Liouville equation is equivalently expressed as³⁷

$$\frac{d}{dt}\mathcal{S}_i = \frac{1}{\hbar} \sum_{j,k=1}^{N^2-1} f_{ijk} \mathcal{H}_j \mathcal{S}_k, \quad (15)$$

which can be viewed as the generalization of the spin precession (see Eq. F7) to N dimensions, originally discovered by Hioe and Eberly.³⁷ This relation was interpreted as the time development (precession) of the N -level coherence vector.³⁷ In the following sections, we will generalize this formalism and develop the corresponding theory when the Hamiltonian explicitly contains nuclear DOFs.

III. STRATONOVICH-WEYL TRANSFORM AND THE SPIN MAPPING FORMALISM

The S-W transform constructs a mapping between an operator in the Hilbert space and a continuous function on the Lie group/manifold. Here, we present the properties of this transformation for a general N -level system. Part of it has been previously discussed in the previous work by Runeson and Richardson.^{35,46} To better help understanding the $SU(N)$ mapping formalism, we also provide the corresponding equations for the two-level system special case ($N = 2$) in Appendix F.

A. Spin Coherent States

For a spin (or equivalently, a two-level system), one can use the following spin coherent states⁴⁹

$$|\mathbf{u}\rangle = \cos \frac{\theta}{2} |1\rangle + \sin \frac{\theta}{2} \cdot e^{i\varphi} |2\rangle \quad (16)$$

as a basis to describe the quantum dynamics,^{35,36} where θ and φ are the angles defining the Bloch vector, with the radius of the Bloch sphere being fixed. The spin coherent states $|\mathbf{u}\rangle$ can be generalized for a N -level system, denoted as $|\boldsymbol{\Omega}\rangle$, through a rigorous procedure using Lie groups and Lie algebras. Mathematically, these generalized spin-coherent states $|\boldsymbol{\Omega}\rangle$ are introduced by acting a parameterized unitary transformation operator on a given diabatic basis $|n\rangle$, *i.e.*, $|\boldsymbol{\Omega}\rangle = \hat{U}(\boldsymbol{\theta}, \varphi)|n\rangle$, where the unitary transformation operator $\hat{U}(\boldsymbol{\theta}, \varphi)$ is an exponential function to linear order of the generators $\hat{\mathcal{S}}$ (Eq. 2-Eq. 4) associated with real parameters $\{\boldsymbol{\theta}, \varphi\}$. The detailed expression of $\hat{U}(\boldsymbol{\theta}, \varphi)$ can be found in Eq. (2.6) of Ref. 53. This particular expression is referred to as the generalized Euler angle parameterization of $\mathfrak{su}(N)$,⁵² which gives rise to a continuous phase space. Actually, one can regard $\hat{U}(\boldsymbol{\theta}, \varphi)$ as a unitary representation^{26,31} of the $SU(N)$ Lie group.⁵⁸

The generalized spin coherent states can be expressed

Eqs (16) and (18) were different from the coherent states (15) and (17) in their first version (online on May 20, 2022). In their first version, the coherent states (17) were incompatible with the deductions (B2) and (B3), leading to serious mistakes when they derived the equations of motion (101) and (105). In this version the authors fixed the problem, where the coherent states (18) were identical to those used by Runeson and Richardson [J. Chem. Phys. 152, 084110 (2020)].

The WRONG coherent states (17) in the first version:

$$\langle n|\Omega \rangle = \begin{cases} \cos \frac{\theta_1}{2} e^{-i\frac{\varphi_1}{2}} & n = 1, \\ \cos \frac{\theta_n}{2} e^{-i\frac{\varphi_n}{2}} \prod_{l=1}^{n-1} \sin \frac{\theta_l}{2} e^{i\frac{\varphi_l}{2}} & 1 < n < N, \\ \prod_{l=1}^{N-1} \sin \frac{\theta_l}{2} e^{i\frac{\varphi_l}{2}} & n = N. \end{cases} \quad (17)$$

This form of integral measure, though not normalized, had long been proposed by Nemoto [J. Phys. A Math. Gen. 33, 3493-3506 (2000)]:

$$d\mu_n = \cos \theta \sin^{2n-3}(\theta) \cos(\xi_1) \sin^{2n-5}(\xi_1) \cdots \cos(\xi_{n-2}) \sin(\xi_{n-2}) d\theta d\xi_1 \cdots d\xi_{n-2} d\varphi d\varphi_1 \cdots d\varphi_{n-1}. \quad (25)$$

though different symbols were used and each angle was divided by two in this manuscript. This original result early in 2000 had not been properly cited here.

as

$$|\Omega\rangle = \sum_{n=1}^N |n\rangle \langle n|\Omega\rangle, \quad (17)$$

where the expansion coefficients are^{46,50-52}

$$\langle n|\Omega \rangle = \begin{cases} \cos \frac{\theta_1}{2} & n = 1, \\ \cos \frac{\theta_n}{2} \prod_{l=1}^{n-1} \sin \frac{\theta_l}{2} e^{i\varphi_l} & 1 < n < N, \\ \prod_{l=1}^{N-1} \sin \frac{\theta_l}{2} e^{i\varphi_l} & n = N. \end{cases} \quad (18)$$

with $\{\theta_n\} \in [0, \pi]$ and $\{\varphi_n\} \in [0, 2\pi]$. The expansion coefficients can be expressed from the usual recursive expression⁴⁶ given in Eq. B1. Note that this is one convenient choice to write down spin coherent states,⁴⁶ such that it is a generalization of Eq. 16 beyond the two level system. These angles can be viewed as the general Euler angles in multi-dimensional Bloch spheres⁴⁶ (also see Fig. 1 for a schematic illustration). The notation of the expansion coefficients $\langle n|\Omega \rangle$ used in Ref. 53 has a reversed order of diabatic state label and a π difference in the definition of $\theta_n/2$.

The spin coherent states $|\Omega\rangle$ are normalized⁵⁰⁻⁵³ such that

$$\langle \Omega|\Omega \rangle = 1, \quad (19)$$

and they also form a resolution of identity

$$\hat{\mathcal{I}} = \int d\Omega |\Omega\rangle \langle \Omega|, \quad (20)$$

where a simple proof is provided in Supplementary Material Sec. III. The differential phase-space volume element $d\Omega$ (which is also referred to as the invariant integration measure on the group), *i.e.*, the Haar measure⁵⁹ is

$$d\Omega = \frac{N!}{(2\pi)^{N-1}} \prod_{n=1}^{N-1} K_n(\theta_n) d\theta_n d\varphi_n, \quad (21)$$

where

$$K_n(\theta_n) = \cos \frac{\theta_n}{2} \left(\sin \frac{\theta_n}{2} \right)^{2(N-n)-1}. \quad (22)$$

For the two-level special case, it reduces to $K(\theta) = \frac{1}{2} \sin \theta$. Our definition of $K_n(\theta_n)$ in Eq. 22 is different⁶⁰ than the one derived by Tilma and Nemoto.^{46,53} We find that this new expression of $d\Omega$ guarantees the identity relation of Eq. 20 and a correct distribution for each angle θ_n . The proof of the current differential phase-space volume element definition is given in Supplemental Materials Sec. III.

Fig. 1 presents a system with $N = 5$ electronic states on the four Bloch spheres, and the distribution of θ_i with the solid curves. As a comparison, the distribution used in Ref. 46 is shown with dashed curves. For a general N states system, we can see that the last Bloch sphere (here $n = 4$ in Fig. 1) always contains only the last two

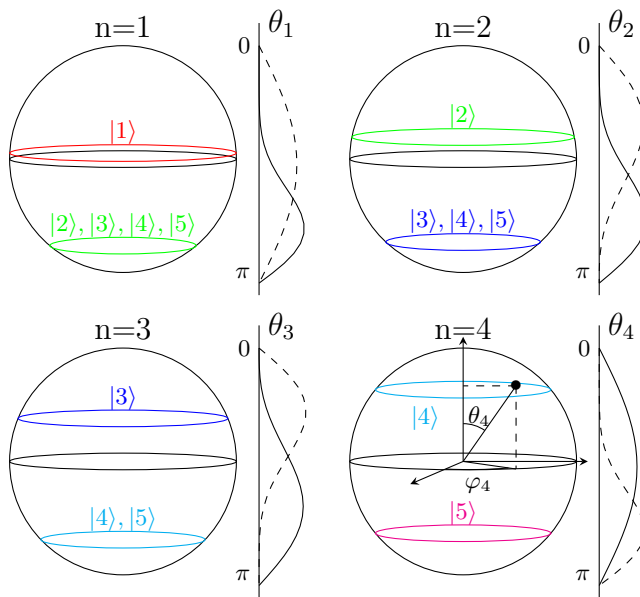


FIG. 1. Schematic representation of the Bloch spheres for a $N = 5$ system (the electronic states are placed for spheres of radius $r_w = \sqrt{N+1}$). On the $n = 4$ sphere are represented θ_4 and φ_4 . On the right of each sphere, the θ_n distribution is sketched from the differential phase space volume element in Eqs. 21-22 (solid lines), and the distribution from the volume element in the previous literature^{46,51-53} (dashed lines).

electronic states, hence requiring a distribution of the last angle, θ_{N-1} , to be symmetric around $\frac{\pi}{2}$. On the contrary, the first Bloch sphere ($n = 1$ in Fig. 1) always puts the first electronic state on the north hemisphere, and all the other electronic states on the south hemisphere, requiring a distribution centered on the south hemisphere. As the index of the Bloch sphere increases (here, for example, $n = 2$ and $n = 3$ in Fig. 1), less states are present on the south hemisphere, and the distribution slowly shifts toward the center. This demonstrates that the differential phase-space volume element in Eqs. 21-22 is the proper one to consider for the spin coherent state representation of $SU(N)$ defined in Eq. 18, whereas the one presented in Ref. 46 was based on a different expansion coefficients $\langle n|\Omega\rangle$ used in Ref. 53, and can not be consistently used with $|\Omega\rangle$ defined in Eq. 18.

To simplify our notation, we define the expectation value of the generalized spin operator as

$$\hbar\Omega_k \equiv \langle \Omega | \hat{S}_k | \Omega \rangle, \quad (23)$$

where $\hbar\Omega$ plays the role of the Bloch vector,^{39,40} and their detailed expressions can be found in Eqs. B2-B4. Further, one can express $|\Omega\rangle\langle\Omega| = C_0\hat{I} + \sum_{k=1}^{N^2-1} C_k\hat{S}_k$ due to the completeness of the generators, similar to the expansion in Eq. 10. To figure out C_j , we perform $\langle\Omega|\hat{S}_j|\Omega\rangle = \text{Tr}_e[\hat{S}_j|\Omega\rangle\langle\Omega|] = C_0\text{Tr}_e[\hat{S}_j] + \sum_{k=1}^{N^2-1} C_k\text{Tr}_e[\hat{S}_j\hat{S}_k] = \hbar^2 C_j/2$ (using Eq. 6 and Eq. 7), thus $C_j = 2\Omega_j/\hbar$. Further, we have $1 = \langle\Omega|\Omega\rangle = \text{Tr}_e[|\Omega\rangle\langle\Omega|] = C_0\text{Tr}_e[\hat{I}] +$

$\sum_{k=1}^{N^2-1} C_k \text{Tr}_e[\hat{\mathcal{S}}_k] = C_0 N$, thus $C_0 = 1/N$. Combining these together, we have

$$|\Omega\rangle\langle\Omega| = \frac{1}{N}\hat{\mathcal{I}} + \frac{2}{\hbar} \sum_{k=1}^{N^2-1} \Omega_k \cdot \hat{\mathcal{S}}_k. \quad (24)$$

This will be a useful results for finding alternative expressions of the kernel of the Stratonovich-Weyl transform in Sec. III B.

B. Basic Properties of the Stratonovich-Weyl Transform

The S-W transform of an operator \hat{A} is defined as

$$[\hat{A}]_s(\Omega) = \text{Tr}_e[\hat{A} \cdot \hat{w}_s], \quad (25)$$

where \hat{w}_s is the kernel of the S-W transform. The generalized S-W kernel \hat{w}_s in Eq. 25 is expressed as^{27,53,61}

$$\begin{aligned} \hat{w}_s(\Omega) &= \frac{1}{N}\hat{\mathcal{I}} + r_s \cdot \frac{2}{\hbar^2} \sum_{k=1}^{N^2-1} \langle\Omega|\hat{\mathcal{S}}_k|\Omega\rangle\hat{\mathcal{S}}_k \\ &\equiv \frac{1}{N}\hat{\mathcal{I}} + r_s \cdot \frac{2}{\hbar} \sum_{k=1}^{N^2-1} \Omega_k \cdot \hat{\mathcal{S}}_k, \end{aligned} \quad (26)$$

where r_s is a constant related to the radius of the Bloch sphere,⁶²⁻⁶⁴ and $|\Omega\rangle$ are the generalized spin-coherent states expressed in Eqs. 17-18. One can clearly see that the S-W kernel depends on both the generators $\hat{\mathcal{S}}$ of the Lie algebra (represented in the Hilbert space) and the parameters $\{\theta_n, \varphi_n\}$ of the manifold. Using the spin coherent states, we can also express the S-W kernel in Eq. 26 as⁶⁵

$$\hat{w}_s(\Omega) = \frac{1 - r_s}{N}\hat{\mathcal{I}} + r_s|\Omega\rangle\langle\Omega|, \quad (27)$$

which can be easily verified by using $|\Omega\rangle\langle\Omega|$ expressed with generators in Eq. 24. Using the MMST-type variables and the diabatic basis $\{|n\rangle\}$, the kernel in Eq. 27 can also be conveniently expressed into its equivalent form (Eq. D7). We want to point out that Eq. 27 can drastically simplify a lot of derivations and can be potentially extremely useful for future theoretical derivations.

Note that when $r_s = 1$ (so called $s = Q$ transform), the kernel is simply the projection operator $\hat{w}_s = |\Omega\rangle\langle\Omega|$ discussed by Brif and Mann.²⁷ The kernel also defines an identity as

$$\int d\Omega \hat{w}_s = \int d\Omega \left(\frac{1 - r_s}{N}\hat{\mathcal{I}} + r_s|\Omega\rangle\langle\Omega| \right) = \hat{\mathcal{I}}, \quad (28)$$

where we have used the fact that $\int d\Omega = N$ and Eq. 20.

The S-W transform in Eq. 25 constructs a mapping between an operator in the Hilbert space to a continuous function whose variables are $\{\theta, \varphi\}$ or $\{\Omega\}$ on the Lie

This expression had been presented in Appendix 3 of WIREs. Comput. Mol. Sci. e1619 (2022)(submitted on February 5, 2022, released on arXiv on May 8, 2022 and officially published on May 13, 2022).

$$\hat{K}_{\text{ele}}^{\text{SU}(F)}(\theta, \varphi; s) = (1+F)^{(1+s)/2} |\theta, \varphi\rangle\langle\theta, \varphi| + \frac{i}{F} \left(1 - (1+F)^{(1+s)/2} \right), \quad s \in \mathbb{R} \quad \text{S41}$$

Also, in Ref. 64(which is a note), Huo and coworkers stated that this was a correction to "for s not equal to Q, there is no simple relation between w_s and out product of Omega" in their previous work Ref. 35. However, when we checked Ref. 35, only the three special cases W, P, Q were mentioned, revealing that they had NO understanding that the parameter space could be continuous! Their original statement was:

We further introduce three functions for the Stratonovich-Weyl (SW) transformation of any operator in the SM representation, named the Q-, P-, and W-functions. These functions depend on the kernel \hat{w}_s and the spin radius r_s as follows.⁵³

$$\hat{w}_s(\mathbf{u}) = \frac{1}{2}\hat{\mathcal{I}} + r_s \mathbf{u} \cdot \hat{\boldsymbol{\sigma}}, \quad s \in \{Q, P, W\}, \quad (8a)$$

$$r_Q = \frac{1}{2}, \quad r_P = \frac{3}{2}, \quad r_W = \frac{\sqrt{3}}{2}, \quad (8b)$$

where $\mathbf{u} \cdot \hat{\boldsymbol{\sigma}} = u_x \cdot \hat{\sigma}_x + u_y \cdot \hat{\sigma}_y + u_z \cdot \hat{\sigma}_z$.

The SCS projection operator is $|\mathbf{u}\rangle\langle\mathbf{u}| = \cos^2 \frac{\theta}{2} |1\rangle\langle 1| + \cos \frac{\theta}{2} \sin \frac{\theta}{2} e^{-i\varphi} |1\rangle\langle 2| + \cos \frac{\theta}{2} \sin \frac{\theta}{2} e^{i\varphi} |2\rangle\langle 1| + \sin^2 \frac{\theta}{2} |2\rangle\langle 2|$. Note that

$$\hat{w}_Q = |\mathbf{u}\rangle\langle\mathbf{u}|, \quad (9)$$

which can be easily verified using elementary trigonometric identities. On the other hand, \hat{w}_P and \hat{w}_W do not have a simple relation with $|\mathbf{u}\rangle\langle\mathbf{u}|$.

The full continuous parameter range was first proposed in our work [J. Phys. Chem. Lett. 12, 2496 (2021)] (submitted on January 22, 2021, Accepted on February 19, 2021 and published online on March 5, 2021).

group/manifold. More specifically, this mapping relation is expressed as

$$\hat{A} \longrightarrow [\hat{A}]_s(\Omega), \quad (29)$$

which is the basic idea of the generalized spin-mapping approach proposed by Runeson and Richardson in Ref. 35 and Ref. 46.

Using the definition of S-W transform, as well as the properties of the generators given in Eqs. 6-7, it is straightforward to show that

$$[\hat{\mathcal{S}}_k]_s(\Omega) = \text{Tr}_e[\hat{\mathcal{S}}_k \cdot \hat{w}_s] = \hbar r_s \Omega_k, \quad (30a)$$

$$[\hat{\mathcal{I}}]_s(\Omega) = \text{Tr}_e[\hat{\mathcal{I}} \cdot \hat{w}_s] = 1. \quad (30b)$$

The property in Eq. 30b means that the S-W transform preserves the identity in the electronic Hilbert subspace, contrarily to the Wigner transform^{66,67} of the identity operator in the MMST formalism.^{22,68} Hence, the spin mapping formalism does not introduce any ambiguity of the identity expression.⁴⁶

To conveniently evaluate any operator $\hat{A}(\hat{R})$ under the S-W transform, one can start by decomposing it on the GGM basis (Eqs 2-4) as follows

$$\hat{A}(\hat{R}) = \mathcal{A}_0(\hat{R}) \cdot \hat{\mathcal{I}} + \frac{1}{\hbar} \sum_{k=1}^{N^2-1} \mathcal{A}_k(\hat{R}) \cdot \hat{\mathcal{S}}_k, \quad (31)$$

where $\mathcal{A}_0(\hat{R}) = \frac{1}{N} \text{Tr}_e[\hat{A}(\hat{R})\hat{\mathcal{I}}] = \frac{1}{N} \sum_{n=1}^N A_{nn}(\hat{R})$ with $A_{nm}(\hat{R}) = \langle n | \hat{A}(\hat{R}) | m \rangle$ and $\mathcal{A}_k(\hat{R}) = \frac{2}{\hbar} \text{Tr}_e[\hat{A}(\hat{R})\hat{\mathcal{S}}_k]$. Here, we explicitly consider a system (with the Hamiltonian in Eq. 1) that contains both electronic and nuclear DOFs. Similar to the expressions in Eq. 12, we can write down each component of \mathcal{A}_i as follows

$$\mathcal{A}_{\alpha_{nm}}(\hat{R}) = A_{mn}(\hat{R}) + A_{nm}(\hat{R}), \quad (32a)$$

$$\mathcal{A}_{\beta_{nm}}(\hat{R}) = i(A_{mn}(\hat{R}) - A_{nm}(\hat{R})), \quad (32b)$$

$$\mathcal{A}_{\gamma_n}(\hat{R}) = \sum_{l=1}^{n-1} \sqrt{\frac{2}{n(n-1)}} A_{ll}(\hat{R}) - \sqrt{\frac{2(n-1)}{n}} A_{nn}(\hat{R}), \quad (32c)$$

with $1 \leq m < n \leq N$ and $2 \leq n \leq N$ as previously introduced (under Eq. 4). To keep our notation concise, we will write \hat{A} instead of $\hat{A}(\hat{R})$ for the following equations, because the S-W transform is performed only on the *electronic* DOFs and does not involve the nuclear DOFs.

Using the expression of \hat{w}_s (Eq. 26), $\hat{A}(\hat{R})$ expressed in Eq. 31 is transformed (through Eq. 25) as

$$[\hat{A}(\hat{R})]_s(\Omega) = \mathcal{A}_0(\hat{R}) + r_s \sum_{k=1}^{N^2-1} \mathcal{A}_k(\hat{R}) \cdot \Omega_k. \quad (33)$$

One of the important properties of the S-W transform is that it can be used to compute a quantum mechanical trace in the continuous phase space as follows

$$\begin{aligned} \int d\Omega [\hat{A}]_s(\Omega) &= \int d\Omega \text{Tr}_e[\hat{A} \cdot \hat{w}_s] = \text{Tr}_e \left[\int d\Omega \hat{w}_s \cdot \hat{A} \right] \\ &= \text{Tr}_e[\hat{A}], \end{aligned} \quad (34)$$

Just repeating our contribution without any citation: In J. Phys. Chem. A 125, 31, 6845-6863 (2021) (submitted on May 19, 2021, released on arXiv on July 7, 2021 (July 31 for the 2nd version) and officially published on August 2, 2021)

$$\sum_{n=1}^F \left[\frac{(x^{(n)})^2 + (p^{(n)})^2}{2} - \gamma \right] = 1 \quad (6)$$

the mapping Hamiltonian eq 4 is equal to the conventional Meyer–Miller Hamiltonian eq 3. This was first proposed in ref 41 for general F -state systems. The simplest way is to use the full constraint electronic space that eq 6 defines, i.e.,

$$S(\mathbf{x}, \mathbf{p}): \delta \left(\sum_{n=1}^F \left[\frac{(x^{(n)})^2 + (p^{(n)})^2}{2} \right] - (1 + F\gamma) \right) \quad (7)$$

for constructing the formulation for physical properties in the mapping approach. The possible value of parameter γ for eq 6 or eq 7 implies $\gamma \in (-\frac{1}{F}, \infty)$.

In J. Phys. Chem. Lett. 12, 2496 (2021)(submitted on January 22, 2021 and published online on March 5, 2021)

$$S(\mathbf{x}, \mathbf{p}): \sum_{n=1}^F \left[\frac{1}{2} ((x^{(n)})^2 + (p^{(n)})^2) \right] = 1 + F\gamma \quad (4)$$

Although we use the diabatic representation to reach eq 4, the constraint holds in the adiabatic representation as well. The constraint (eq 4) has already been implied in eqs 43 and 44 of ref 17, and used in ref 15 where $\gamma = 0$ is considered. The physical meaning of eq 4 requires only $\gamma > -1/F$. This confirms that negative values for the ZPE parameter, γ , are possible!

In Acc. Chem. Res. 54, 23, 4215-4228 (2021)(submitted on August 14, 2021 and published online on November 10, 2021)

$$S(\mathbf{x}, \mathbf{p}): \delta \left(\sum_{n=1}^F \frac{(x^{(n)})^2 + (p^{(n)})^2}{2} - (1 + F\gamma) \right) \quad (34)$$

for developing the formulation for evaluation of physical observables. In eq 34, the possible value of parameter γ lies in $(-\frac{1}{F}, \infty)$. The trace of a product of two operators is expressed

The full continuous parameter range was first proposed in J. Phys. Chem. Lett. 12, 2496 (2021)(submitted on January 22, 2021 and published online on March 5, 2021). Huo and coworkers did not cite these contributions above in this place at all!

where we have used the identity given in Eq. 28.

For two operators $\hat{A}(\hat{R})$ and $\hat{B}(\hat{R})$, one cannot compute the trace of a product of operators $\text{Tr}_e[\hat{A}\hat{B}]$ as $\int d\Omega [\hat{A}]_s [\hat{B}]_s(\Omega)$ for a given value of r_s , because generally $[\hat{A}\hat{B}]_s(\Omega) \neq [\hat{A}]_s(\Omega) \cdot [\hat{B}]_s(\Omega)$ (see Eq. 42). To get the separate S-W transform of \hat{A} and \hat{B} , it is required to use two matching values of the radius, r_s and $r_{\bar{s}}$, with complementing indices s and \bar{s} which will be defined in Eq. 39. It can be shown that the S-W transform has the following property

$$\begin{aligned} \text{Tr}_e[\hat{A}\hat{B}] &= \int d\Omega [\hat{A}\hat{B}]_s(\Omega) \\ &= \int d\Omega [\hat{A}]_s(\Omega) \cdot [\hat{B}]_{\bar{s}}(\Omega) = \int d\Omega [\hat{A}]_{\bar{s}}(\Omega) \cdot [\hat{B}]_s(\Omega), \end{aligned} \quad (35)$$

where $[\dots]_{\bar{s}}(\Omega)$ is S-W transformed through Eq. 33 using $r_{\bar{s}}$. The proof is given in Supplementary Material Sec. IV.

The sum of the squares of the generators (the so-called Casimir operator of $\mathfrak{su}(N)$) can be expressed with the identity operator as follows⁴⁶

$$\sum_{k=1}^{N^2-1} \hat{\mathcal{S}}_k^2 = \hbar^2 \frac{N^2-1}{2N} \hat{\mathcal{I}}, \quad (36)$$

where the proof can be found in Appendix A of Ref. 46. Performing the S-W transform on both sides of the above identity leads to the squared spin magnitude as follows

$$\sum_{k=1}^{N^2-1} [\hat{\mathcal{S}}_k]_s [\hat{\mathcal{S}}_k]_{\bar{s}} = \hbar^2 r_s r_{\bar{s}} \sum_{k=1}^{N^2-1} \Omega_k^2 = \hbar^2 \frac{N^2-1}{2N}, \quad (37)$$

which is a conserved quantity. Using the fact⁴⁶ that $\sum_{k=1}^{N^2-1} \Omega_k^2 = \frac{N-1}{2N}$ (see the proof in Appendix E of Ref. 46) together with the identity in Eq. 37, one has⁴⁶

$$r_s \cdot r_{\bar{s}} = N + 1. \quad (38)$$

The commonly used values^{28,46} for r_s and $r_{\bar{s}}$ are

$$r_s = r_{\bar{s}} = \sqrt{N+1}, \quad (\text{for } s = \bar{s} = W), \quad (39a)$$

$$r_s = 1, \quad r_{\bar{s}} = N+1, \quad (\text{for } s = Q, \quad \bar{s} = P), \quad (39b)$$

$$r_s = N+1, \quad r_{\bar{s}} = 1, \quad (\text{for } s = P, \quad \bar{s} = Q). \quad (39c)$$

Note that these parameters are not restricted to the above special cases, and in principle they can take any value in the range of $r_s \in (0, \infty)$. More detailed discussions can be found in Appendix D (see Eq. D6 and the discussion below).

Using the complementing $r_{\bar{s}}$, one can define the inverse S-W transform⁴⁸ as follows

$$\hat{A} = \int d\Omega \hat{w}_s(\Omega) [\hat{A}]_{\bar{s}}(\Omega), \quad (40)$$

where $[\hat{A}]_{\bar{s}}(\Omega)$ is defined in Eq. 33 with the radius $r_{\bar{s}}$. A simple proof of Eq. 40 is given in the Supplementary Material Sec. IV.

It indicates that parameter r_s lies in a continuous range, $(0, \infty)$

parameter range

discrete values:

SM:
Stratonovich
Phase space

| | | | |
|-------|---|--------------|-------|
| r_s | 1 | $\sqrt{1+F}$ | $1+F$ |
| | Q | W | P |

CMM:
phase space
with MM
variables

| | | | |
|----------|---|--------------------|---|
| γ | 0 | $(\sqrt{F+1}-1)/F$ | 1 |
|----------|---|--------------------|---|

continuous range:

$\gamma \in (-1/F, \infty)$

Only realized $s \in \{Q, W, P\}$

Plagiarized the idea of the continuous parameter range as their first finding:
 $r_s \in (0, \infty)$ and $\gamma \in (-1/F, \infty)$

$(-\frac{1}{F}, \infty)$ to make eq 23 hold. We note that the so-called spin mapping model of refs 43 and 44 intrinsically based on the Meyer–Miller mapping Hamiltonian model (especially when $F \geq 3$ electronic states are involved) is only a special case of the exact phase space mapping formulation that we established first in refs 13 and 41 and then in ref 42, i.e., parameter $\gamma = 0$, $(\sqrt{F+1} - 1)/F$, or 1 in our exact phase space mapping formulation corresponds to the Q-version, W-version, or P-version of refs 43 and 44, respectively.

Richardson and his coworkers

J. Chem. Phys. 152, 084110 (2020).

Liu and his coworkers

J. Phys. Chem. A 125, 6845 (2021)
Acc. Chem. Res. 54, 4215 (2021)

J. Phys. Chem. Lett. 12, 2496 (2021)

Huo and his coworkers

J. Chem. Phys. 154, 184106 (2021)

ChemRxiv Version 1 (May 20, 2022)

ChemRxiv Version 2 (May 27, 2022)

J. Chem. Phys. 2022, accepted.

doi:10.1063/5.0094893

We had pointed out that spin mapping method with P, Q, W versions are only three special cases of CMM in J. Phys. Chem. A 125, 6845 -6863, (2021) (submitted on May 19, 2021, released on arXiv on July 7, 2021 and officially published on August 2, 2021):

$(-\frac{1}{F}, \infty)$ to make eq 23 hold. We note that the so-called spin mapping model of refs 43 and 44 intrinsically based on the Meyer–Miller mapping Hamiltonian model (especially when $F \geq 3$ electronic states are involved) is only a special case of the exact phase space mapping formulation that we established first in refs 13 and 41 and then in ref 42, i.e., parameter $\gamma = 0$, $(\sqrt{F+1} - 1)/F$, or 1 in our exact phase space mapping formulation corresponds to the Q-version, W-version, or P-version of refs 43 and 44, respectively. Interestingly, the

Also in Acc. Chem. Res. 54, 23, 4215-4228 (2021)
(submitted on August 14, 2021 and published online on November 10, 2021):

As pointed out in ref 42, it is trivial to show that the Q-version, W-version, or P-version of ref 36 corresponds to parameter $\gamma = 0$, $(\sqrt{F+1} - 1)/F$, or 1 of the exact phase space mapping formulation that we *first* proposed in refs 1 and 3 and then in ref 4, respectively. It will be interesting to use our general phase space mapping formulation to include or reformulate other approaches that use the Meyer–Miller mapping model.^{21,25,28–30,34,37,41,45,48}

The commonly used values^{28,40} for r_s and $r_{\bar{s}}$ are

$$r_s = r_{\bar{s}} = \sqrt{N+1}, \quad (\text{for } s = \bar{s} = W), \quad (39a)$$

$$r_s = 1, \quad r_{\bar{s}} = N+1, \quad (\text{for } s = Q, \quad \bar{s} = P), \quad (39b)$$

$$r_s = N+1, \quad r_{\bar{s}} = 1, \quad (\text{for } s = P, \quad \bar{s} = Q). \quad (39c)$$

Note that these parameters are not restricted to the above special cases, and in principle they can take any value in the range of $r_s \in (0, \infty)$. More detailed discussions can be found in Appendix D (see Eq. D6 and the discussion below).

Using the complementing $r_{\bar{s}}$, one can define the inverse S-W transform⁴⁸ as follows

$$\hat{A} = \int d\Omega \hat{w}_s(\Omega) [\hat{A}]_{\bar{s}}(\Omega), \quad (40)$$

where $[\hat{A}]_{\bar{s}}(\Omega)$ is defined in Eq. 33 with the radius $r_{\bar{s}}$. A simple proof of Eq. 40 is given in the Supplementary Material Sec. IV.

It is also useful to derive the expression of the S-W transform of the product of two electronic operators $[\hat{A}\hat{B}]_s$ in order to evaluate commutation and anti-commutation relations. To proceed, we use the detailed expressions of \hat{A} and \hat{B} in their $\mathfrak{su}(N)$ representation, and express $[\hat{A}\hat{B}]_s$ as follows

$$\begin{aligned} [\hat{A}\hat{B}]_s(\Omega) &= \left[\left(\mathcal{A}_0(\hat{R}) \cdot \hat{\mathcal{I}} + \frac{1}{\hbar} \sum_{k=1}^{N^2-1} \mathcal{A}_k(\hat{R}) \cdot \hat{\mathcal{S}}_k \right) \right]_s (41) \\ &\quad \times \left(\mathcal{B}_0(\hat{R}) \cdot \hat{\mathcal{I}} + \frac{1}{\hbar} \sum_{k=1}^{N^2-1} \mathcal{B}_k(\hat{R}) \cdot \hat{\mathcal{S}}_k \right)_s \\ &= \left[\mathcal{A}_0\mathcal{B}_0 \cdot \hat{\mathcal{I}} + \frac{\mathcal{A}_0}{\hbar} \sum_{k=1}^{N^2-1} \mathcal{B}_k \cdot \hat{\mathcal{S}}_k + \frac{\mathcal{B}_0}{\hbar} \sum_{k=1}^{N^2-1} \mathcal{A}_k \cdot \hat{\mathcal{S}}_k \right. \\ &\quad \left. + \frac{1}{\hbar^2} \sum_{j,k=1}^{N^2-1} \mathcal{A}_j \mathcal{B}_k \cdot \hat{\mathcal{S}}_j \hat{\mathcal{S}}_k \right]_s. \end{aligned}$$

Using the fact that

$$\hat{\mathcal{S}}_j \hat{\mathcal{S}}_k = \frac{1}{2} ([\hat{\mathcal{S}}_j, \hat{\mathcal{S}}_k] + \{\hat{\mathcal{S}}_j, \hat{\mathcal{S}}_k\}_+),$$

together with Eqs. 8 and 30, we can evaluate $[\hat{A}\hat{B}]_s(\Omega)$ as follows

$$\begin{aligned} [\hat{A}\hat{B}]_s(\Omega) &= \mathcal{A}_0\mathcal{B}_0 + \frac{1}{2N} \sum_{i=1}^{N^2-1} \mathcal{A}_i\mathcal{B}_i \quad (42) \\ &\quad + r_s \sum_{i=1}^{N^2-1} (\Omega_i \mathcal{A}_i \mathcal{B}_0 + \Omega_i \mathcal{A}_0 \mathcal{B}_i) \\ &\quad + \frac{r_s}{2} \sum_{i,j,k=1}^{N^2-1} \Omega_i \mathcal{A}_j \mathcal{B}_k (d_{ijk} + i f_{ijk}), \end{aligned}$$

where $\mathcal{A}_i(\hat{R})$ and $\mathcal{B}_i(\hat{R})$ are expressed in Eq. 32. A generalization of this expression for both S-W transform (on the electronic DOF) and the Wigner transform (on the nuclear DOF) is provided in Eq. S66 in the Supplementary Material Sec. IV.

C. Mapping Formalism using the Stratonovich-Weyl Transform

Performing the S-W transform of the Hamiltonian \hat{H} (Eq. 10) through Eq. 25, we have

$$[\hat{H}(\hat{R})]_s(\Omega) = \mathcal{H}_0(\hat{R}) + r_s \sum_{k=1}^{N^2-1} \mathcal{H}_k(\hat{R}) \cdot \Omega_k, \quad (43)$$

where \mathcal{H}_0 is expressed in Eq. 11a and \mathcal{H}_k is expressed in Eq. 12. This is the mapping Hamiltonian expression in terms of the expectation values of the generalized spin operators.^{46,54}

In addition, we can also perform the S-W transform for electronic projection operators and obtain

$$\begin{aligned} [|n\rangle\langle n|]_s &= \text{Tr}_e [|n\rangle\langle n| \hat{w}_s] \quad (44) \\ &= \frac{1}{N} + r_s \sum_{m=n+1}^N \sqrt{\frac{2}{m(m-1)}} \Omega_{\gamma_m} - r_s \sqrt{\frac{2(n-1)}{n}} \Omega_{\gamma_n}, \end{aligned}$$

with $1 \leq n \leq N$. The complementary expression $[|n\rangle\langle n|]_{\bar{s}}$ can be obtained by replacing r_s in Eq. 44 by $r_{\bar{s}}$. Note that the first sum in Eq. 44 is null when the condition $m > n$ is not satisfied, *i.e.* when $n = N$, and the last term is null when $n = 1$. The population estimators only depend on the expectation values of the diagonal spin operators $\{\Omega_{\gamma_m}\}$ (see Eq. B4), hence they are independent of the mapping variables $\{\varphi_m\}$ for $m \in \{1, \dots, N-1\}$. As expected, summing all the state population estimators gives a total population equal to 1, because the S-W transformation explicitly preserves the identity in the electronic subspace (see Eq. 30b).

For an off-diagonal electronic operator with $m < n$, the S-W transform is

$$[|n\rangle\langle m|]_s = r_s (\Omega_{\alpha_{nm}} - i\Omega_{\beta_{nm}}), \quad (45a)$$

$$[|m\rangle\langle n|]_s = r_s (\Omega_{\alpha_{nm}} + i\Omega_{\beta_{nm}}), \quad (45b)$$

where the detailed expressions of $\Omega_{\alpha_{nm}}$ and $\Omega_{\beta_{nm}}$ are provided in Eq. B2 and Eq. B3, respectively. Using Eq. 44 and Eq. 45, one can also perform the S-W transform on \hat{H} (Eq. 1) and derive

$$\begin{aligned} [\hat{H}]_s &= [\hat{T}_R + U_0(\hat{R})] \quad (46) \\ &+ \sum_n V_{nn}(\hat{R}) [|n\rangle\langle n|]_s + \sum_{n \neq m} V_{nm}(\hat{R}) [|n\rangle\langle m|]_s, \end{aligned}$$

which is identical to Eq. 43 (when using \mathcal{H}_k expressed in Eq. 12).

Upon a variable transform,⁴⁶ the Hamiltonian $[\hat{H}(\hat{R})]_s(\boldsymbol{\Omega})$ (in Eq. 43) can be reformulated into a Meyer-Miller-Stock-Thoss (MMST) form. In particular, one can introduce the following transformation^{46,69}

$$c_n = \langle n | \boldsymbol{\Omega} \rangle \cdot e^{i\Phi} = \frac{1}{\sqrt{2r_s}} (q_n + ip_n), \quad (47)$$

where $q_n/\sqrt{2r_s}$ is the real part of c_n and $p_n/\sqrt{2r_s}$ is the imaginary part of c_n , and $e^{i\Phi}$ is a *constant global phase* variable to *all* of the coefficients $\langle n | \boldsymbol{\Omega} \rangle$. For a purely real Hamiltonian, using the transform defined in Eq. 47, the spin mapping Hamiltonian $[\hat{H}(\hat{R})]_s$ in Eq. 43 can be expressed as the well-known MMST mapping Hamiltonian^{7,8,10}

$$\begin{aligned} \mathcal{H} &= \mathcal{H}_0(\hat{R}) + \sum_n \frac{1}{2} [V_{nn}(\hat{R}) - \bar{V}(\hat{R})] (q_n^2 + p_n^2 - \gamma) \quad (48) \\ &+ \sum_{n < m} V_{nm}(\hat{R}) (q_n q_m + p_n p_m), \end{aligned}$$

Similar to comment on eq (D1).

where $\bar{V}(\hat{R}) = \frac{1}{N} \sum_l V_{ll}(\hat{R})$, $\mathcal{H}_0(\hat{R}) = \frac{\hat{P}^2}{2m} + U_0(\hat{R}) + \bar{V}(\hat{R})$ is the trace part of the potential, which is naturally separated from the trace-less part. Previous work by Runeson and Richardson⁴⁶ have already shown this connection using the transform expressed in Eq. 47. The detailed discussion of connections and differences between the $SU(N)$ mapping formalism and the MMST mapping formalism is provided in Appendix D. Further, the expression of the S-W kernel \hat{w}_s (Eq. 27) and estimator $[\langle n \rangle \langle m \rangle]_s$ using MMST variables are presented in Eq. D7 and Eq. D8, respectively. The details are provided in Appendix D.

IV. TIME-CORRELATION FUNCTION IN THE MIXED WIGNER/STRATONOVICH-WEYL REPRESENTATION

In this section, we derive the exact expression of the time correlation function (TCF) and the expression of estimators for different types of quantum operators. The exact and approximate forms of the Liouvillian will be discussed in Sec. V.

A. Time-Correlation Functions (TCF)

The regular quantum TCF is expressed as

$$C_{AB}(t) = \frac{1}{Z} \text{Tr}_e \text{Tr}_n [e^{-\beta \hat{H}} \hat{A}(0) \hat{B}(t)], \quad (49)$$

with the Hamiltonian defined in Eq. 1, and $\beta = 1/k_B T$. The density matrix under the canonical equilibrium condition is $\hat{\rho}_{eq} = e^{-\beta \hat{H}} / Z$ and the partition function is defined as $Z = \text{Tr}_e \text{Tr}_n [e^{-\beta \hat{H}}]$. In order to compute the nuclear trace Tr_n , we insert the identity $\hat{1}_{R'} = \int dR' |R'\rangle \langle R'|$. To compute the electronic trace we use the property of the S-W transform in Eq. 34. This leads to

$$C_{AB}(t) = \frac{1}{Z} \int dR' \int d\Omega [\langle R' | e^{-\beta \hat{H}} \hat{A}(0) \hat{B}(t) | R' \rangle]_s(\Omega). \quad (50)$$

To proceed, we use the property given in Eq. 35 and identify $e^{-\beta \hat{H}} \hat{A}(0)$ and $\hat{B}(t)$ as two operators to compute the trace of $\int d\Omega$. By adding another nuclear identity $\hat{1}_{R''} = \int dR'' |R''\rangle \langle R''|$ between two operators, we can re-express Eq. 50 as

$$C_{AB}(t) = \frac{1}{Z} \int dR' \int dR'' \int d\Omega \times [\langle R' | e^{-\beta \hat{H}} \hat{A}(0) | R'' \rangle]_{\bar{s}}(\Omega) [\langle R'' | \hat{B}(t) | R' \rangle]_s(\Omega). \quad (51)$$

Introducing the nuclear mean path and path difference variables^{70–72}

$$R = \frac{1}{2}(R' + R''), \quad \Delta = R' - R'', \quad (52)$$

and inserting the following identity of the nuclear DOFs^{73,74}

$$\hat{\mathbb{1}}_R = \int d\Delta' \delta(\Delta + \Delta') = \frac{1}{2\pi\hbar} \int d\Delta' \int dP e^{\frac{i}{\hbar} P(\Delta + \Delta')} \quad (53)$$

into the TCF, Eq. 51 becomes

$$\begin{aligned} C_{AB}(t) &= \frac{1}{2\pi\hbar Z} \int dR \int d\Delta \int d\Delta' \int dP e^{\frac{i}{\hbar} P(\Delta + \Delta')} \int d\Omega \\ &\times [\langle R + \frac{\Delta}{2} | e^{-\beta \hat{H}} \hat{A}(0) | R - \frac{\Delta}{2} \rangle]_{\text{S}}(\Omega) \\ &\times [\langle R - \frac{\Delta'}{2} | \hat{B}(t) | R + \frac{\Delta'}{2} \rangle]_{\text{s}}(\Omega). \end{aligned} \quad (54)$$

The above equation has an explicit Wigner transform^{66,75,76} over the nuclear DOFs, which is defined for an operator $\hat{O}(\hat{R})$ as follows

$$[\hat{O}(\hat{R})]_{\text{w}} = \int d\Delta e^{\frac{i}{\hbar} P\Delta} \langle R - \frac{\Delta}{2} | \hat{O}(\hat{R}) | R + \frac{\Delta}{2} \rangle. \quad (55)$$

Note that the lower case w used here represents the Wigner transform, whereas the capital case W represents a special choice of the S-W transform through $r_W = \sqrt{N+1}$.

With the above definition, we can rewrite Eq. 54 as

$$\begin{aligned} C_{AB}(t) &= \frac{1}{2\pi\hbar Z} \int dR \int dP \int d\Omega [e^{-\beta \hat{H}} \hat{A}(0)]_{\text{ws}} [\hat{B}(t)]_{\text{ws}}, \\ &= \frac{1}{2\pi\hbar Z} \int dR \int dP \int d\Omega [e^{-\beta \hat{H}} \hat{A}(0)]_{\text{ws}} e^{\hat{\mathcal{L}}t} [\hat{B}(0)]_{\text{ws}}, \end{aligned} \quad (56)$$

where $[\hat{A}(\hat{R})]_{\text{ws}}$ is a Wigner transform of the nuclear DOFs (defined in Eq. 55) and a S-W transform of the electronic DOFs in the $SU(N)$ representation (defined in Eq. 25 or Eq. 34). The time evolved expectation value $[\hat{B}(t)]_{\text{ws}}$ is written using the quantum Liouvillian $\hat{\mathcal{L}}$ to update $[\hat{B}(0)]_{\text{ws}}$. The exact expression of $\hat{\mathcal{L}}$ is derived in Sec. V. From now on, we will simply denote $\hat{A}(0)$ as \hat{A} and $\hat{B}(0)$ as \hat{B} . To compute the transform of the operator $[e^{-\beta \hat{H}} \hat{A}(0)]_{\text{ws}}$, we need to perform the Wigner transform of the nuclear DOFs and S-W transform of the electronic DOFs for a product of two operators. The details are provided in the Supplementary Materials Sec. IV.

B. Population Dynamics expressed as the TCF

For a given photo-induced process, we are often interested in the reduced density matrix dynamics upon an initial excitation of the molecular system. In this case, the system is initially prepared in its ground state, with the ground state Hamiltonian

$$\hat{H}_g = (\hat{T}_R + U_g(\hat{R})), \quad (57)$$

and $U_g(\hat{R})$ is the ground state potential. Upon the initial photo-excitation of the system, the system is excited to

state $|n\rangle$. The reduced density matrix element can be expressed as

$$\rho_{ij}(t) = \text{Tr}_e \text{Tr}_n [\hat{\rho}(0) e^{\frac{i}{\hbar} \hat{H} t} |i\rangle \langle j| e^{-\frac{i}{\hbar} \hat{H} t}], \quad (58)$$

where the initial density operator $\hat{\rho}(0)$ is expressed as a tensor product of the electronic and nuclear DOFs as $\hat{\rho}(0) = |n\rangle \langle n| \otimes \frac{1}{Z} e^{-\beta \hat{H}_g}$, where $Z = \text{Tr}[e^{-\beta \hat{H}_g}]$, and \hat{H}_g is the ground state Hamiltonian in Eq. 57.

The reduced density matrix $\rho_{ij}(t)$ can also be equivalently expressed as a correlation function

$$\rho_{ij}(t) = C_{AB}(t) = \frac{1}{Z} \text{Tr}_e \text{Tr}_n [e^{-\beta \hat{H}_g} \hat{A} e^{\frac{i}{\hbar} \hat{H} t} \hat{B} e^{-\frac{i}{\hbar} \hat{H} t}], \quad (59)$$

where $\hat{A} = |n\rangle \langle n|$ is the initially occupied electronic state, and $\hat{B} = |i\rangle \langle j|$. Using the mixed Wigner/S-W representation for the TCF, we have

$$C_{AB}(t) = \frac{1}{2\pi\hbar Z} \int dR \int dP \int d\Omega \times [|n\rangle \langle n|]_s [e^{-\beta \hat{H}_g}]_w e^{\hat{\mathcal{L}}t} [|i\rangle \langle j|]_s. \quad (60)$$

One can numerically perform the integrals over $d\Omega$ by sampling the initial conditions according to the differential phase space volume element expression in Eq. 21, and explicitly using the expression of $[|n\rangle \langle n|]_s$ (Eq. 44 with r_s , or Eq. D10 in terms of the MMST mapping variables).

C. The Focused Initial Condition for Mapping Variables

Another numerically advantageous but *approximate* method is to focus the initial electronic state.^{35,46,77} The focused method requires to know what values to attribute to the mapping variables in order to enforce an initial projection onto state $|n\rangle$. As proposed in the previous work of spin-LSC, this requires to replace $[|n\rangle \langle n|]_s$ in Eq. 60 by $[|n\rangle \langle n|]_s$ in order to achieve a properly normalized initial population.^{35,46} To this end, we first introduce the following variables

$$\Theta_n \equiv nr_s \sum_{k=n+1}^N \sqrt{\frac{2}{k(k-1)}} \Omega_{\gamma_k} = r_s \left(\frac{N-n}{N} - \prod_{k=1}^n \sin^2 \frac{\theta_k}{2} \right), \quad (61)$$

where $n \in \{1, \dots, N-1\}$. The derivation of the second equality in Eq. 61 is provided in the Supplementary Material Sec. V B. We further introduce the proper boundaries $\Theta_N = \Theta_0 = 0$. Later, in Sec. VI A, we will show that this Θ_n is actually the canonical conjugate variable of φ_n (Eq. 90), which plays a role similar to the role the traditional MMST action variable (see Eq. 100a) plays in the MMST mapping formalism.^{9,23}

We then write the estimator in Eq. 44 with these new

variables $\{\Theta_n\}$ as follows

$$\begin{aligned} [|n\rangle\langle n|]_s &= \frac{1}{N} + \frac{1}{n}\Theta_n - (n-1)\left(\frac{1}{n-1}\Theta_{n-1} - \frac{1}{n}\Theta_n\right) \\ &= \frac{1}{N} + \Theta_n - \Theta_{n-1} \\ &= \frac{1}{N} + r_s\left(-\frac{1}{N} + \cos^2 \frac{\theta_n}{2} \prod_{k=1}^{n-1} \sin^2 \frac{\theta_k}{2}\right), \quad (62) \end{aligned}$$

in the last line, $\cos^2 \frac{\theta_n}{2}$ and $\prod_{k=1}^{n-1} \sin^2 \frac{\theta_k}{2}$ are replaced by 1 when $n = N$ and $n = 1$, respectively.

For $m < n$, the non-diagonal elements in Eq. 45 can be expressed in terms of θ_n and φ_n using the explicit expressions of $\Omega_{\alpha_{nm}}$ (Eq. B2) and $\Omega_{\beta_{nm}}$ (Eq. B3), resulting in

$$\begin{aligned} [|n\rangle\langle m|]_s &= r_s \prod_{j=1}^{m-1} \sin^2 \frac{\theta_j}{2} \cos \frac{\theta_m}{2} \prod_{k=m}^{n-1} \sin \frac{\theta_k}{2} \\ &\times \cos \frac{(1 - \delta_{nN})\theta_n}{2} \prod_{k=m}^{n-1} e^{-i\varphi_k}. \quad (63) \end{aligned}$$

The term $\prod_{j=1}^{m-1} \sin^2 \frac{\theta_j}{2}$ is replaced by 1 when $m = 1$. Using the definition of Θ_n (Eq. 61) one can further express it into Eq. 64. Alternatively, we can use the kernel expressed in Eq. 27 to evaluate

$$[|n\rangle\langle m|]_s = \text{Tr}_e [|n\rangle\langle m|\hat{w}_s(\boldsymbol{\Omega})] = r_s \langle \boldsymbol{\Omega}|n\rangle\langle m|\boldsymbol{\Omega}\rangle,$$

then using the definition of $\langle n|\boldsymbol{\Omega}\rangle$ (Eq. 18) to get

$$\begin{aligned} [|n\rangle\langle m|]_s &= \sqrt{\left(\Theta_n - \Theta_{n-1} + \frac{r_s}{N}\right)\left(\Theta_m - \Theta_{m-1} + \frac{r_s}{N}\right)} \cdot \prod_{k=m}^{n-1} e^{-i\varphi_k}, \quad (64) \end{aligned}$$

where $[|m\rangle\langle n|]_s$ is the complex conjugate of Eq. 64. Note that $\{\theta_n\} \in [0, \pi]$, thus all the $\sin(\theta_k/2)$ and $\cos(\theta_k/2)$ in Eq. 63 are the square root of Eq. 64 gives non-negative result.

To obtain the focused initial conditions for an initially populated state $|n\rangle$, one requires that⁴⁶

$$[|n\rangle\langle n|]_s = 1; \quad [|j\rangle\langle j|]_s = 0, \quad (j \neq n). \quad (65)$$

As Eq. 62 is recursive, we derive the expression starting from state 1 toward state N , and obtain the values of the $\{\Theta_j\}$ as

$$\Theta_{j < n} = -\frac{j}{N}; \quad \Theta_{j \geq n} = \frac{N-j}{N}. \quad (66)$$

More generally, when focusing on any combination of state with, for each state $|j\rangle$ an initial population P_j (such that $\sum_{j=1}^N P_j = 1$), we have the expression

$$\Theta_j = \sum_{k=1}^j P_k - \frac{j}{N}, \quad (67)$$

where the proof is provided in the Supplementary Material Sec. V A. The above focused initial conditions only affect angles $\{\theta_j\}$ for $j \in \{1, \dots, N-1\}$, whereas the $\{\varphi_j\}$ angles are sampled randomly in the range $[0, 2\pi]$. This effectively evaluates the integrals over $\{\theta_j\}$, but leaves the original integrals over $\{\varphi_j\}$. From Eq. 61, we further derive the expression of the angles $\{\theta_n\}$ as follows

$$\cos \theta_n = 1 - 2 \left(\frac{N-n}{N} - \frac{\Theta_n}{r_s} \right), \quad n = 1, \quad (68a)$$

$$\cos \theta_n = 1 - \frac{2 \left(\frac{N-n}{N} - \frac{\Theta_n}{r_s} \right)}{\prod_{k=1}^{n-1} \sin^2 \frac{\theta_k}{2}}, \quad 2 \leq n \leq N-1. \quad (68b)$$

The sines in the denominator of Eq. 68b can only be zero for $s = Q$, and in this case the equation for $\cos \theta_n$ is expressed in Eq. 68a. From the above equations, we note that any angle θ_n only depends on Θ_n and on the angles $\{\theta_j\}$ for $j < n$. Thus, the focused initial conditions in Eq. 66 (or more generally, Eq. 67) can be used to recursively generate values of θ_n based on Eq. 68.

In terms of the conjugate MMST mapping variables, the corresponding focused initial conditions in Eq. 65 are

$$q_n^2 + p_n^2 = 2 + \gamma; \quad q_j^2 + p_j^2 = \gamma, \quad (j \neq n), \quad (69)$$

based on the expression of the estimator in Eq. D9. These are the focused initial conditions proposed in the recently developed spin-LSC approach.⁴⁶ However, the latter focused conditions do not provide any specific choice of $\{\varphi_j\}$ in generalized Euler angle variables (see Eq. 18), and based on the expression of $d\Omega$ (Eq. 21) it should be uniformly sampled. In principle, any algorithm that uses $\{q_n, p_n\}$ should generate a uniform distribution of $\{\varphi_j\}$ in the range $[0, 2\pi]$, required by the $\int d\Omega$ integral (see expression of $d\Omega$ in Eq. 21). In the spin-LSC approach, it is proposed that the corresponding angle variable ϕ_n (Eq. 100b) should be sampled uniformly, as the original MMST formalism suggested.^{9,23} We shall see that $\varphi_n = \phi_{n+1} - \phi_n$ (Eq. 103), thus randomly sample ϕ_n is equivalent to randomly sample φ_n . Our rigorous theoretical framework thus helps to justify the empirical choices made by the previous simulation method.⁴⁶

V. QUANTUM LIOUVILLIAN IN THE MIXED WIGNER/STRATONOVICH-WEYL REPRESENTATION

A. Exact Liouvillian Expression

In this section, we derive the exact expression of the quantum Liouvillian $\hat{\mathcal{L}}$ in Eq. 56. Using the Heisenberg EOMs in the Wigner/S-W representation, we can

derive⁷⁸

$$\begin{aligned} \frac{d}{dt} [\hat{B}]_{ws} &= \frac{i}{\hbar} [\hat{H}, \hat{B}]_{ws} \equiv \hat{\mathcal{L}}[\hat{B}]_{ws} \quad (70) \\ &= \frac{2}{\hbar} [\mathcal{H}_0]_w \sin \frac{\hat{\Lambda}\hbar}{2} [\mathcal{B}_0]_w + \frac{1}{\hbar N} \sum_{i=1}^{N^2-1} [\mathcal{H}_i]_w \sin \frac{\hat{\Lambda}\hbar}{2} [\mathcal{B}_i]_w \\ &\quad + \frac{2r_s}{\hbar} \sum_{i=1}^{N^2-1} \Omega_i \left([\mathcal{H}_i]_w \sin \frac{\hat{\Lambda}\hbar}{2} [\mathcal{B}_0]_w + [\mathcal{H}_0]_w \sin \frac{\hat{\Lambda}\hbar}{2} [\mathcal{B}_i]_w \right) \\ &\quad + \frac{r_s}{\hbar} \sum_{i,j,k=1}^{N^2-1} d_{ijk} [\mathcal{H}_j]_w \Omega_k \sin \frac{\hat{\Lambda}\hbar}{2} [\mathcal{B}_i]_w \\ &\quad + \frac{r_s}{\hbar} \sum_{i,j,k=1}^{N^2-1} f_{ijk} [\mathcal{H}_j]_w \Omega_k \cos \frac{\hat{\Lambda}\hbar}{2} [\mathcal{B}_i]_w, \end{aligned}$$

where we have explicitly used the property in Eq. 42 for the S-W transform and the property of the Wigner transform $[\hat{A}\hat{B}]_w = [\hat{A}]_w e^{-i\hat{\Lambda}\hbar/2} [\hat{B}]_w$ (see Supplementary Material Sec. IV for details), and

$$\hat{\Lambda} = \frac{\overleftarrow{\partial}}{\partial P} \frac{\overrightarrow{\partial}}{\partial R} - \frac{\overleftarrow{\partial}}{\partial R} \frac{\overrightarrow{\partial}}{\partial P} \quad (71)$$

is the negative Poisson operator associated with the nuclear DOFs.^{75,79,80}

Based on Eq. 70, we identify a state-independent part and a state-dependent part of the Liouvillian, acting respectively on the state-independent and state-dependent components of the operator \hat{B} . By rewriting the total time-derivative of operator $[\hat{B}]_{ws}$ we have

$$\begin{aligned} \frac{d}{dt} [\hat{B}]_{ws} &= \frac{d}{dt} [\mathcal{B}_0 \hat{\mathcal{I}}]_{ws} + \sum_{i=1}^{N^2-1} \frac{d}{dt} [\mathcal{B}_i \cdot \frac{1}{\hbar} \hat{\mathcal{S}}_i]_{ws} \quad (72) \\ &= \frac{d}{dt} [\mathcal{B}_0]_w + \sum_{i=1}^{N^2-1} \frac{d}{dt} ([\mathcal{B}_i]_w \cdot r_s \Omega_i) \\ &\equiv \hat{\mathcal{L}}_0 [\mathcal{B}_0]_w + r_s \sum_{i=1}^{N^2-1} \hat{\mathcal{L}}_i (\Omega_i [\mathcal{B}_i]_w). \end{aligned}$$

By comparing Eq. 70 and Eq. 72, the state-independent Liouvillian is expressed as

$$\hat{\mathcal{L}}_0 [\mathcal{B}_0]_w \equiv \frac{2}{\hbar} H_s \sin \frac{\hat{\Lambda}\hbar}{2} [\mathcal{B}_0]_w, \quad (73)$$

with H_s expressed as

$$\begin{aligned} H_s(R, P) &= [\hat{H}(\hat{R}, \hat{P})]_{ws} = [\mathcal{H}_0]_w + r_s \sum_{j=1}^{N^2-1} \Omega_j [\mathcal{H}_j]_w \\ &= \mathcal{H}_0(R, P) + r_s \sum_{j=1}^{N^2-1} \Omega_j \mathcal{H}_j(R). \quad (74) \end{aligned}$$

For the last line of the above equation, we have used the fact that $[\mathcal{H}_i(\hat{R})]_w = \mathcal{H}_i(R)$ (see Eq. 11b or Eq. 12 for

its expression) and $[\mathcal{H}_0(\hat{R}, \hat{P})]_w = \mathcal{H}_0(R, P)$ because the Wigner transform of a function of position operator is the same function, and $\mathcal{H}_0(\hat{R}, \hat{P})$ only contains \hat{P} up to the quadratic order.⁷⁶

The state-dependent Liouvillian is expressed as

$$\begin{aligned} \hat{\mathcal{L}}_i(r_s\Omega_i[\mathcal{B}_i]_w) &\equiv \frac{1}{\hbar} \left[\left(\frac{1}{N} \mathcal{H}_i + 2r_s\Omega_i\mathcal{H}_0 \right) \sin \frac{\hat{\Lambda}\hbar}{2} \right. \\ &+ r_s \sum_{j,k=1}^{N^2-1} d_{ijk} \mathcal{H}_j \Omega_k \sin \frac{\hat{\Lambda}\hbar}{2} + r_s \sum_{j,k=1}^{N^2-1} f_{ijk} \mathcal{H}_j \Omega_k \cos \frac{\hat{\Lambda}\hbar}{2} \left. \right] [\mathcal{B}_i]_w \end{aligned} \quad (75)$$

We further identify two terms in $\hat{\mathcal{L}}_i$ as $\hat{\mathcal{L}}_i = \hat{\mathcal{L}}_i^e + \hat{\mathcal{L}}_i^n$. The first term evolves $\Omega_i[\mathcal{B}_i]_w$ as follows

$$\hat{\mathcal{L}}_i^e(r_s\Omega_i[\mathcal{B}_i]_w) \equiv \frac{1}{\hbar} r_s \sum_{j,k=1}^{N^2-1} f_{ijk} \mathcal{H}_j \Omega_k \cos \frac{\hat{\Lambda}\hbar}{2} [\mathcal{B}_i]_w, \quad (76)$$

where the leading term $\cos \frac{\hat{\Lambda}\hbar}{2} \approx 1$ evolves only the spin mapping variables. The second term evolves the nuclear DOFs through the coupling between the spin mapping variables and the nuclear DOFs as follows

$$\begin{aligned} \hat{\mathcal{L}}_i^n(r_s\Omega_i[\mathcal{B}_i]_w) &\quad (77) \\ &\equiv \frac{1}{\hbar} \left(\frac{1}{N} \mathcal{H}_i + 2r_s\Omega_i\mathcal{H}_0 + r_s \sum_{j,k=1}^{N^2-1} d_{ijk} \mathcal{H}_j \Omega_k \right) \sin \frac{\hat{\Lambda}\hbar}{2} [\mathcal{B}_i]_w. \end{aligned}$$

Naturally, if there is no state-dependent Hamiltonian ($H_s = [\mathcal{H}_0]_w$ and $\forall j, \mathcal{H}_i = 0$), the Liouvillian expression in Eq. 70 reduces back to the original Wigner-Moyal series⁶⁷ as follows

$$\frac{d}{dt} [\hat{B}]_{ws} = \hat{\mathcal{L}} \left([\mathcal{B}_0]_w + r_s \sum_{i=1}^{N^2-1} \Omega_i [\mathcal{B}_i]_w \right) \quad (78a)$$

$$\hat{\mathcal{L}} = \frac{P}{m} \overrightarrow{\partial_R} - \frac{2}{\hbar} U_0(R) \sin \left(\frac{\hbar}{2} \overleftarrow{\partial_R} \overrightarrow{\partial_P} \right), \quad (78b)$$

where the details of the derivation is provided in the Supplementary Materials Sec. VI.

Further, in the special case where there is no nuclear dependency, the only remaining term in the Liouvillian (Eq. 76) is

$$\hat{\mathcal{L}}_i^e(r_s\Omega_i) = \frac{1}{\hbar} r_s \sum_{j,k=1}^{N^2-1} f_{ijk} \mathcal{H}_j \Omega_k, \quad (79)$$

which goes back, as expected, to the expression of the EOMs derived by Hioe and Eberly³⁷ given in Eq. 15.

To summarize, the TCF (Eq. 56) with the exact Liouvillian is expressed as

$$\begin{aligned} C_{AB}(t) &= \frac{1}{2\pi\hbar Z} \int dR \int dP \int d\Omega [e^{-\beta\hat{H}} \hat{A}]_{ws} \quad (80) \\ &\times [e^{\hat{\mathcal{L}}_0 t} [\mathcal{B}_0]_w + r_s \sum_{i=1}^{N^2-1} e^{\hat{\mathcal{L}}_i t} \Omega_i [\mathcal{B}_i]_w], \end{aligned}$$

where $\hat{\mathcal{L}}_0$ and $\hat{\mathcal{L}}_i$ are expressed in Eq. 73 and Eq. 75, respectively. This is the *first key result* of this paper.

Note that this exact non-adiabatic Liouvillian based upon the $SU(N)$ mapping formalism has a different expression compared to the previous exact non-adiabatic Liouvillian based on the MMST mapping formalism,⁸¹ due to the different symmetry used in the mapping procedure. In particular, the current formalism might be more advantageous as it avoids a double derivative term on the mapping variables (which couples higher-order derivatives of nuclear and electronic motion, see Eq. 45 in Ref. 81). This term is difficult to evaluate^{82,83} but it does appear in all of the MMST based non-adiabatic Liouvillians.^{74,81,82}

B. Linearization Approximation and the Equations of Motion

So far, we have not made any approximation to the TCF expression. Solving Eq. 80 will be as difficult as solving the exact quantum dynamics, if not more. To simplify the task, we use the linearized path-integral approximation,^{11,84} or equivalently, linearizing the sines and cosines⁸¹ of $\hat{\Lambda}$ in Eq. 70 as follows

$$\cos \frac{\hat{\Lambda} \hbar}{2} \approx 1 + \mathcal{O}(\hbar^2), \quad \sin \frac{\hat{\Lambda} \hbar}{2} \approx \frac{\hat{\Lambda} \hbar}{2} + \mathcal{O}(\hbar^3). \quad (81)$$

This linearization approximation is equivalent to the approximation used in Linearized Semiclassical-Initial Value Representation (LSC-IVR).^{11,85,86} with the difference that the current approach uses the generalized spin mapping variables as opposed to the original MMST mapping variables.^{8,10} The detail of the derivation of the linearization of the Liouvillian is done in Supplementary Material Sec. VI.

Within the linearized approximation, we obtain the EOMs for the state-independent component (in Eq. 73) as follows

$$\frac{d}{dt} [\mathcal{B}_0]_w \approx \left[\frac{P}{m} \vec{\partial}_R - (\partial_R \mathcal{H}_0 + r_s \sum_{j=1}^{N^2-1} \partial_R \mathcal{H}_j \Omega_j) \vec{\partial}_P \right] [\mathcal{B}_0]_w. \quad (82)$$

The state-dependent time-derivatives (in Eqs. 72 and 75) after the linearization approximation become

$$\begin{aligned} r_s \frac{d}{dt} (\Omega_i [\mathcal{B}_i]_w) &= r_s \frac{d\Omega_i}{dt} \cdot [\mathcal{B}_i]_w + r_s \Omega_i \cdot \frac{d}{dt} [\mathcal{B}_i]_w \quad (83) \\ &\approx \frac{1}{\hbar} \left[r_s \sum_{j,k=1}^{N^2-1} f_{ijk} \mathcal{H}_j \Omega_k + \left(2r_s \Omega_i \mathcal{H}_0 + \frac{1}{N} \mathcal{H}_i \right) \frac{\hat{\Lambda} \hbar}{2} \right. \\ &\quad \left. + r_s \sum_{j,k=1}^{N^2-1} d_{ijk} \mathcal{H}_j \Omega_k \frac{\hat{\Lambda} \hbar}{2} \right] [\mathcal{B}_i]_w. \end{aligned}$$

Note that Ω_i (see Eq. 23) is an independent variable of the nuclear DOFs, $\{R, P\}$. Thus, the first term on the

As mentioned in Appendix 5 of WIREs. Comput. Mol. Sci. e1619 (2022)(submitted on February 5, 2022, released on arXiv on May 8, 2022 and officially published on May 13, 2022), the first-order truncation of \hbar [eq (93)] does not lead the EOMs that one obtains from LSC-IVR/Classical Wigner model, i.e., the mean-field trajectories.

right hand side of Eq. 83, which is independent of both R and P , must be equal to $r_s \frac{d\Omega_i}{dt} [\mathcal{B}_i]_w$, whereas the remaining terms on the right hand side of Eq. 83, which in principle depends on R and P , must be equal to $r_s \Omega_i \cdot \frac{d}{dt} [\mathcal{B}_i]_w$. This helps to identify the individual time derivatives for Ω_i as follows

$$\frac{d}{dt} \Omega_i = \frac{1}{\hbar} \sum_{j,k=1}^{N^2-1} f_{ijk} \mathcal{H}_j \Omega_k, \quad (84)$$

which is identical to Eq. 15, as well as time-derivative of $[\mathcal{B}_i]_w$ as follows

$$\begin{aligned} \frac{d}{dt} [\mathcal{B}_i]_w = & \left[\frac{P}{m} \overrightarrow{\partial_R} - \left(\partial_R \mathcal{H}_0 + \frac{1}{2Nr_s \Omega_i} \partial_R \mathcal{H}_i \right. \right. \\ & \left. \left. + \sum_{j,k=1}^{N^2-1} d_{ijk} \frac{\Omega_k}{2\Omega_i} \partial_R \mathcal{H}_j \right) \overrightarrow{\partial_P} \right] [\mathcal{B}_i]_w. \end{aligned} \quad (85)$$

The Liouvillians acting on $[\mathcal{B}_0]_w$ (Eq. 82) and on $[\mathcal{B}_i]_w$ (Eq. 85) are different, which is the feature of the spin mapping formalism. We emphasize that these equations are in principle exact for Hamiltonian with only linear state-dependent potentials \mathcal{H}_k and quadratic state-independent potential \mathcal{H}_0 , such as the spin-boson model and the conical intersection model. This is because under such a condition, \mathcal{H}_0 is a function up to R^2 and \mathcal{H}_k is a linear function of R , and thus the truncation in Eq. 81 becomes exact because those higher order terms of $\hat{\Lambda}$ will not act on \mathcal{H}_0 or \mathcal{H}_k in Eq. 70.

In the practical implementations of this approximation, such as in the recently proposed spin-LSC,³⁵ the nuclear DOFs were proposed to be updated with the Liouvillian in Eq. 82. This should be viewed as an independent approximation, in addition to the linearized approximation expressed in Eq. 81. Future investigations will be carried out to develop new propagation schemes taking into account the two Liouvillian components for a trajectory based method.

C. Equations of Motion with the Bloch vector

Thus, under the linearization approximation and using Eq. 82 to propagate the nuclear DOFs, we have the following classical EOMs, which is the *second key result* of this paper

$$\dot{R} = \frac{P}{m}, \quad (86a)$$

$$\dot{P} = -\frac{\partial \mathcal{H}_0}{\partial R} - r_s \sum_{k=1}^{N^2-1} \frac{\partial \mathcal{H}_k}{\partial R} \Omega_k = -\frac{\partial H_s(R, P)}{\partial R}, \quad (86b)$$

$$\frac{d}{dt} \Omega_i = \frac{1}{\hbar} \sum_{j,k=1}^{N^2-1} f_{ijk} \mathcal{H}_j(R) \Omega_k, \quad (86c)$$

where $H_s(R, P)$ is expressed in Eq. 74. The analytic expressions of the structure constants f_{ijk} are provided

in Eq. A1. Note that we choose to propagate the nuclear DOFs following the state-independent Liouvillian \mathcal{L}_0 that leads to Eq. 82, not considering the state-dependent Liouvillian \mathcal{L}_i^n which corresponds to Eq. 85. The above EOMs can be viewed as the generalization of the N -dimensional spin precession theory (Eq. 15) of Hioe and Eberly³⁷, where the electronic-nuclear coupling is explicitly considered here.

The above equations were recently *proposed* as the EOMs for the Generalized Discrete Truncated Wigner Approximation (GDTWA) approach⁵⁴ by choosing $r_s = \sqrt{N+1}$ (or $s = W$). In that work,⁵⁴ the EOMs were argued as the classical limit of the Heisenberg EOMs for the corresponding operators \hat{R} , \hat{P} , and \hat{S}_k . Here, we present a rigorous derivation of these EOMs. One can propagate quantum dynamics based on the EOMs outlined in Eq. 86. The initial conditions for the electronic DOFs can be sampled based on the phase space volume element in $\int d\Omega$ (Eqs. 21-22), which provides initial values of $\{\theta_n\}$ and $\{\varphi_n\}$, and then provide the values of $\{\Omega_k\}$ through Eq. B2-B4. The nuclear DOFs will be sampled through the initial Wigner density (for example, $[e^{-\beta\hat{H}_g}]_w$ in Eq. 60). These variables will be numerically propagated according to EOMs in Eq. 86. The formal numerical scaling for solving Eq. 86c is $\mathcal{O}(N^4)$, due to the N^2 dimensionality of both \mathcal{H}_j and Ω_k . It is thus ideal to find alternative but equivalent EOMs that reduce this scaling. Below, we derive three sets of linearized EOMs that are equivalent to the EOMs in Eq. 86c.

VI. ALTERNATIVE EXPRESSIONS OF THE LINEARIZED EQUATIONS OF MOTION

A. Equations of Motion with the Action-Angle Type Variables

In order to obtain equivalent EOMs in terms of the $2N - 2$ variables, we want to find a set of canonical variables. We recognize that in the two-state special case,^{36,87} the conjugate momentum of φ_1 is $\frac{1}{2}r_s \cos \theta_1 \equiv r_s \Omega_{\gamma_2}$, where γ_2 is the index of the diagonal generator (see Eq. 5c). Hence, we expect a conjugate momentum of any φ_n being a combination of $\{\Omega_{\gamma_j}\}$ for $j \in \{2, \dots, N\}$, which to the best of our knowledge, is unknown in the literature. Based on this conjectured conjugate relationship, we postulate the following Hamilton's EOMs

$$r_s \sum_{j=1}^N C_n(j) \frac{d}{dt} \Omega_{\gamma_j} = -\frac{\partial H_s}{\partial \varphi_n} \quad (87a)$$

$$r_s \frac{d}{dt} \varphi_n = \frac{\partial H_s}{\partial \sum_{j=1}^N C_n(j) \Omega_{\gamma_j}}, \quad (87b)$$

where H_s is expressed in Eq. 74. Here, $C_n(j)$ is the coefficient depending on the index of the generator γ_j , and the index of the *conjugate general coordinate* φ_n . Using Eq. 86c and our closed formulas for the structure

constants of $\mathfrak{su}(N)$ (see Appendix A), we derive the coefficients as follows

$$C_n(j \leq n) = 0; \quad C_n(j > n) = n \sqrt{\frac{2}{j(j-1)}}, \quad (88)$$

the derivation can be found in Appendix C. The general expression of the *conjugate variable of* φ_n for N -state systems, considering the coefficients found above, is

$$n \cdot r_s \sum_{j=n+1}^N \sqrt{\frac{2}{j(j-1)}} \Omega_{\gamma_j} \equiv \Theta_n, \quad (89)$$

which exactly corresponds to the variable Θ_n defined in Eq. 61. With the above finding, Eq. 87 can be rigorously expressed as

$$\dot{\Theta}_n = -\frac{\partial H_s}{\partial \varphi_n}; \quad \dot{\varphi}_n = \frac{\partial H_s}{\partial \Theta_n}, \quad (90)$$

with H_s expressed in Eq. 74, and the nuclear DOFs obey Eq. 86a-86b. Thus, we have discovered conjugate variables $\{\Theta_n, \varphi_n\}$ which decompose the $N^2 - 1$ coupled equations in Eq. 86c into $2N - 2$ coupled equations. In fact, Θ_n and φ_n play a similar role as the “action” and the “angle” variables in the original Meyer-Miller mapping formalism.⁹ This is not very surprising, as the action variables are related to the population of states, and Θ_n is directly related to the population estimator (see Eq. 62) and thus related to the action variable (Eq. 100) as well.

In order to derive the closed formula of the EOMs in Eq. 90 with variables $\{\Theta_n, \varphi_n\}$, we express the Hamiltonian in terms of these variables. Using Eq. 62 and Eq. 64, the mapping Hamiltonian in Eq. D13 (with replacing \vec{R} to R upon nuclear Wigner transform) can be expressed as

$$\begin{aligned} H_s = & \frac{P^2}{2M} + U_0(R) + \sum_{n=1}^N \left(\Theta_n - \Theta_{n-1} + \frac{1}{N} \right) \cdot V_{nn}(R) \\ & + 2 \sum_{n=2}^N \sum_{m=1}^{n-1} \sqrt{\left(\Theta_n - \Theta_{n-1} + \frac{r_s}{N} \right) \left(\Theta_m - \Theta_{m-1} + \frac{r_s}{N} \right)} \\ & \times \cos \left(\sum_{k=m}^{n-1} \varphi_k \right) \cdot V_{nm}(R), \end{aligned} \quad (91)$$

which is reminiscent to the Meyer-Miller mapping Hamiltonian in the form of the action-angle variables^{9,23} (see Eq. 104) and the transformation to the cartesian mapping variables $\{p_n, q_n\}$ are provided in Eq. 98a and Eq. 98b. Note that we have assumed a purely real Hamiltonian when expressing Eq. 91. The general form of the mapping Hamiltonian can be found in Eq. C7, and the two-state special case of Eq. 91 is provided in Eq. F12. More interestingly, it seems that the early work of Miller and McCurdy³⁴ had suggested the same mapping Hamiltonian for $N = 2$ case (based on the linear interpolation of Heisenberg correspondence principle), where Eq. 3.20 in Ref. 34 is equivalent to Eq. F12 when setting $r_s = 1$.

Using the expression of H_s in Eq. 91, the Hamilton's EOMs in Eq. 90 can be expressed in Eq. C8 of Appendix C. This EOM in Eq. C8 share a similar form of those original Meyer-Miller mapping EOMs expressed in the action-angle variables⁹ (see Eq. 105a), because the conjugate variables $\{\Theta_n, \varphi_n\}$ are closely related to the Meyer-Miller action-angle variables (see Eq. 102 and Eq. 103). The advantage of using the conjugate variable relationship between Θ_n and φ_n in Eq. C8, instead of the EOMs expressed in Eq. 86c with $\{\Omega_j\}$ is that in the former case there are $2N - 2$ variables to explicitly propagate, as opposed to the $N^2 - 1$ variables of the latter.

B. Equations of Motion with the MMST mapping Variables

Instead of using conjugated variables $\{\varphi_n, \Theta_n\}$ (Eq. E5), one can use $\{q_n, p_n\}$ defined in Eq. D4, which are also conjugated variables.⁴⁶ Here, we explicitly show this using the EOMs. The electronic EOMs in Eq. 86c under the linearization approximation are equivalent to the following equation

$$i\hbar \frac{\partial}{\partial t} \hat{w}_s = [\hat{V}_e(R), \hat{w}_s], \quad (92)$$

where $\hat{V}_e(R)$ is defined as

$$\hat{V}_e(R) = \frac{1}{\hbar} \sum_{k=1}^{N^2-1} \mathcal{H}_k \cdot \hat{\mathcal{S}}_k, \quad (93)$$

and $\mathcal{H}_k(R) = \frac{2}{\hbar} \text{Tr}_e[\hat{H} \cdot \hat{\mathcal{S}}_k] = \frac{2}{\hbar} \text{Tr}_e[\hat{V}_e(R) \cdot \hat{\mathcal{S}}_k]$. Plugging the expression of $\hat{V}_e(R)$ (Eq. 93) as well as the expression of \hat{w}_s (Eq. 26) into Eq. 92, one can easily verify its equivalence with Eq. 86c.

We then re-express Eq. 92 using the kernel expressed in Eq. D7, leading to

$$i\hbar \frac{\partial}{\partial t} \left(\sum_{na} c_n c_a^* |n\rangle \langle a| \right) = [\hat{V}_e(R), \sum_{mb} c_m c_b^* |m\rangle \langle b|],$$

which can be used to derive

$$i\hbar \dot{c}_n = \sum_m V_{nm}(R) \cdot c_m \quad (94)$$

and its complex conjugate equation. This means that Eq. 84 is equivalent to the Ehrenfest dynamics for the electronic DOFs. The nuclear force described in Eq. 86b, on the other hand, differs from the Ehrenfest dynamics if $r_s \neq 1$ ($s \neq Q$).

Using the transformation defined in Eq. 47, one can rewrite the EOMs in Eq. 94 as the coupled equations for the conjugated variables $\{q_n, p_n\}$ as follows⁸⁸

$$\dot{q}_n = \sum_m V_{nm}(R) \cdot p_m = \frac{\partial \mathcal{H}}{\partial p_n}, \quad (95a)$$

$$\dot{p}_n = - \sum_m V_{nm}(R) \cdot q_m = - \frac{\partial \mathcal{H}}{\partial q_m}. \quad (95b)$$

Thus, Eq. 95 can be viewed as the mapping equation corresponding to the time-dependent Schrödinger's equation, which is equivalent to the mapping equation corresponding to the Quantum Liouville-von Neumann equation in Eq. 86c (also see Eq. 15). In Eq. 95, the MMST mapping Hamiltonian is

$$\mathcal{H} = \frac{P^2}{2M} + U_0(R) + \sum_n \frac{1}{2} V_{nn}(R)(q_n^2 + p_n^2 - \gamma) \quad (96)$$

$$+ \sum_{n < m} V_{nm}(R)(q_n q_m + p_n p_m),$$

where \mathcal{H} (Eq. 96) is equivalent to $H_s(R, P)$ (Eq. 74) through the transform defined in Eq. D4 (or equivalently in Eq. 47). The Hamiltonian \mathcal{H} in Eq. 96 can be viewed as Eq. 48 with the Wigner transform over only the nuclear DOFs. Further, using the transformation defined in Eq. D4, the nuclear EOMs in Eq. 86 can be expressed as

$$\dot{R} = \frac{\partial \mathcal{H}}{\partial P}, \quad \dot{P} = -\frac{\partial \mathcal{H}}{\partial R}. \quad (97)$$

Note that Eq. 95 are the classical Hamilton's EOMs of \mathcal{H} (Eq. 96), with the conjugated variables $\{q_n, p_n\}$.

Similarly, Eq. C8 is also the Hamilton's EOMs of H_s , with the conjugate variables $\{\Theta_n, \varphi_n\}$. Thus, the transformation that convert $H_s(\Theta_n, \varphi_n)$ (Eq. 91) to $\mathcal{H}(q_n, p_n)$ (Eq. 96) is a canonical transform that preserves the form of Hamilton's EOMs. More specifically, this canonical transformation that connects the generalized conjugate variables $\{\Theta_n, \varphi_n\}$ to the conjugate position and momentum is expressed as

$$\Theta_n = \left(\frac{1}{n} - \frac{1}{N} \right) \sum_{m=1}^n \frac{1}{2} (q_m^2 + p_m^2) - \frac{n}{N} \sum_{m=n+1}^N \frac{1}{2} (q_m^2 + p_m^2), \quad (98a)$$

$$\varphi_n = \tan^{-1} \left(\frac{p_{n+1} \cdot q_n - q_{n+1} \cdot p_n}{q_{n+1} \cdot q_n + p_{n+1} \cdot p_n} \right), \quad (98b)$$

where we have used the transform defined in Eq. D4 to convert Eq. 89 into Eq. 98a, and convert Eq. E2 into Eq. 98b. The inverse transform from $\{\varphi_n, \theta_n\}$ to the MMST mapping variables $\{q_n, p_n\}$ (based on Eq. 47) are

$$q_n = \sqrt{2r_s} \cdot \text{Re}[\langle n | \Omega \rangle \cdot e^{i\Phi}], \quad (99a)$$

$$p_n = \sqrt{2r_s} \cdot \text{Im}[\langle n | \Omega \rangle \cdot e^{i\Phi}], \quad (99b)$$

where the explicit expression of $\langle n | \Omega \rangle$ as a function of $\{\varphi_n, \theta_n\}$ can be found in Eq. 18.

Note that the EOMs in Eq. 95 and Eq. 97 are identical to the EOMs commonly used in the MMST mapping formalism.^{23,44} These EOMs are also used in the spin-LSC approach,⁴⁶ by the argument⁴⁶ that they are Hamilton's EOMs of \mathcal{H} (Eq. 96). Here, we rigorously prove that they are equivalent to the EOMs in Eq. 86, thus can be derived as the linearization approximation

Similar to comment on eq (D1). The importance of global phase in SU(F) Stratonovich phase space was already stressed in Appendix 3 of WIREs. Comput. Mol. Sci. e1619 (2022)(submitted on February 5, 2022, released on arXiv on May 8, 2022 and officially published on May 13, 2022), while completely absent in first version of this manuscript (online on May 20, 2022) and abruptly involved here (online on July 29, 2022). The eq (121) here was different with the corresponding eq (113) in previous version:

$$q_n = \sqrt{2r_s} \cdot \text{Re}[\langle n | \Omega \rangle] \quad (113a)$$

$$p_n = \sqrt{2r_s} \cdot \text{Im}[\langle n | \Omega \rangle], \quad (113b)$$

where the global phase disappeared. The authors copied key ideas from our paper WIREs. Comput. Mol. Sci. e1619 (2022) where we clearly pointed out in eq (S54),

$$\begin{pmatrix} x^{(n)} \\ p^{(n)} \end{pmatrix} = \sqrt{2\lambda} \begin{pmatrix} \cos\psi & -\sin\psi \\ \sin\psi & \cos\psi \end{pmatrix} \begin{pmatrix} \text{Re}\langle n | \theta, \phi \rangle \\ \text{Im}\langle n | \theta, \phi \rangle \end{pmatrix}, \quad S54$$

which involved the global phase. Moreover, the correct form of canonical Hamilton's equations of motion in Meyer-Miller variables could not be derived with a constant global phase!

Timeline

Liu and his coworkers'
WCMS paper
submitted on Feb 5, 2022
revised on April 8, 2022
realized on arXiv on May 8, 2022
published on May 13, 2022

Huo and his coworkers'
ChemRxiv Version 1
online on May 20, 2022

Huo and his coworkers'
ChemRxiv Version 2
online on May 27, 2022

Huo and his coworkers'
JCP accepted Version
online on July 29, 2022

representations

one-to-one **exact** mapping
between Stratonovich space
and CMM phase space

$$\begin{pmatrix} x^{(s)} \\ p^{(s)} \end{pmatrix} = \sqrt{2\lambda} \begin{pmatrix} \cos\psi & -\sin\psi \\ \sin\psi & \cos\psi \end{pmatrix} \begin{pmatrix} \text{Re}(n|\theta, \phi) \\ \text{Im}(n|\theta, \phi) \end{pmatrix}, \quad S54$$

$$\sqrt{\lambda} e^{i\psi} |\theta, \phi\rangle \equiv |x, p\rangle$$

lost global phase in such
relation! (**incorrect**)

$$q_n = \sqrt{2r_s} \cdot \text{Re}[\langle n|\Omega \rangle] \quad (113a)$$

$$p_n = \sqrt{2r_s} \cdot \text{Im}[\langle n|\Omega \rangle], \quad (113b)$$

plagiarized the idea of global
phase from

$$q_n = \sqrt{2r_s} \cdot \text{Re}[\langle n|\Omega \rangle \cdot e^{i\Phi}], \quad (121a)$$

$$p_n = \sqrt{2r_s} \cdot \text{Im}[\langle n|\Omega \rangle \cdot e^{i\Phi}], \quad (121b)$$

$$q_n = \sqrt{2r_s} \cdot \text{Re}[\langle n|\Omega \rangle \cdot e^{i\Phi}], \quad (99a)$$

$$p_n = \sqrt{2r_s} \cdot \text{Im}[\langle n|\Omega \rangle \cdot e^{i\Phi}], \quad (99b)$$

dynamics

full description of EOMs

$$\dot{\lambda} = \frac{\partial}{\partial \psi} H_C^{(\lambda)}(\theta, \phi; s) = 0$$

$$\dot{\psi} = \left[-\frac{\partial}{\partial \lambda} + \frac{\tan \theta_{F-1}}{2\lambda} \frac{\partial}{\partial \theta_{F-1}} \right] H_C^{(\lambda)}(\theta, \phi; s) \quad S53$$

$$\dot{\theta}_i = -\sum_{j=1}^{F-1} \frac{A_{ji}}{\lambda} \frac{\partial}{\partial \varphi_j} H_C^{(\lambda)}(\theta, \phi; s) - \delta_{i,F-1} \frac{\tan \theta_{F-1}}{2\lambda} \frac{\partial}{\partial \psi} H_C^{(\lambda)}(\theta, \phi; s)$$

$$\dot{\phi}_i = +\sum_{j=1}^{F-1} \frac{A_{ij}}{\lambda} \frac{\partial}{\partial \theta_j} H_C^{(\lambda)}(\theta, \phi; s)$$

WRONG EOMs eq (105)
with coherent states in eq (17).

wrong even until May 20, 2022.

plagiarized the idea from
our EOMs to derive the correct EOMs only for 2F-2
variables of Stratonovich phase space
in their paper [eq (113) with eq (18)]

also plagiarized the idea from our EOMs
in eq (E9) with eq (18)

$$q_n = \sqrt{2r_s} \cdot \text{Re}[\langle n|\Omega \rangle \cdot e^{i\Phi}], \quad (99a)$$

$$p_n = \sqrt{2r_s} \cdot \text{Im}[\langle n|\Omega \rangle \cdot e^{i\Phi}], \quad (99b)$$

where the explicit expression of $\langle n|\Omega \rangle$ as a function of $\{\varphi_n, \theta_n\}$ can be found in Eq. 18.

Note that the EOMs in Eq. 95 and Eq. 97 are identical to the EOMs commonly used in the MMST mapping formalism.^{23,44} These EOMs are also used in the spin-LSC approach,⁴⁶ by the argument⁴⁶ that they are Hamilton's EOMs of \mathcal{H} (Eq. 96). Here, we rigorously prove that they are equivalent to the EOMs in Eq. 86, thus can be derived as the linearization approximation

from the exact quantum Liouvillian (Eq. 73 and Eq. 75). The $2N$ MMST mapping variables are subject to a constraint given in Eq. D11. Further, there is an overall phase factor among the $\{q_n, p_n\}$ variables which does not influence the dynamics (see Eq. 47). Thus, there are still $2N - 2$ truly independent variables, in agreement with the $2N - 2$ generalized Euler angle variables $\{\varphi_n, \theta_n\}$ or the $2N - 2$ conjugate variables $\{\varphi_n, \Theta_n\}$. The EOMs with $\{q_n, p_n\}$ in Eq. 95 are indeed analytically simpler than the EOMs with $\{\varphi_n, \theta_n\}$ in Eq. E9, making them more appealing for practical implementations.

C. Connections among Different Formalisms

For these MMST variables, one often define action-angle variables^{7,23,44} $\{\eta_n, \phi_n\}$ associated with the phase space mapping variables as follows

$$\eta_n = \frac{1}{2}(q_n^2 + p_n^2 - \gamma), \quad (100a)$$

$$\phi_n = \tan^{-1}\left(\frac{p_n}{q_n}\right), \quad (100b)$$

or the inverse transform

$$q_n = \eta_n \cdot \cos \phi_n; \quad p_n = \eta_n \cdot \sin \phi_n. \quad (101)$$

Thus, Θ_n in Eq. 98a is a function of the action variables $\{\eta_n\}$ (as we already expected from the expression in Eq. 91), and φ_n in Eq. 98b is a function of the MMST angle variables $\{\phi_n\}$. In fact, using Eq. 62 and Eq. D9 (as well as the definition of η_n in Eq. 100a), we have

$$\eta_n = \Theta_n - \Theta_{n-1} + \frac{1}{N}. \quad (102)$$

Further, we can plug Eq. 101 into Eq. 98b and obtain

$$\begin{aligned} \varphi_n &= \tan^{-1}\left(\frac{\sin \phi_{n+1} \cdot \cos \phi_n - \cos \phi_{n+1} \cdot \sin \phi_n}{\cos \phi_{n+1} \cdot \cos \phi_n + \sin \phi_{n+1} \cdot \sin \phi_n}\right) \\ &= \tan^{-1}\left(\frac{\sin(\phi_{n+1} - \phi_n)}{\cos(\phi_{n+1} - \phi_n)}\right) = \phi_{n+1} - \phi_n. \end{aligned} \quad (103)$$

Thus, the meaning of φ_n is the phase difference for state $|n\rangle$ and state $|n+1\rangle$ in the angle variables of the MMST mapping formalism. This explains why numerically one can also uniformly sample the angle ϕ_n in the MMST mapping,⁴⁶ which is equivalent to the uniform sampling of φ_n .

Moreover, it is well-known that the MMST Hamiltonian (Eq. 96) can also be expressed as the action-angle variables (Eq. 100 or Eq. 101) as^{9,23}

$$\begin{aligned} \mathcal{H} &= \frac{P^2}{2M} + U_0(R) + \sum_n V_{nn}(R) \cdot \eta_n \\ &\quad + 2 \sum_{m < n} V_{nm}(R) \sqrt{\left(\eta_n + \frac{\gamma}{2}\right) \left(\eta_m + \frac{\gamma}{2}\right)} \cos(\phi_n - \phi_m), \end{aligned} \quad (104)$$

and the corresponding EOMs as⁹

$$\dot{\eta}_n = -\frac{\partial \mathcal{H}}{\partial \phi_n} \quad (105a)$$

$$= 2 \sum_{m < n} \sqrt{\left(\eta_n + \frac{\gamma}{2}\right) \left(\eta_m + \frac{\gamma}{2}\right)} \cdot \sin(\phi_n - \phi_m) \cdot V_{nm}(R)$$

$$\dot{\phi}_n = \frac{\partial \mathcal{H}}{\partial \eta_n} \quad (105b)$$

$$= \sum_{m < n} \sqrt{\frac{\eta_m + \frac{\gamma}{2}}{\eta_n + \frac{\gamma}{2}}} \cdot \cos(\phi_n - \phi_m) \cdot V_{nm}(R)$$

These EOMs are closely related to those in Eq. C8 which are expressed in $\{\Theta_n, \varphi_n\}$ variables. Actually, using Eq. 102 and Eq. 103, one can easily verify that $\mathcal{H}(\Theta, \varphi)$ of Eq. 91 is equivalent to $\mathcal{H}(\eta, \phi)$ of Eq. 104 (by noticing $r_s = 1 + N\gamma/2$, see Eq. D6).

Though "related", it was never hand-waving to start from eq (105) to recover the canonical Hamilton's equations of motion of Meyer-Miller variables in eq (95). The evolving global phase was completely neglected.

VII. COMPUTATIONAL DETAILS

Here, we provide the computational implementation of the method. Details of the model systems, as well as the initial conditions of the simulations are provided in Supplementary Material Sec. VII.

Using the EOMs expressed in Eq. 86 or Eq. C8, and the out-of-equilibrium TCF expressions that we derived in Eq. 60, we can apply the linearized spin mapping approach to study the non-adiabatic dynamics of model systems. Here, we briefly summarize the details of the propagation algorithm. In this paper, we present numerical results with both sampled and focused initial conditions. The sampling of $\{\theta_n\}$ or $\{\Theta_n\}$ and $\{\varphi_n\}$ is done over the phase space volume element $\int d\Omega$ defined in Eqs. 21-22, through a Metropolis-Hastings algorithm. The results are presented using $r_s = r_{\bar{s}} = r_W$. The focused initial conditions and the procedure are described in Sec. IV C. To propagate the dynamics, we use the simple Verlet algorithm because of the conjugate relation between Θ_n and φ_n (see Eq. E5), as well as the relation between $\dot{\Theta}_n$ and $\dot{\varphi}_n$ in Eq. E5a (to use the EOMs in Eq. E9).

First, the generalized conjugate variables $\{\varphi_n, \Theta_n\}$ are propagated by a half time-step, which is done using the Verlet algorithm as follows

$$\Theta_n(t + \frac{\Delta t}{4}) = \Theta_n(t) + \dot{\Theta}_n(t) \frac{\Delta t}{4}, \quad (106a)$$

$$\varphi_n(t + \frac{\Delta t}{2}) = \varphi_n(t) + \dot{\varphi}_n(t + \frac{\Delta t}{4}) \frac{\Delta t}{2}, \quad (106b)$$

$$\Theta_n(t + \frac{\Delta t}{2}) = \Theta_n(t + \frac{\Delta t}{4}) + \dot{\Theta}_n(t + \frac{\Delta t}{2}) \frac{\Delta t}{4}, \quad (106c)$$

Comment: The algorithm was changed from eq 115 in their first version (online one May 20, 2022). But the Monte Carlo simulation results remained HIGHLY SIMILAR.

or equivalently with θ_n instead of Θ_n , where $\dot{\theta}_n$ and $\dot{\varphi}_n$ are expressed in Eq. E9a-E9b and $\dot{\Theta}_n$ and $\dot{\varphi}_n$ in Eq. C8a-C8b. In theory it is possible to have a singular value for $\dot{\theta}_n$ (Eq. E9a) or $\dot{\varphi}_n$ (Eq. C8b) due to a possible zero value of the denominator. In practice, for the calculations performed in this study, this situation rarely occurs

for the sampled initial condition for $s = W$ approach, but may happen for the first time-step of the focused initial conditions with the choice of $s = Q$. Nevertheless, for the time-step where this situation occurs, one can switch back to Eq. 86c to avoid these rare numerical singularities in $\dot{\theta}_n$. In this case, one can switch to use a Verlet algorithm with $\dot{\Omega}_i$ and $\ddot{\Omega}_i = \frac{1}{\hbar} \sum_{j,k=1}^{N^2-1} f_{ijk} \mathcal{H}_j \dot{\Omega}_k$, or to the MMST variables by propagating Eq. 95.

The above half-propagation step for the electronic DOFs is followed by a propagation of the nuclear variables using the Verlet algorithm,

$$P(t + \frac{\Delta t}{2}) = P(t) + \dot{P}(t) \frac{\Delta t}{2}, \quad (107a)$$

$$R(t + \Delta t) = R(t) + \dot{R}(t + \frac{\Delta t}{2}) \Delta t, \quad (107b)$$

$$P(t + \Delta t) = P(t + \frac{\Delta t}{2}) + \dot{P}(t + \Delta t) \frac{\Delta t}{2}, \quad (107c)$$

and finally by the second half time-step of the mapping variables $\{\varphi_n, \theta_n\}$ with a similar Verlet scheme as outlined in Eq. 106. Thus, in principle, the non-adiabatic mapping dynamics in the $SU(N)$ representation does not need the MMST mapping variables.

On the other hand, an *alternative* but *numerically simpler* way to propagate dynamics (compare to solving the dynamics using $\{\Theta_n, \varphi_n\}$ variables) is to obtain the initial values of the angles for $\{\varphi_n, \theta_n\}$ through either the sampling or focusing approach described in Sec. IV, then transform them into the MMST Cartesian mapping variables $\{q_n, p_n\}$ through Eq. 99, and directly propagate the EOMs with these MMST variables through Eq. 95 and Eq. 97. This is an *easier approach to implement into computer code*, because these equations are simpler than the corresponding EOMs for $\{\varphi_n, \theta_n\}$ or $\{\varphi_n, \Theta_n\}$. In addition, there are several previously developed symplectic integrators^{21,89} to propagate these EOMs, which one can take advantage of. Our numerical tests suggest that identical numerical accuracy of the results are generated from this approach and the approach in Eq. 106.

VIII. RESULTS AND DISCUSSIONS

In this section, we refer to the linearized method in the $SU(N)$ mapping formalism as the spin mapping (SM) approach, with the EOMs described in Eq. 86, or equivalently, in Eq. E9 or in Eq. 95. Here, we compare the numerical results obtained from the spin mapping formalism with other methods, including the LSC-IVR^{11,85,86} as well as the simple trajectory Ehrenfest method.^{90–92} Note that the current Spin Mapping approach is derived entirely based on the $SU(N)$ formalism, without the necessity to convert back to the Cartesian mapping variables of the MMST formalism that spin-LSC uses. Nevertheless, we found that the current approach generates numerically similar results compared to spin-LSC.^{35,46} As we have discussed, the underlying EOMs for the generalized spin mapping approach (within the linearization

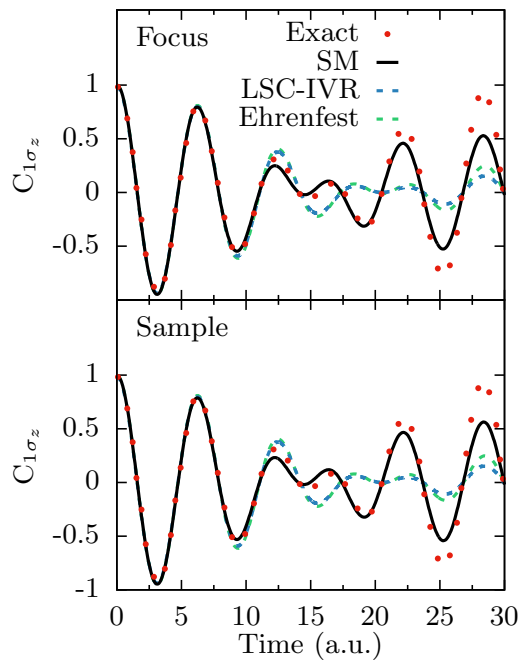


FIG. 2. Population dynamics of the 1-D spin boson models, obtained from focused initial conditions (top panel) and sampled initial conditions (bottom panel). The Spin-Mapping results (black solid lines) are compared against the LSC-IVR (blue dashed lines), Ehrenfest (green dashed lines) and exact results (red dots).

approximation) are identical to Ehrenfest dynamics and the MMST-based approach under a specific choice of r_s . Nuclear initial conditions for all of these methods are also obtained from the Wigner transform of the initial nuclear density operator. In Supplementary Material Sec. IX, we provide the connection and difference of several previously developed methods with the current method in the language of the $SU(N)$ mapping formalism.

Fig. 2 presents the population dynamics $\langle \sigma_z(t) \rangle = C_{1\sigma_z}(t)$ for a 1-D spin-boson model,⁹³ with a Hamiltonian $\hat{H} = (\frac{\hat{P}^2}{2m} + \frac{1}{2}m\omega^2\hat{R}^2)\hat{I} + \sqrt{2}\zeta\hat{R}\hat{\sigma}_z + \Delta\hat{\sigma}_x$. We choose $2\Delta = \omega = m = 1$ and increasing values of the coupling strength parameter, the temperature is chosen in order to have $\beta = 16$, and the coupling parameter is $\xi = 0.1$. The initial electronic state is prepared on state $|1\rangle$. A time-step of $dt = 0.01$ a.u. and 10^4 (focused initial conditions) and 10^5 (sampled initial conditions) are used. The population dynamics of the spin mapping approach are compared to the numerically exact calculations (red dots), LSC-IVR (blue) and Ehrenfest dynamics (green). The results obtained from the SM approach (with both sampled and focused initial conditions) are in a very good agreement with the exact calculations. Additional results with regular spin-boson models (which has bath and spectral density) are provided in the Supplementary Materials Sec. VIII.

The LSC-IVR approach and the Ehrenfest dynamics in Fig. 2, on the other hand, capture the initial electronic os-

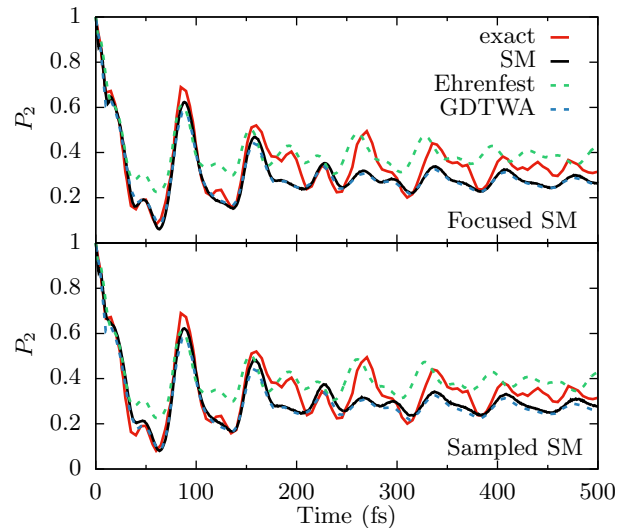


FIG. 3. Population dynamics of the pyrazine model with focused (upper panel) and sampled initial conditions (lower panel) for the Spin Mapping approach. The results obtained from Spin Mapping (black solid lines) are compared to the Ehrenfest method (green dashed line), the GDTWA approach⁵⁴ (blue dashed line), and exact results (red solid line).

cillations but fail to reproduce the longer time recurrence. This less accurate longer time dynamics from LSC-IVR or Ehrenfest was thought⁹³ to be caused by the zero point energy (ZPE) leakage problem associated with the classical Wigner dynamics of the nuclear DOF,^{94,95} which is typical for linearized path-integral approaches based on the classical Wigner dynamics.^{71,84,96} The ZPE leakage originates from the fact that classical dynamics does not preserve the ZPE incorporated in the nuclear initial Wigner distribution,^{94,95} causing an incorrect energy flow from the nuclear DOF to the electronic DOFs,⁹⁷ equalizing the longer time populations and giving $\langle \sigma_z(t) \rangle = 0$. In our previous work on non-adiabatic ring polymer molecular dynamics,⁹³ we have shown that quantizing the nuclear DOF with a ring polymer can effectively incorporate nuclear quantum distribution and alleviate ZPE leaking problem, even when using the MMST mapping formalism. Here, our numerical results suggest that by using the $SU(N)$ mapping formalism which exactly preserves the size of the electronic Hilbert space, this problem can be largely alleviated, compare to the traditional MMST mapping formalism which can get outside of the singly excited oscillator (SEO) mapping subspace, even though the classical Wigner type of dynamics is used for the nuclear DOF. Additional results with a larger system-bath coupling parameter ξ are presented in the Supplementary Materials Sec. VIII.

Fig. 3 presents the population dynamics of state $|2\rangle$ in the pyrazine model.⁹⁹ For the Spin Mapping results presented here, we used 10^5 trajectories for the sampled

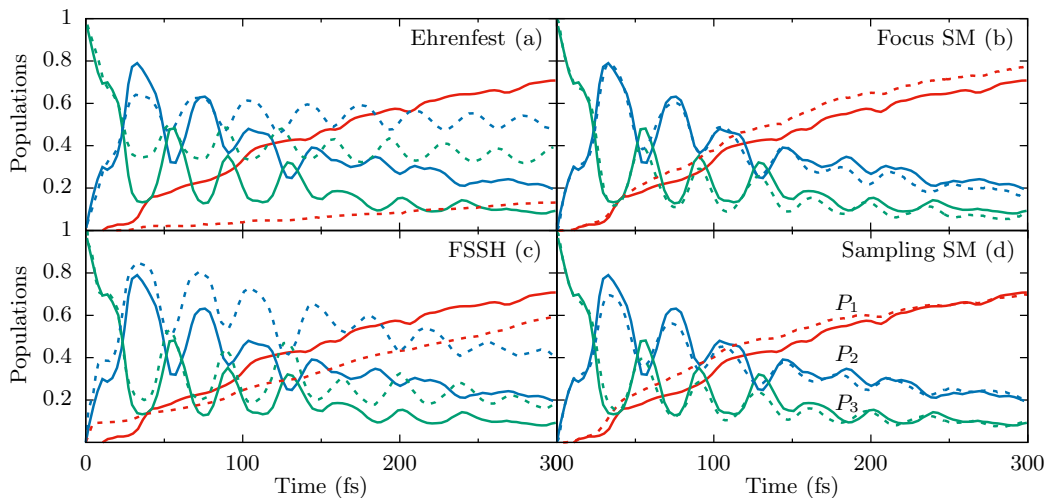


FIG. 4. Electronic populations of the benzene cation model, obtained from (a) Ehrenfest dynamics, (b) Spin Mapping formalism with focused initial condition, (c) fewest switches surface hopping (FSSH) as obtained from Ref. 98, and (d) Spin Mapping with sampled initial conditions. The population dynamics of state 1 (red), state 2 (blue) and state 3 (green) are presented (dashed lines) and compared to exact dynamics (solid lines).

initial condition and 10^4 for the focused initial condition, and a nuclear time-step of $dt = 0.5$ a.u. as well as a mapping time-step of $dt_{\text{map}} = dt_{\text{nuc}}/16$. The results are obtained from the current Spin Mapping approach (red solid) with both focused and sampled initial conditions, and compared to Ehrenfest dynamics (green dash), as well as to the recently developed Generalized Discrete Truncated Wigner Approximation (GDTWA)⁵⁴ approach (blue dashed line). The Spin Mapping approach generates very accurate population dynamics compared to the exact results, regardless of the initial conditions of the mapping variables, although the early dynamics is slightly more accurate when focusing the initial conditions, while the long-time dynamics seems closer to the exact result when using the sampled initial conditions. The current Spin Mapping approach perfectly coincides with the GDTWA approach when focused initial conditions are used, and is close when sampled initial conditions are used. This was expected as it was claimed⁵⁴ that in the GDTWA approach, the discrete sampling of the phase space is the key to provide more accurate results compared to the spin mapping formalism when $N > 2$ states are considered, for $N = 2$ those two approaches (GDTWA and focused spin-LSC) are equivalent.

Fig. 4 presents the numerical results of a three-state model for the benzene radical cation.^{100,101} Same number of trajectories and time-step are used as for the pyrazine model. This is a particularly challenging model due to the multi-state dynamics and the presence of conical intersection, especially for traditional mixed quantum-classical methods such as Ehrenfest (panel a) and Fewest Switches Surface Hopping³ (panel c), both of which generate less accurate population dynamics.⁹⁸ The spin map-

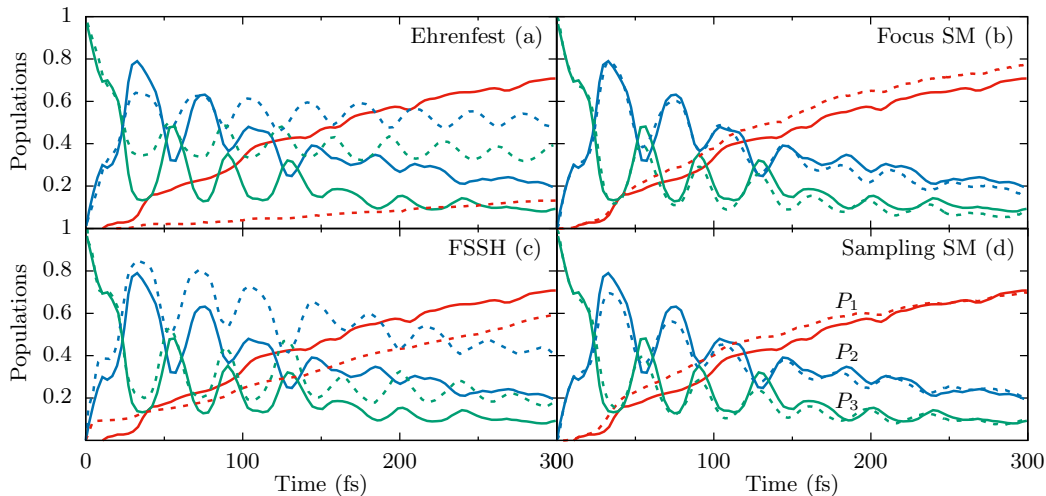


FIG. 4. Electronic populations of the benzene cation model, obtained from (a) Ehrenfest dynamics, (b) Spin Mapping formalism with focused initial condition, (c) fewest switches surface hopping (FSSH) as obtained from Ref. 98, and (d) Spin Mapping with sampled initial conditions. The population dynamics of state 1 (red), state 2 (blue) and state 3 (green) are presented (dashed lines) and compared to exact dynamics (solid lines).

ping formalism, on the other hand, gives almost quantitatively accurate dynamics for this challenging system. While the focused initial conditions provide slightly more accurate short-time dynamics up to 150 fs (panel b), the sampled initial conditions seem to generate population closer to the exact result at a longer time. An additional figure comparing the results obtained from the recently developed γ -SQC method¹⁰² is presented in Supplementary Material Sec. VIII, which demonstrates that the current linearized spin mapping approach slightly outperforms the γ -SQC method,¹⁰² both of which, on the other hand, are more accurate than traditional MQC methods such as Ehrenfest dynamics and FSSH.¹⁰³

Fig. 5 presents the results of population dynamics in the three-state coupled Morse potential.¹² Here, we present the Spin Mapping results only using focused initial conditions (solid lines). A time-step of 1 a.u., and 10^5 to 5×10^5 trajectories were used. The sampled initial conditions for spin mapping variables generates less accurate population as the initial nuclear force does not respect the physical occupancy of the electronic states.¹⁰² This has been extensively discussed in the recent work on trajectory-adjusted electronic zero point energy in classical Meyer-Miller vibronic dynamics.¹⁰² Nevertheless, the population dynamics of the Spin Mapping method with the focused initial conditions give almost exact results compared to the numerically exact calculations (dots), and outperform Ehrenfest dynamics (dashed lines). The Spin Mapping approach generates both accurate short time branching dynamics among three states as well as long time plateau value of the population, that is almost exact for models presented in panel (a) and (c). For the model presented in panel (b), the spin mapping formalism slightly outperforms the state-of-the-art γ -SQC

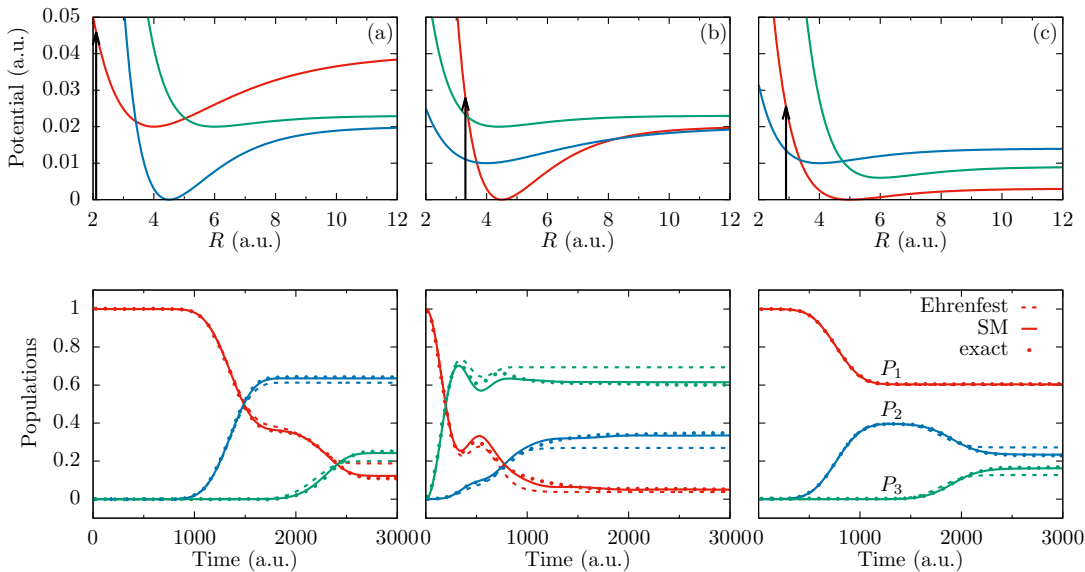


FIG. 5. Diabatic potential energy surfaces (top panels) and the population dynamics (bottom panels) for the three-state coupled Morse models (a) IA, (b) IB and (c) IC,. Details of the model are provided in the Supplementary Material Sec. VII. The vertical black arrows in top panels indicate the Franck-Condon vertical photo-excitations. State 1 (red), state 2 (blue) and state 3 (green) populations are calculated with the focused spin-mapping approach (solid lines), and compared with the Ehrenfest dynamics (dashed lines) as well as the exact results (dots).

approach,¹⁰² as well as the non-adiabatic ring polymer molecular dynamics approach.⁹³

IX. CONCLUSION

We present the rigorous analytical derivation of the non-adiabatic dynamics using the generators (generalized spin matrices) of the $\mathfrak{su}(N)$ Lie algebra, which was first introduced by Runeson and Richardson.^{35,46} Applying the S-W transform on the $SU(N)$ -based mapping Hamiltonian provides the continuous variables (generalized spin coherent states) that can be viewed as the angle variables on a multi-dimensional Bloch sphere (or so-called general Euler angles^{51,52}), hence establishing a mapping between discrete electronic states and continuous variables. The main advantage of the $SU(N)$ representation is that the corresponding S-W transform exactly preserves the identity operator in the N dimensional Hilbert space,⁴⁶ as opposed to the MMST formalism where the identity is not preserved through the mapping and there is an ambiguity of how to evaluate it.²² This is because the MMST representation has a larger size of Hilbert space (that contains other states outside the single excitation manifold of the mapping oscillators) compared to the original electronic subspace, which then requires a projection back to the single excitation subspace of the mapping oscillators to obtain accurate results. The $SU(N)$ representation, on the other hand, completely alleviates these problems and is the most nat-

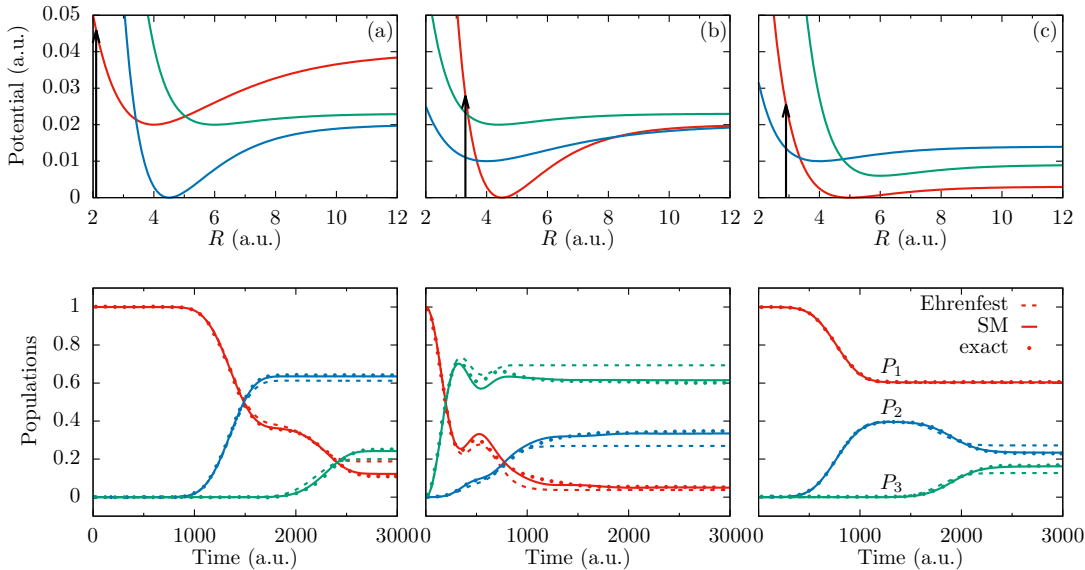


FIG. 5. Diabatic potential energy surfaces (top panels) and the population dynamics (bottom panels) for the three-state coupled Morse models (a) IA, (b) IB and (c) IC,. Details of the model are provided in the Supplementary Material Sec. VII. The vertical black arrows in top panels indicate the Franck-Condon vertical photo-excitations. State 1 (red), state 2 (blue) and state 3 (green) populations are calculated with the focused spin-mapping approach (solid lines), and compared with the Ehrenfest dynamics (dashed lines) as well as the exact results (dots).

ural way to map a N -level system into a classical phase space. More discussions can be found in Supplemental Material Sec. IX.

Using a mixed Wigner/S-W formalism, we derive a general expression of the time-correlation function, where the Wigner representation is used for the nuclear DOFs, and the S-W transform is applied to the generalized spin matrices associated to the electronic DOFs. We obtain the expression of the exact quantum Liouvillian in this formalism. Further making a linearization approximation, we obtain a set of EOMs that describe the coupled dynamics between the electronic and nuclear DOFs. We further connect EOMs with different mapping variables, including the spin coherence state variables, generalized Bloch spherical coordinates, as well as the MMST mapping variables. We formally establish the equivalence of these EOMs with different mapping variables. We also connect a variety of previously developed methods with the current formalism in the language of the $SU(N)$ mapping formalism. A detailed summary of the theoretical contribution of the current work can be found in Supplementary Material Sec. X.

Finally, we perform numerical simulations to assess the accuracy of the generalized spin mapping approach under the linearization approximation. We compute the population dynamics of systems with multiple electronic states coupled to the nuclear DOFs, including a 1D spin-boson model system, two conical intersection models, and an anharmonic three-state Morse model for photo-dissociation dynamics. The current formalism provides

an excellent agreement compared to the numerically exact results, and a significant improvement compared to the Ehrenfest dynamics or LSC-IVR which is based on the MMST mapping formalism.

Overall, the theoretical framework presented in this work provides a rigorous foundation to formally derive non-adiabatic quantum dynamics approaches with continuous mapping variables.

ACKNOWLEDGMENTS

This work was supported by the National Science Foundation CAREER Award under Grant No. CHE-1845747. Computing resources were provided by the Center for Integrated Research Computing (CIRC) at the University of Rochester. P.H. appreciates valuable discussions with W. H. Miller, especially for pointing out the connection with the earlier work in the spin mapping formalism. We would like to thank Braden M. Weight for valuable suggestions to the original manuscript. The authors want to express their gratitude to the valuable help from the journal editor for improving the quality of this work.

CONFLICT OF INTEREST

The authors have no conflicts to disclose.

SUPPLEMENTARY MATERIAL

See Supplementary Material for the Details of the Proofs in the structure constant derivations in Sec. I-II; Proof of the infinitesimal volume element of $\mathfrak{su}(N)$ in Sec. III; Proof of properties of the Stratonovich-Weyl transformation in Sec. IV; Proofs related to Θ_n in Sec. V; Details on the linearization of the Liouvillian in Sec. VI; Parameters of the model system presented in Sec. VII; Additional numerical results in Sec. VIII; Connection with previous methods in Sec. IX; Theoretical contribution of this work in Sec. X.

AVAILABILITY OF DATA

The data that support the findings of this study are available from the corresponding author upon a reasonable request.

Appendix A: Analytic expression of the structure constants

Despite the extensive usage and the crucial role these structure constants play in modern physics, to the best of our knowledge,¹⁰⁴ there is no analytic expression (closed formulas) of f_{ijk} and d_{ijk} . Here, we derive closed analytic

formulas for these structure constants without requiring any matrix multiplication or involving the generator expressions. Their analytic expressions are listed in Eq. A1 (for f_{ijk}) and Eq. A2 (for d_{ijk}). The detailed derivation is presented in Supplementary Material Sec. I-II.

All of the non-zero totally anti-symmetric structure constants are expressed as follows

$$\begin{aligned} f_{\alpha_{nm}\alpha_{kn}\beta_{km}} &= f_{\alpha_{nm}\alpha_{nk}\beta_{km}} = f_{\alpha_{nm}\alpha_{km}\beta_{kn}} = \frac{1}{2}, & (\text{A1}) \\ f_{\beta_{nm}\beta_{km}\beta_{kn}} &= \frac{1}{2}, \\ f_{\alpha_{nm}\beta_{nm}\gamma_m} &= -\sqrt{\frac{m-1}{2m}}, \quad f_{\alpha_{nm}\beta_{nm}\gamma_n} = \sqrt{\frac{n}{2(n-1)}}, \\ f_{\alpha_{nm}\beta_{nm}\gamma_k} &= \sqrt{\frac{1}{2k(k-1)}}, \quad m < k < n. \end{aligned}$$

All the non-zero totally symmetric structure constants as follows

$$\begin{aligned} d_{\alpha_{nm}\alpha_{kn}\alpha_{km}} &= d_{\alpha_{nm}\beta_{kn}\beta_{km}} = d_{\alpha_{nm}\beta_{mk}\beta_{nk}} = \frac{1}{2}, & (\text{A2}) \\ d_{\alpha_{nm}\beta_{nk}\beta_{km}} &= -\frac{1}{2}, \\ d_{\alpha_{nm}\alpha_{nm}\gamma_m} &= d_{\beta_{nm}\beta_{nm}\gamma_m} = -\sqrt{\frac{m-1}{2m}}, \\ d_{\alpha_{nm}\alpha_{nm}\gamma_k} &= d_{\beta_{nm}\beta_{nm}\gamma_k} = \sqrt{\frac{1}{2k(k-1)}}, \quad m < k < n, \\ d_{\alpha_{nm}\alpha_{nm}\gamma_n} &= d_{\beta_{nm}\beta_{nm}\gamma_n} = \frac{2-n}{\sqrt{2n(n-1)}}, \\ d_{\alpha_{nm}\alpha_{nm}\gamma_k} &= d_{\beta_{nm}\beta_{nm}\gamma_k} = \sqrt{\frac{2}{k(k-1)}}, \quad n < k, \\ d_{\gamma_n\gamma_k\gamma_k} &= \sqrt{\frac{2}{n(n-1)}}, \quad k < n, \\ d_{\gamma_n\gamma_n\gamma_n} &= (2-n)\sqrt{\frac{2}{n(n-1)}}. \end{aligned}$$

We hope that these expressions can be widely used for analytical and computational interest in Physics, as they are valid for any dimension N of the $\mathfrak{su}(N)$ Lie algebra without needing to explicitly compute the commutation and anti-commutation relations (through Eq. 9), which requires laborious effort of combining the $N^2 - 1$ different generators of $\mathfrak{su}(N)$.

Appendix B: Coherent state basis and expectation value of the spin operator

The expansion coefficients of the coherent state basis in the N -level diabatic basis are^{46,50}

$$\langle n|\Omega \rangle_N = \begin{cases} \langle n|\Omega \rangle_{N-1}, & 1 \leq n < N-1, \\ \langle N-1|\Omega \rangle_{N-1} \cos \frac{\theta_{N-1}}{2}, & n = N-1, \\ \langle N-1|\Omega \rangle_{N-1} \sin \frac{\theta_{N-1}}{2}, & n = N, \end{cases} \quad (\text{B1})$$

where $\langle 1|\Omega \rangle_1 = 1$, and for $N > 1$ the spin coherent states are defined recursively. This is equivalent to the expression in Eq. 18.

Using the definition of the spin coherent states presented here (or defined in Eq. 18), and the definition of the generators of $\mathfrak{su}(N)$ in Eqs. 2-4, we can derive a general expression of the expectation value of the spin operators. The expression of the expectation value of the symmetric spin operator is

$$\begin{aligned} \hbar\Omega_{\alpha_{nm}} &\equiv \langle \Omega | \hat{\mathcal{S}}_{\alpha_{nm}} | \Omega \rangle \\ &= \frac{\hbar}{2} \left(\cos \frac{\theta_m}{2} \prod_{j=1}^{m-1} e^{-i\varphi_j} \sin \frac{\theta_j}{2} \cos \frac{(1-\delta_{nN})\theta_n}{2} \prod_{k=1}^{n-1} e^{i\varphi_k} \right. \\ &\quad \times \sin \frac{\theta_k}{2} + \cos \frac{\theta_m}{2} \prod_{j=1}^{m-1} e^{i\varphi_j} \sin \frac{\theta_j}{2} \cos \frac{(1-\delta_{nN})\theta_n}{2} \\ &\quad \times \left. \prod_{k=1}^{n-1} e^{-i\varphi_k} \sin \frac{\theta_k}{2} \right) \\ &= \hbar \prod_{j=1}^{m-1} \sin^2 \frac{\theta_j}{2} \cos \frac{\theta_m}{2} \prod_{k=m}^{n-1} \sin \frac{\theta_k}{2} \cos \frac{(1-\delta_{nN})\theta_n}{2} \\ &\quad \times \cos \left(\sum_{l=m}^{n-1} \varphi_l \right), \end{aligned} \quad (\text{B2})$$

where $1 \leq m < n \leq N$. When $m = 1$, $\prod_{j=1}^{m-1} \sin^2 \frac{\theta_j}{2}$ is replaced by 1.

Similarly, for the anti-symmetric spin operator, we have

$$\begin{aligned} \hbar\Omega_{\beta_{nm}} &\equiv \langle \Omega | \hat{\mathcal{S}}_{\beta_{nm}} | \Omega \rangle \\ &= \hbar \prod_{j=1}^{m-1} \sin^2 \frac{\theta_j}{2} \cos \frac{\theta_m}{2} \prod_{k=m}^{n-1} \sin \frac{\theta_k}{2} \cos \frac{(1-\delta_{nN})\theta_n}{2} \\ &\quad \times \sin \left(\sum_{l=m}^{n-1} \varphi_l \right), \end{aligned} \quad (\text{B3})$$

and when $m = 1$, the term $\prod_{j=1}^{m-1} \sin^2 \frac{\theta_j}{2}$ is replaced by 1.

For the diagonal spin operator there is only one index

$1 < n \leq N$ and the expression is

$$\begin{aligned}\hbar\Omega_{\gamma_n} &\equiv \langle \boldsymbol{\Omega} | \hat{\mathcal{S}}_{\gamma_n} | \boldsymbol{\Omega} \rangle \\ &= \frac{\hbar}{\sqrt{2n(n-1)}} \left(\sum_{j=1}^{n-1} \cos^2 \frac{\theta_j}{2} \prod_{k=1}^{j-1} \sin^2 \frac{\theta_k}{2} \right. \\ &\quad \left. + (1-n) \cos^2 \frac{(1-\delta_{nN})\theta_n}{2} \prod_{j=1}^{n-1} \sin^2 \frac{\theta_j}{2} \right),\end{aligned}\quad (\text{B4})$$

where $\prod_{k=1}^{j-1} \sin^2 \frac{\theta_k}{2}$ is replaced by 1 when $n = 2$ (or $j = 1$).

Appendix C: Derivation of the conjugate relationship between φ and Θ

We begin with the proposed conjugate relation

$$r_{\bar{s}} \sum_{j=1}^N C_n(j) \frac{d}{dt} \Omega_{\gamma_j} = - \frac{\partial H_{\bar{s}}}{\partial \varphi_n} \quad (\text{C1a})$$

$$r_{\bar{s}} \frac{d}{dt} \varphi_n = \frac{\partial H_{\bar{s}}}{\partial \sum_{j=1}^N C_n(j) \Omega_{\gamma_j}}, \quad (\text{C1b})$$

and compute $-\frac{\partial H_{\bar{s}}}{\partial \varphi_n}$ (using Eq. B2 and Eq. B3) as follows

$$-\frac{\partial H_{\bar{s}}}{\partial \varphi_n} = r_{\bar{s}} \sum_{j=n+1}^N \sum_{k=1}^n (\mathcal{H}_{\alpha_{jk}} \Omega_{\beta_{jk}} - \mathcal{H}_{\beta_{jk}} \Omega_{\alpha_{jk}}), \quad (\text{C2})$$

and compare it to $r_{\bar{s}} \sum_{j=1}^N C_n(j) \frac{d}{dt} \Omega_{\gamma_j}$ (using Eq. 84) to determine the coefficients $C_n(j)$. We derived in Appendix A the closed formulas for the structure constants of $\mathfrak{su}(N)$ and hence can explicitly express the derivatives of Eq. 84 as

$$\begin{aligned}\frac{d}{dt} \Omega_{\gamma_j} &= \frac{1}{\hbar} \left[\sqrt{\frac{j}{2(j-1)}} \sum_{k=1}^j (\mathcal{H}_{\alpha_{jk}} \Omega_{\beta_{jk}} - \mathcal{H}_{\beta_{jk}} \Omega_{\alpha_{jk}}) \right. \\ &\quad - \sqrt{\frac{j-1}{2j}} \sum_{k=j+1}^N (\mathcal{H}_{\alpha_{kj}} \Omega_{\beta_{kj}} - \mathcal{H}_{\beta_{kj}} \Omega_{\alpha_{kj}}) \\ &\quad \left. + \sqrt{\frac{1}{2j(j-1)}} \sum_{k=j+1}^N \sum_{l=1}^{j-1} (\mathcal{H}_{\alpha_{kl}} \Omega_{\beta_{kl}} - \mathcal{H}_{\beta_{kl}} \Omega_{\alpha_{kl}}) \right].\end{aligned}\quad (\text{C3})$$

Starting from φ_n , $n = 1$, and solving iteratively Eq. C1a for every element $\mathcal{H}_{\alpha_{kl}} \Omega_{\beta_{kl}} - \mathcal{H}_{\beta_{kl}} \Omega_{\alpha_{kl}}$ (from $k = 2$, $l = 1$ and ascending) until deducing the expression of the coefficients $C_1(j)$, then using the same approach for $n > 1$, we obtain a formula that can be generalized, hence an expression for any coefficient

$$C_n(j \leq n) = 0; \quad C_n(j > n) = n \sqrt{\frac{2}{j(j-1)}}. \quad (\text{C4})$$

Further, the analytical expression of the time derivative of the symmetric generators is (we write $n + 1 \equiv k$ for convenience)

$$\begin{aligned} \frac{d}{dt}\Omega_{\alpha_{k,n}} = & \frac{1}{\hbar} \left[\sqrt{\frac{n-1}{2n}} (\mathcal{H}_{\gamma_n} \Omega_{\beta_{kn}} - \mathcal{H}_{\beta_{kn}} \Omega_{\gamma_n}) \right. \\ & - \sqrt{\frac{n+1}{2n}} (\mathcal{H}_{\gamma_k} \Omega_{\beta_{kn}} - \mathcal{H}_{\beta_{kn}} \Omega_{\gamma_k}) \\ & + \frac{1}{2} \sum_{j=1}^{n-1} (\mathcal{H}_{\beta_{nj}} \Omega_{\alpha_{kj}} - \mathcal{H}_{\alpha_{kj}} \Omega_{\beta_{nj}} - \mathcal{H}_{\alpha_{nj}} \Omega_{\beta_{kj}} + \mathcal{H}_{\beta_{kj}} \Omega_{\alpha_{nj}}) \\ & \left. + \frac{1}{2} \sum_{l=n+2}^N (\mathcal{H}_{\alpha_{ln}} \Omega_{\beta_{lk}} - \mathcal{H}_{\beta_{lk}} \Omega_{\alpha_{ln}} - \mathcal{H}_{\beta_{ln}} \Omega_{\alpha_{lk}} + \mathcal{H}_{\alpha_{lk}} \Omega_{\beta_{ln}}) \right] \end{aligned} \quad (\text{C5})$$

$$\dot{\Theta}_n = -\frac{\partial H_s}{\partial \varphi_n} = 2 \sum_{l=n+1}^N \sum_{m=1}^n V_{lm}(R) \sqrt{\left(\Theta_l - \Theta_{l-1} + \frac{r_s}{N}\right)} \sqrt{\left(\Theta_m - \Theta_{m-1} + \frac{r_s}{N}\right)} \cdot \sin \left(\sum_{k=m}^{l-1} \varphi_k \right), \quad (\text{C8a})$$

$$\dot{\varphi}_n = \frac{\partial H_s}{\partial \Theta_n} = V_{nn}(R) - V_{n+1,n+1}(R) \quad (\text{C8b})$$

$$+ \left[\sum_{m \neq n}^N V_{nm}(R) \sqrt{\frac{\Theta_m - \Theta_{m-1} + \frac{r_s}{N}}{\Theta_n - \Theta_{n-1} + \frac{r_s}{N}}} \cdot \cos \left(\sum_{k=\min\{m,n\}}^{\max\{m,n\}-1} \varphi_k \right) - \sum_{m \neq n+1}^N V_{nm}(R) \sqrt{\frac{\Theta_m - \Theta_{m-1} + \frac{r_s}{N}}{\Theta_{n+1} - \Theta_n + \frac{r_s}{N}}} \cdot \cos \left(\sum_{k=\min\{m,n+1\}}^{\max\{m-1,n\}} \varphi_k \right) \right],$$

where the nuclear DOFs obey Eq. 86a-86b. The two-state special case of the above EOMs are provided in Eq. F13.

Appendix D: Connections with the MMST Mapping Hamiltonian

Following the previous work of spin mapping,⁴⁶ we express the expansion coefficients $\langle n | \Omega \rangle$ in Eq. 17 (with

and the time derivative of anti-symmetric generators are

$$\begin{aligned} \frac{d}{dt}\Omega_{\beta_{kn}} &= \frac{1}{\hbar} \left[\sqrt{\frac{n+1}{2n}} (\mathcal{H}_{\gamma_k} \Omega_{\alpha_{kn}} - \mathcal{H}_{\alpha_{kn}} \Omega_{\gamma_k}) \right. \\ &\quad \left. - \sqrt{\frac{n-1}{2n}} (\mathcal{H}_{\gamma_n} \Omega_{\alpha_{kn}} - \mathcal{H}_{\alpha_{kn}} \Omega_{\gamma_n}) \right. \\ &\quad \left. + \frac{1}{2} \sum_{j=1}^{n-1} (\mathcal{H}_{\alpha_{nj}} \Omega_{\alpha_{kj}} - \mathcal{H}_{\alpha_{kj}} \Omega_{\alpha_{nj}} + \mathcal{H}_{\beta_{nj}} \Omega_{\beta_{kj}} - \mathcal{H}_{\beta_{kj}} \Omega_{\beta_{nj}}) \right. \\ &\quad \left. + \frac{1}{2} \sum_{l=n+2}^N (\mathcal{H}_{\alpha_{ln}} \Omega_{\alpha_{lk}} - \mathcal{H}_{\alpha_{lk}} \Omega_{\alpha_{ln}} + \mathcal{H}_{\beta_{ln}} \Omega_{\beta_{lk}} - \mathcal{H}_{\beta_{lk}} \Omega_{\beta_{ln}}) \right], \end{aligned} \quad (\text{C6})$$

where the elements of the sum are null when the conditions cannot be satisfied.

Using Eq. 62 and Eq. 64, the mapping Hamiltonian in Eq. 74 can be expressed as

$$\begin{aligned} H_s &= \mathcal{H}_0 \\ &+ \sum_{n=2}^N \sum_{m=1}^{n-1} \sqrt{\left(\Theta_n - \Theta_{n-1} + \frac{r_s}{N} \right) \left(\Theta_m - \Theta_{m-1} + \frac{r_s}{N} \right)} \\ &\quad \times \left(\mathcal{H}_{\alpha_{nm}} \cos \left(\sum_{k=m}^{n-1} \varphi_k \right) + \mathcal{H}_{\beta_{nm}} \sin \left(\sum_{k=m}^{n-1} \varphi_k \right) \right) \\ &+ \sum_{n=2}^N \mathcal{H}_{\gamma_n} \left(\sqrt{\frac{n}{2(n-1)}} \Theta_{n-1} - \sqrt{\frac{n-1}{2n}} \Theta_n \right). \end{aligned} \quad (\text{C7})$$

Under the special case of a purely real Hamiltonian ($\mathcal{H}_{\beta_{nm}} = 0$), the above mapping Hamiltonian is expressed as Eq. 91 of the main text.

Using the expression of H_s in Eq. 91, the Hamilton's EOMs in Eq. 90 can be expressed in details as follows

detailed expressions in Eq. 18) into its real and imaginary parts. To this end, we introduce a *constant global phase* variable $e^{i\Phi}$ to all of the coefficients $\langle n|\Omega \rangle$, with the range $\Phi \in (0, 2\pi)$, and define^{46,69}

$$c_n = \langle n|\Omega \rangle \cdot e^{i\Phi} = \frac{1}{\sqrt{2r_s}} (q_n + ip_n), \quad (\text{D1})$$

where we introduced $q_n/\sqrt{2r_s}$ as the real part of c_n and $p_n/\sqrt{2r_s}$ as the imaginary part of c_n . This phase $e^{i\Phi}$ is a

In fact, the virtue of writing each c_n with a coordinate and a momentum had long been proposed in Appendix B of J. Chem. Phys. 145, 204105 (2016).

$$c_n(t) = x^{(n)}(t) + ip^{(n)}(t), \quad (\text{B2})$$

The importance of global phase in SU(F) Stratonovich phase space was already stressed in Appendix 3 of WIREs. Comput. Mol. Sci. e1619 (2022)(submitted on February 5, 2022, released on arXiv on May 8, 2022 and officially published on May 13,2022), while completely absent in first version of this manuscript (online on May 20, 2022) and abruptly involved here (online on July 29, 2022). The eq (D1) here was different with the corresponding eq (44) in previous version:

$$c_n = \langle n|\Omega \rangle = \frac{1}{\sqrt{2r_s}} (q_n + ip_n), \quad (\text{44})$$

where the global phase was not appeared. The authors plagiarized key ideas in WIREs. Comput. Mol. Sci. e1619 (2022) (submitted on February 5, 2022, revised on April 8, 2022, accepted on April 11, 2022, released on arXiv on May 8, 2022 and officially published on May 13, 2022), where we clearly pointed out the importance of an evolving global phase. The eq (S54) of WIREs. Comput. Mol. Sci. e1619 (2022) read,

$$\begin{pmatrix} x^{(n)} \\ p^{(n)} \end{pmatrix} = \sqrt{2\lambda} \begin{pmatrix} \cos\psi & -\sin\psi \\ \sin\psi & \cos\psi \end{pmatrix} \begin{pmatrix} \text{Re}\langle n|\theta, \phi \rangle \\ \text{Im}\langle n|\theta, \phi \rangle \end{pmatrix}, \quad \text{S54}$$

where the global phase had been involved. Moreover, a constant global phase still could not lead to correct form of canonical Hamilton's equations of motion in Meyer-Miller variables.

constant. The transformation in Eq. D1 provides the connection between a given pair of q_n and p_n and the angle variables of the generalized spin coherent states $\{\theta_n, \varphi_n\}$ through Eq. 18. Because we want to convert $2N - 2$ real independent variables of $\{\theta_n, \varphi_n\}$ into $2N$ variables $\{q_n, p_n\}$ that are subjects to a total population constraint (see Eq. D11 or Eq. D12), we need to introduce one more independent variable $e^{i\Phi}$ to define $\{q_n, p_n\}$. Further, this phase is necessary to introduce q_1 and p_1 variables, because $\langle 1|\Omega \rangle = \cos \frac{\theta_1}{2}$ in Eq. 18 is purely real.¹⁰⁵

Using the coefficients defined in Eq. D1, the expectation value of the spin operator (Eq. 23) is expressed as

$$\begin{aligned} \hbar\Omega_k &= \langle \Omega | \hat{S}_k | \Omega \rangle = \sum_{n,m} e^{-i\Phi} \cdot \langle \Omega | n \rangle \langle n | \hat{S}_k | m \rangle \langle m | \Omega \rangle \cdot e^{i\Phi} \\ &= \sum_{n,m} \langle n | \hat{S}_k | m \rangle \cdot c_n^* c_m, \end{aligned} \quad (\text{D2})$$

which is commonly referred to as the components of the generalized Bloch vector in $N^2 - 1$ dimensions.^{37,39,40} Note that the global phase cancels in any physical expectation values, such that it is not *explicitly* present in $\hbar\Omega_k$. Using the transform defined in Eq. D1, Eq. D2 becomes

$$2r_s\Omega_k = \sum_{n,m} \langle n | \hat{S}_k | m \rangle \cdot (q_n - ip_n)(q_m + ip_m). \quad (\text{D3})$$

Explicitly using the matrix elements of $\langle n | \hat{S}_k | m \rangle$ (see Eqs. 2-4), Eq. D3 becomes

$$2r_s\Omega_{\alpha_{nm}} = q_n q_m + p_n p_m, \quad (\text{D4a})$$

$$2r_s\Omega_{\beta_{nm}} = p_n q_m - q_n p_m, \quad (\text{D4b})$$

$$2r_s\Omega_{\gamma_n} = \frac{1}{\sqrt{2n(n-1)}} \left(\sum_{l=1}^{n-1} q_l^2 + p_l^2 - (n-1)(q_n^2 + p_n^2) \right). \quad (\text{D4c})$$

Note that this transformation *does depend on the choice* of r_s , which must match the index in the mapped Hamiltonian that evolves the dynamics (see Sec. IV).

For a purely real Hamiltonian (such that in Eq. 12b $\mathcal{H}_{\beta_{nm}} = 0$), using the transform defined in Eq. D4, the spin mapping Hamiltonian $[\hat{H}(\hat{R})]_s$ in Eq. 43 can be expressed as the well-known MMST mapping Hamiltonian^{7,8,10}

$$\begin{aligned} \mathcal{H} &= \mathcal{H}_0(\hat{R}) + \sum_n \frac{1}{2} [V_{nn}(\hat{R}) - \bar{V}(\hat{R})](q_n^2 + p_n^2 - \gamma) \quad (\text{D5}) \\ &\quad + \sum_{n < m} V_{nm}(\hat{R})(q_n q_m + p_n p_m), \end{aligned}$$

where $\bar{V}(\hat{R}) = \frac{1}{N} \sum_l V_{ll}(\hat{R})$, $\mathcal{H}_0(\hat{R}) = \frac{\hat{P}^2}{2m} + U_0(\hat{R}) + \bar{V}(\hat{R})$ is the trace part of the potential, which is naturally separated from the traceless part. Previous work by Runeson and Richardson⁴⁶ have already shown this connection using the transform expressed in Eq. D1. Note that the

Some statements by Huo and coworkers in Ref. 105 were incorrect. Please refer to our discussions around Ref. 105 in the end of this file.

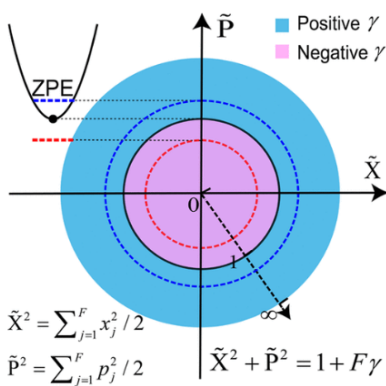
This was repeating of J. Phys. Chem. Lett. 12, 2496 (2021)(submitted on January 22, 2021 and published online on March 5, 2021). We had already wrote,

$$\mathcal{S}(\mathbf{x}, \mathbf{p}): \sum_{n=1}^F \left[\frac{1}{2}((x^{(n)})^2 + (p^{(n)})^2) \right] = 1 + F\gamma \quad (4)$$

Although we use the diabatic representation to reach eq 4, the constraint holds in the adiabatic representation as well. The constraint (eq 4) has already been implied in eqs 43 and 44 of ref 17, and used in ref 15 where $\gamma = 0$ is considered. The physical meaning of eq 4 requires only $\gamma > -1/F$. This confirms that negative values for the ZPE parameter, γ , are possible!

The full continuous parameter range, not only the so-called "negative values", should be cited!

And also, the intuitive picture had been already drawn on the FIRST page of [J. Phys. Chem. Lett. 12, 2496 (2021)], illustrating clearly that the square of radius is proportional to $1+F\gamma$. The statement "the constraint of the radius leads to corresponding constraint of ZPE parameter" was never a new idea, as both the radius and ZPE parameter were altogether given out in [J. Phys. Chem. Lett. 12, 2496 (2021)]. The illustration on first page:



Comments: CMM never applies oscillators in mapping, and (x, p) play the role as phase space variables other than quantum operators. CMM is a phase space mapping other than oscillator mapping (though we use oscillator's zero-point energy to illustrate the parameter gamma!). It was just a misunderstanding of authors by themselves.

MMST form of the mapping Hamiltonian does not explicitly contain the global phase $e^{i\Phi}$ (introduced in Eq. D1), due to the cancellation of this phase.

Further, in Eq. D5, the parameter γ is expressed⁴⁶ as follows

$$\gamma = \frac{2}{N}(r_s - 1), \quad (D6)$$

or equivalently, $r_s = 1 + N\gamma/2$. In the MMST mapping formalism, this parameter is viewed as the zero-point energy (ZPE) parameter of the mapping oscillators.^{23,46,97,102,106,107} In the $SU(N)$ mapping formalism, it is the parameter related to the choice of r_s . Nevertheless, Eq. D6, which was first derived in Ref. 46, helps to establish the connection between the boundaries on the S-W radius and the boundaries on the γ parameter in the MMST mapping. The constraint of the radius $r_s \in (0, \infty)$ leads to a corresponding constraint for the ZPE parameter, $\gamma \in (-\frac{2}{N}, \infty)$. The negative values of the ZPE parameter has been proposed in the MMST framework,¹⁰⁷ and simply correspond to $r_s \leq r_Q = 1$. In our own opinion, it might be more intuitive to understand the choice of radius of Bloch sphere⁴⁶ (that should be larger than 0) rather than the negative ZPE of quantum mapping oscillators.¹⁰⁷

Using the conjugate variables $\{q_n, p_n\}$ defined in Eq. 47, the S-W kernel in Eq. 27 can also be equivalently expressed in the diabatic electronic basis as follows

$$\begin{aligned} \hat{w}_s &= \frac{1 - r_s}{N} \hat{\mathcal{I}} + r_s \sum_{a,b} c_a c_b^* |a\rangle \langle b| \\ &= \frac{1 - r_s}{N} \hat{\mathcal{I}} + \frac{1}{2} \sum_{a,b} (q_a + ip_a)(q_b - ip_b) |a\rangle \langle b| \\ &= \frac{1}{2} \sum_{a,b} [(q_a + ip_a)(q_b - ip_b) - \gamma \delta_{ab}] |a\rangle \langle b|, \end{aligned} \quad (D7)$$

where we have used $r_s = N\gamma/2 + 1$. The kernel in Eq. D7 is identical to the one expressed in Eq. 7 of Ref. 107, which is derived in the extended classical mapping model (eCMM).^{25,107}

Using the S-W kernel expressed in Eq. D7, the S-W transform (Eq. 25) of operator $|n\rangle \langle m|$ is

$$\begin{aligned} [|n\rangle \langle m|]_s &= \frac{1 - r_s}{N} \delta_{nm} + \frac{1}{2} (q_m + ip_m)(q_n - ip_n) \\ &= -\frac{\gamma}{2} \delta_{nm} + \frac{1}{2} (q_m + ip_m)(q_n - ip_n). \end{aligned} \quad (D8)$$

The same result can also be obtained by performing the transform defined in Eq. D4 directly on Eq. 44 and Eq. 45. For the diagonal projection operators ($n = m$), Eq. D8 becomes

$$[|n\rangle \langle n|]_s = \frac{1}{2} (q_n^2 + p_n^2 - \gamma). \quad (D9)$$

Similar to Eq. D8, for the complementary index \bar{s} , the expression $[|n\rangle \langle n|]_{\bar{s}} = \text{Tr}_e[|n\rangle \langle n| \hat{w}_{\bar{s}}]$ (using the kernel in

Eq. D7 with r_s) is

$$\begin{aligned} [|\langle n \rangle \langle n |]_s &= \frac{1 - r_s}{N} + \frac{1}{2} \cdot \frac{r_s}{r_s} (q_n^2 + p_n^2) = \frac{1}{2} \left[\frac{r_s}{r_s} (q_n^2 + p_n^2) - \gamma_s \right] \\ &= \frac{N+1}{2(1+\frac{N\gamma}{2})^2} \cdot (q_n^2 + p_n^2) - \frac{1 - \frac{\gamma}{2}}{1 + \frac{N\gamma}{2}}, \quad (\text{D10}) \end{aligned}$$

where we define $\gamma = \frac{2}{N}(r_s - 1)$ in the second equality, and used $r_s/r_s = (N+1)/r_s^2 = (N+1)/(\frac{N\gamma}{2} + 1)^2$ and $r_s = (N+1)/(\frac{N\gamma}{2} + 1)$ based on Eq. D6 and Eq. 38 for the third equality. Thus, the estimators (Eq. D9 and Eq. D10) used in the Spin-LSC⁴⁶ are identical to those used in the eCMM¹⁰⁷ approach (second line of Eq. D10).

In the $SU(N)$ mapping formalism, the total population constraint on the $2N$ -dimensional phase space comes *naturally from the normalization* of the generalized spin coherent states^{69,108} as follows

$$\langle \Omega | \Omega \rangle = \sum_n c_n^* c_n = \frac{1}{2r_s} \sum_{n=1}^N (q_n^2 + p_n^2) = 1, \quad (\text{D11})$$

which properly enforces the total electronic diabatic population to be one (see Eq. D6) for these MMST mapping variables

$$\sum_{n=1}^N \frac{1}{2} (q_n^2 + p_n^2 - \gamma) = 1. \quad (\text{D12})$$

Alternatively, one can obtain this condition from the basic property of the S-W transform that preserves the trace of the electronic identity operator (Eq. 30) as follows

$$[\hat{I}]_s = \sum_{n=1}^N [|\langle n \rangle \langle n |]_s = 1 - r_s + \sum_n \frac{1}{2} (q_n^2 + p_n^2) = 1.$$

Note that the recent work of the eCMM is developed based on *manually adding* an extra total population constraint (as described in Eq. D12) on the MMST mapping oscillator phase space. Historically, it was realized¹⁰⁸ that a mapping from the quantum Schrödinger's equation to $2N$ classical phase space Hamilton's EOMs is incorrect, unless a total population constraints is applied.¹⁰⁸ In the $SU(N)$ framework, on the other hand, the total population constraint is *naturally* satisfied through the S-W transform, without the necessity to introduce it as an additional constraint. Nevertheless, the eCMM approach derives equivalent kernel as the S-W kernel in Eq. D7 (hence also equivalent estimators in Eq. D9 and Eq. D10) from a seemingly different procedure that applies population constraint on the MMST mapping oscillator phase space.¹⁰⁷ The mathematical reason behind the equivalence of two kernels is: using the additional population constraint, the $2N$ -dimensional MMST phase space of $\{q_n, p_n\}$ is reduced to a complex projective (CP) space, mathematically denoted⁶⁹ as $CP(N-1)$, which is in fact a subspace¹⁰⁸ of the parameterized manifold of $SU(N)$.

Comment: It had been clarified in [J. Chem. Phys., 151, 024105 (2019)] the constraint is naturally from the normalization of electronic DOFs:

The conservation of the total population Eq. (16) is implicitly used for the kinetic energy term in Eq. (23). (This is a new observation that is essentially the key point of this paper.) The classical

Here, the trace over the electronic DOFs is replaced by an integral over the mapping phase space (x, p_x, y, p_y) with the constraint that the total population is 1. That is,

$$\sum_{n=1}^F P_n(0) = 1 \text{ and } 0 \leq P_n(0) \leq 1 \quad (\forall n). \quad (28)$$

This physical constraint is consistent with the implicit employment of Eq. (16) (the conservation of the total population) in deriving

And the one-to-one mapping connection between "I" and 1 had also clarified in [J. Phys. Chem. Lett. 12, 2496 (2021)].

Supporting Information. As expected, the kernel and its inverse are properly normalized

$$\begin{aligned} \text{Tr}_e[\hat{K}(x, p)] &= \text{Tr}_e[\hat{K}^{-1}(x, p)] = 1 \\ \int_{S(x,p)} d\mu(x, p) \hat{K}(x, p) &= \int_{S(x,p)} d\mu(x, p) \hat{K}^{-1}(x, p) = \hat{I}_e \end{aligned} \quad (9)$$

Authors presented nothing beyond but just attributed our first ideas as theirs.

In fact, in CMM framework the dynamics is intrinsically exact for electronic DOFs, as the constraint eq (D12) comes from the mapping property of the identity operator, and is strictly protected by the Meyer-Miller Hamiltonian, thus always holds during the corresponding dynamics. Thus, this statement in this manuscript is totally WRONG!

Using Eq. D8 and the Hamiltonian in Eq. 1, one can also directly obtain the mapping Hamiltonian expression

$$\begin{aligned} [\hat{H}(\hat{R})]_s = & \hat{T}_R + U_0(\hat{R}) + \sum_n \frac{1}{2} V_{nn}(\hat{R})(q_n^2 + p_n^2 - \gamma) \\ & + \sum_{n < m} V_{nm}(\hat{R})(q_n q_m + p_n p_m), \end{aligned} \quad (\text{D13})$$

which is indeed equivalent to Eq. 48 due to the constraint on the total population in Eq. D12. Despite the similar expression of $[\hat{H}(\hat{R})]_s$ compared to the seminal MMST mapping Hamiltonian,^{8–10} the $SU(N)$ mapping formalism should be viewed as a different mapping procedure compared to the MMST mapping formalism.

Historically, the MMST mapping Hamiltonian (Eq. 48) is established through the Stock-Thoss mapping procedure^{8,10} by representing the N -level system with N harmonic oscillators' singly excited states

$$|n\rangle \rightarrow |0_1, \dots, 1_n, \dots, 0_N\rangle = \hat{a}_n^\dagger |0_1, \dots, 0_n, \dots, 0_N\rangle, \quad (\text{D14})$$

where $\hat{a}_n^\dagger = \frac{1}{\sqrt{2}}(\hat{q}_n - i\hat{p}_n)$, $\hat{a}_n = \frac{1}{\sqrt{2}}(\hat{q}_n + i\hat{p}_n)$ are harmonic oscillator's raising and lowering operators, and the commutator $[\hat{q}_n, \hat{p}_m] = i\delta_{nm}$ is valid in the complete Hilbert space of the mapping oscillator. This can be viewed as a generalized Schwinger's bosonization approach.¹⁰ Using the mapping relation

$$\sum_{nm} V_{nm}(\hat{R}) |n\rangle \langle m| \rightarrow \sum_{nm} V_{nm}(\hat{R}) \hat{a}_n^\dagger \hat{a}_m, \quad (\text{D15})$$

the Stock-Thoss mapping Hamiltonian is expressed as

$$\begin{aligned} \hat{H}_{\text{MMST}} = & \hat{T}_R + U_0(\hat{R}) + \sum_n \frac{1}{2} V_{nn}(\hat{R})(\hat{q}_n^2 + \hat{p}_n^2 - 1) \\ & + \sum_{n < m} V_{nm}(\hat{R})(\hat{q}_n \hat{q}_m + \hat{p}_n \hat{p}_m), \end{aligned} \quad (\text{D16})$$

when $V_{nm}(\hat{R})$ is purely real. This argument leads to the ZPE parameter $\gamma = 1$, and without the constraint provided in Eq. D12, even though $\sum_{n=1}^N \frac{1}{2}(q_n^2 + p_n^2 - \gamma)$ is a constant of motion. Most of the existing mapping approaches are based upon this mapping procedure,^{11,14} or a modified one that constraint the operators within the SEO subspace. One can further downgrade these mapping operators into classical variables, for example, using the Wigner transform through the mixed quantum-classical approximation,¹⁰⁹ linearization approximation,^{11,86} or the Husimi representation (coherent state basis) for these mapping variables through the semi-classical approximation^{8,10,12,13,77,110} or the partial linearization approximation.^{15,16,111,112}

The MMST mapping formalism should be viewed as a fundamentally different mapping procedure compared to the $SU(N)$ formalism. This is because that the MMST mapping operators \hat{a}_n^\dagger and \hat{a}_n (or \hat{q}_n , \hat{p}_n) live in a *larger* Hilbert space than the electronic Hilbert space of the original Hamiltonian.^{10,20,21} Truncating the larger

Hilbert space to include only SEO subspace²⁴ ruins the simple commutation relation between \hat{p}_n and \hat{q}_n , such that $[\hat{q}_n, \hat{p}_n] \neq i$ in the truncated Hilbert space.^{24,113} A detailed expression of $[\hat{q}_n, \hat{p}_n]$ in the truncated SEO mapping space can be found in Eq. 17 of Ref. 114. Thus, when applying truncation of the mapping Hilbert space (such as done for the mapping formalism in Ref. 24), this additional commutator $[\hat{q}_n, \hat{p}_n]$ need to be explicitly included to replace $\gamma = 1$ in \hat{H}_{MMST} Hamiltonian (Eq. D16), and is required to be evaluated through additional approximations.²⁵

As opposed to the Stock-Thoss mapping procedure, the starting point of the $SU(N)$ mapping formalism is completely different. The $SU(N)$ mapping formalism uses the generators of the $\mathfrak{su}(N)$ Lie algebra which exactly preserves the commutation relations among operators as well as the original electronic Hilbert space. As a result, there is no need for additional Hilbert space projection nor truncation that ruins the simple commutation relations of mapping operators^{24,25} (see Supplementary Materials Sec. IX for detailed discussions) or necessity of projecting back to the subspace as required by MMST formalism.^{20,21} The exact quantum Liouvillian from the current $SU(N)$ mapping formalism (see Sec. V) is also different than the exact Liouvillian of the MMST formalism.^{74,81,82}

Appendix E: Equations of Motion with the Generalized Euler Angles

Similarly, one can formulate the EOMs in terms of the generalized Euler angles $\{\theta_n, \varphi_n\}$. The EOMs with these variables are a bit more complicated and non-linear in terms of $\{\theta_n, \varphi_n\}$, as oppose to the case of $\{\Theta_n, \varphi_n\}$. This is because θ_n is not the conjugate variable of φ_n , but Θ_n is. To this end, we express the EOMs in Eq. 90 in terms of $\{\Omega_k\}$, which in turn depends on $\{\theta_n, \varphi_n\}$ (see Eq. B2-Eq. B4). To obtain $\partial H_s / \partial \varphi_n$, we use the expression of H_s in Eq. 74 and explicitly take the derivative with respect to φ_n . Note that only $\Omega_{\alpha_{jk}}$ and $\Omega_{\beta_{jk}}$ contain φ_n , whereas Ω_{γ_k} only contains $\{\theta_j\}$. Using the detailed expressions of $\Omega_{\alpha_{jk}}$ (Eq. B2) and $\Omega_{\beta_{jk}}$ (Eq. B3), we have

$$-\frac{\partial H_s}{\partial \varphi_n} = r_s \sum_{j=n+1}^N \sum_{k=1}^n (\mathcal{H}_{\alpha_{jk}} \Omega_{\beta_{jk}} - \mathcal{H}_{\beta_{jk}} \Omega_{\alpha_{jk}}). \quad (\text{E1})$$

To obtain the time derivative of φ_n , we try to¹¹⁵ find an expression in terms of the generators that have a well defined time derivative in Eq. 84. From the expressions of $\Omega_{\alpha_{nm}}$ (Eq. B2) and $\Omega_{\beta_{nm}}$ (Eq. B3), we know that

$$\tan \varphi_n = \frac{\Omega_{\beta_{n+1,n}}}{\Omega_{\alpha_{n+1,n}}}, \quad (\text{E2})$$

which leads to the expression of the time derivative of φ_n

as

$$\begin{aligned}\dot{\varphi}_n &= \frac{d}{dt} \left(\arctan \frac{\Omega_{\beta_{n+1,n}}}{\Omega_{\alpha_{n+1,n}}} \right) \\ &= \frac{\dot{\Omega}_{\beta_{n+1,n}} \Omega_{\alpha_{n+1,n}} - \Omega_{\beta_{n+1,n}} \dot{\Omega}_{\alpha_{n+1,n}}}{\Omega_{\alpha_{n+1,n}}^2 + \Omega_{\beta_{n+1,n}}^2}.\end{aligned}\quad (\text{E3})$$

Using the analytical expressions of the $\mathfrak{su}(N)$ structure constants (Appendix A), we can obtain the closed analytic expression of $\dot{\Omega}_{\alpha_{n+1,n}}$ (Eq. C5) and $\dot{\Omega}_{\beta_{n+1,n}}$ (Eq. C6). Thus, using the transform between $\{\Omega\}$ and $\{\varphi_n, \Theta_n\}$ as follows

$$\Theta_n = n \cdot r_s \sum_{j=n+1}^N \sqrt{\frac{2}{j(j-1)}} \Omega_{\gamma_j}, \quad (\text{E4a})$$

$$\varphi_n = \tan^{-1} \frac{\Omega_{\beta_{n+1,n}}}{\Omega_{\alpha_{n+1,n}}}, \quad (\text{E4b})$$

the EOMs in Eq. 90 (which is equivalent to Eq. 86) are expressed with the conjugate variables $\{\Theta_n, \varphi_n\}$ as

$$\dot{\Theta}_n = -\frac{\partial H_s}{\partial \varphi_n} = r_s \sum_{j=n+1}^N \sum_{k=1}^n (\mathcal{H}_{\alpha_{jk}} \Omega_{\beta_{jk}} - \mathcal{H}_{\beta_{jk}} \Omega_{\alpha_{jk}}) \quad (\text{E5a})$$

$$\dot{\varphi}_n = \frac{\partial H_s}{\partial \Theta_n} = \frac{\dot{\Omega}_{\beta_{n+1,n}} \Omega_{\alpha_{n+1,n}} - \Omega_{\beta_{n+1,n}} \dot{\Omega}_{\alpha_{n+1,n}}}{\Omega_{\alpha_{n+1,n}}^2 + \Omega_{\beta_{n+1,n}}^2}, \quad (\text{E5b})$$

where H_s is expressed in Eq. 74, and the nuclear DOFs obeys Eq. 86a-Eq. 86b.

Further, one can also express the EOMs in Eq. 90 directly in terms of the generalized Euler angles $\{\theta_n, \varphi_n\}$, without using the conjugated variables $\{\Theta_n, \varphi_n\}$. To this end, we use the expression of $\Theta_n(\{\theta_k\})$ in Eq. 61 and directly work out its time derivative (through the chain rule with θ_n) as follows

$$\dot{\Theta}_n = -\frac{\partial H_s}{\partial \varphi_n} = -\sum_{j=1}^n r_s \dot{\theta}_j \frac{\sin \theta_j}{2} \prod_{\substack{k=1 \\ k \neq j}}^n \sin^2 \frac{\theta_k}{2}. \quad (\text{E6})$$

The above equation can be expressed as an equivalent but recursive expression as follows

$$-\frac{\partial H_s}{\partial \varphi_n} = -\frac{\partial H_s}{\partial \varphi_{n-1}} \sin^2 \frac{\theta_n}{2} - r_s \dot{\theta}_n \frac{\sin \theta_n}{2} \prod_{j=1}^{n-1} \sin^2 \frac{\theta_j}{2}. \quad (\text{E7})$$

The above equation gives a numerically efficient recursive expression of $\dot{\theta}_n$ as follows

$$\dot{\theta}_n = \left(\frac{\partial H_s}{\partial \varphi_n} \frac{2}{\sin \theta_n} - \frac{\partial H_s}{\partial \varphi_{n-1}} \tan \frac{\theta_n}{2} \right) / \left(r_s \prod_{j=1}^{n-1} \sin^2 \frac{\theta_j}{2} \right), \quad (\text{E8})$$

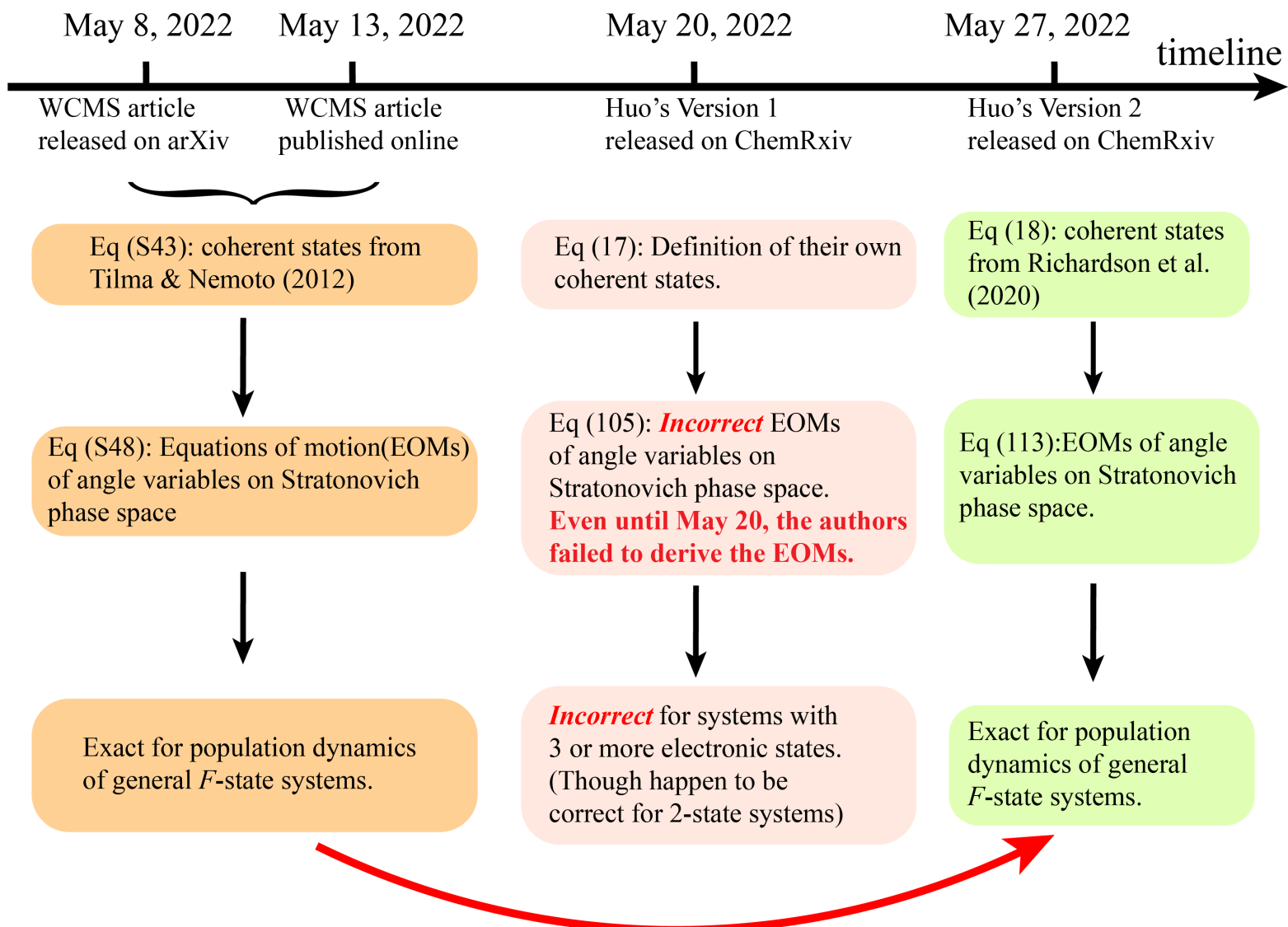
where for $n = 1$ the denominator is replaced by r_s because there is no θ_0 variable and the numerator only has the term that includes $\frac{\partial H_s}{\partial \varphi_n}$ as there is no φ_{n-1} .

Thus, the EOMs in Eq. 86 can be expressed with the generalized Euler angles $\{\theta_n, \varphi_n\}$ as

$$\dot{\theta}_n = \left(\frac{\partial H_s}{\partial \varphi_n} \frac{2}{\sin \theta_n} - \frac{\partial H_s}{\partial \varphi_{n-1}} \tan \frac{\theta_n}{2} \right) / \left(r_s \prod_{j=1}^{n-1} \sin^2 \frac{\theta_j}{2} \right), \quad (\text{E9a})$$

$$\dot{\varphi}_n = \frac{\dot{\Omega}_{\beta_{n+1,n}} \Omega_{\alpha_{n+1,n}} - \Omega_{\beta_{n+1,n}} \dot{\Omega}_{\alpha_{n+1,n}}}{\Omega_{\alpha_{n+1,n}}^2 + \Omega_{\beta_{n+1,n}}^2}, \quad (\text{E9b})$$

Timeline of the Equations of Motion on SU(F) Stratonovich Phase Space



Plagiarized the ideas from the WCMS article after it was released nearly 3 weeks.

See details in Evidence #6 of evidence.pdf.

where the nuclear DOFs obeys Eq. 86a-Eq. 86b. To solve Eq. E9b, one can use the expressions of $\dot{\Omega}_{\alpha_{n+1,n}}$ and $\dot{\Omega}_{\beta_{n+1,n}}$ in Eq. C5 and Eq. C6, respectively, which are only functions of Ω_k (Eq. B2-Eq. B4) that depends on $\{\theta_n, \varphi_n\}$. For a two-level system, it is straightforward to show that Eqs. E8-E3 reduce back to Eqs. F9a-F9b, which are the EOMs for the $SU(2)$ mapping formalism derived in the previous work of spin mapping non-adiabatic ring polymer molecular dynamics.³⁶

One can evolve each Θ_n , or equivalently θ_n by using the chain rule in Eq. E6, and φ_n using a velocity Verlet algorithm ($\{\Theta_n\}$ being the *generalized conjugate momenta* of $\{\varphi_n\}$), which does not require using the derivative of the potential.

Appendix F: Mapping of Two-Level Systems under the $SU(2)$ Representation

For a two-level system $\hat{H} = \frac{\hat{P}^2}{2M}\hat{\mathcal{I}} + U_0(\hat{R})\hat{\mathcal{I}} + \hat{V}_e(\hat{R})$ where $\hat{\mathcal{I}}$ is the 2×2 identity matrix, and

$$\hat{V}_e(\hat{R}) = \begin{pmatrix} V_{11}(\hat{R}) & V_{12}(\hat{R}) \\ V_{21}(\hat{R}) & V_{22}(\hat{R}) \end{pmatrix}. \quad (\text{F1})$$

For this special case, $f_{ijk} = \varepsilon_{ijk}$ and $d_{ijk} = 0$, all of the equations in the main text remain general. Nevertheless, it will be beneficial to explicitly give several key equations under this special limit, whereas more detailed discussion of the $SU(2)$ can be found in the previous work of Spin-LSC³⁵ as well as in spin-mapping non-adiabatic RPMD (SM-NRPMD).³⁶

Using the $SU(2)$ representation, one can express the original two-states Hamiltonian as follows³⁵

$$\hat{H} = \mathcal{H}_0\hat{\mathcal{I}} + \frac{1}{\hbar}\mathbf{H}\cdot\hat{\mathbf{S}} = H_0\hat{\mathcal{I}} + \frac{1}{\hbar}(\mathcal{H}_x\cdot\hat{\mathcal{S}}_x + \mathcal{H}_y\cdot\hat{\mathcal{S}}_y + \mathcal{H}_z\cdot\hat{\mathcal{S}}_z), \quad (\text{F2})$$

where $\hat{S}_i = \frac{\hbar}{2}\hat{\sigma}_i$ (for $i \in \{x, y, z\}$) is the quantum spin operator, with $\hat{\sigma}_i$ as the Pauli matrices expressed in Eq. 2, and $\mathcal{H}_0 = \frac{\hat{P}^2}{2m} + U_0(\hat{R}) + \frac{1}{2}(V_{11}(\hat{R}) + V_{22}(\hat{R}))$, $\mathcal{H}_x = 2\text{Re}(V_{12}(\hat{R}))$, $\mathcal{H}_y = 2\text{Im}(V_{12}(\hat{R}))$, $\mathcal{H}_z = V_{11}(\hat{R}) - V_{22}(\hat{R})$, which are the $N = 2$ limit of Eq. 12. This Hamiltonian was first introduced by Meyer and Miller (Eq. 2.4-2.6 in Ref. 7), and later by Thoss and Stock¹⁰ as well as by Runeson and Richardson.³⁵

Using the spin coherent state for $N = 2$ (Eq. 16), the expectation value of the spin operator is

$$\hbar\Omega_i(\mathbf{u}) = \langle \mathbf{u} | \hat{S}_i | \mathbf{u} \rangle = \frac{\hbar}{2} u_i, \quad i \in \{x, y, z\}, \quad (\text{F3})$$

where $u_x = \sin \theta \cos \varphi$, $u_y = \sin \theta \sin \varphi$, $u_z = \cos \theta$ as the special case of Eqs. B2-B4. The identity in Eq. 20 becomes $\hat{\mathcal{I}} = \int d\mathbf{u} |\mathbf{u}\rangle\langle\mathbf{u}|$, where $\int d\mathbf{u} = \frac{1}{2\pi} \int_0^\pi d\theta \sin \theta \int_0^{2\pi} d\varphi$ is the $N = 2$ limit of Eq. 21.

Under the $\mathfrak{su}(2)$ Lie algebra, the S-W kernel in Eq. 26 becomes

$$\hat{w}_s = \frac{1}{2} \hat{\mathcal{I}} + r_s \boldsymbol{\Omega} \cdot \hat{\boldsymbol{\sigma}}, \quad (\text{F4})$$

where $\boldsymbol{\Omega} \cdot \hat{\boldsymbol{\sigma}} = \Omega_x \cdot \hat{\sigma}_x + \Omega_y \cdot \hat{\sigma}_y + \Omega_z \cdot \hat{\sigma}_z$. Note that the r_s used in this paper is twice the one defined in the previous work,^{35,36} (see the factor between $\boldsymbol{\Omega}$ and \mathbf{u} in Eq. F3).

The S-W transform of the Hamiltonian becomes

$$\begin{aligned} [\hat{H}]_s(\boldsymbol{\Omega}) &= \mathcal{H}_0 + r_s \mathcal{H} \cdot \boldsymbol{\Omega} \\ &= \frac{P^2}{2m} + U_0 + \left(\frac{1}{2} + \frac{r_s}{2} \cos \theta \right) \cdot V_{11}(\hat{R}) \\ &\quad + \left(\frac{1}{2} - \frac{r_s}{2} \cos \theta \right) \cdot V_{22}(\hat{R}) + r_s \sin \theta \cos \varphi \cdot \text{Re}[V_{12}(\hat{R})] \\ &\quad + i r_s \sin \theta \sin \varphi \cdot \text{Im}[V_{12}(\hat{R})], \end{aligned} \quad (\text{F5})$$

which was first derived in Ref. 35. The projection operators are transformed as³⁵

$$\begin{aligned} [|1\rangle\langle 1|]_s &= \left[\frac{1}{2} \hat{\mathcal{I}} + \frac{1}{\hbar} \hat{S}_z \right]_s = \frac{1}{2} + \frac{r_s}{2} \cos \theta, \\ [|2\rangle\langle 2|]_s &= \left[\frac{1}{2} \hat{\mathcal{I}} - \frac{1}{\hbar} \hat{S}_z \right]_s = \frac{1}{2} - \frac{r_s}{2} \cos \theta, \\ [|1\rangle\langle 2| + |2\rangle\langle 1|]_s &= 2 \left[\frac{1}{\hbar} \hat{S}_x \right]_s = r_s \sin \theta \cos \varphi \\ [|1\rangle\langle 2| - |2\rangle\langle 1|]_s &= 2i \left[\frac{1}{\hbar} \hat{S}_y \right]_s = ir_s \sin \theta \sin \varphi. \end{aligned}$$

The derivation procedure of the TCF and exact Liouvillian are same as outlined in the main text. The electronic EOMs under the linearization approximation is

$$\frac{d}{dt} \Omega_i = \frac{1}{\hbar} \sum_{j,k=1}^3 \varepsilon_{ijk} H_j(R) \Omega_k, \quad (\text{F7})$$

which is the $N = 2$ limit of Eq. 86c. Here, ε_{ijk} is the Levi-Civita symbol, which is the structure constant of the $\mathfrak{su}(2)$ Lie algebra. Eq. F7 is commonly written as^{32,33}

$$\frac{d}{dt} \boldsymbol{\Omega} = \frac{1}{\hbar} \mathbf{H}(\hat{R}) \times \boldsymbol{\Omega}. \quad (\text{F8})$$

For a two-level system, Eq. E9 reduce back to³⁶

$$\dot{\theta} = -\mathcal{H}_x \sin \varphi + \mathcal{H}_y \cos \varphi, \quad (\text{F9a})$$

$$\dot{\varphi} = \mathcal{H}_z - \mathcal{H}_x \frac{\cos \varphi}{\tan \theta} - \mathcal{H}_y \frac{\sin \varphi}{\tan \theta}, \quad (\text{F9b})$$

The same equation was derived by Thoss and Stock in their spin mapping formalism (see Eq. 4.5c and 4.5d in Ref. 10). It is interesting to note³⁶ that the above equations are equivalent to

$$\dot{\theta} = \frac{1}{\frac{1}{2}r_s \sin \theta} \frac{\partial H_s}{\partial \varphi} \quad (\text{F10a})$$

$$\dot{\varphi} = - \frac{1}{\frac{1}{2}r_s \sin \theta} \frac{\partial H_s}{\partial \theta} \quad (\text{F10b})$$

from which we obtain the conjugate variables $\dot{\varphi}$ and $\frac{1}{2}r_s \cos \theta$ related to the spin mapping representation, where the latter plays the role of conjugate momentum⁸⁷ to φ as

$$\frac{d}{dt} \left(\frac{1}{2}r_s \cos \theta \right) = - \frac{\partial H_s}{\partial \varphi} \quad (\text{F11a})$$

$$\dot{\varphi} = \frac{\partial H_s}{\partial \left(\frac{1}{2}r_s \cos \theta \right)}. \quad (\text{F11b})$$

This helps to inspire the relation we conjectured in Eq. 87, and one notice that when $N = 2$, the expression of Θ (Eq. 61) indeed reduces to $\Theta = r_s \left(\frac{2-1}{2} - \sin^2 \frac{\theta}{2} \right) = \frac{1}{2}r_s \cos \theta$, which is the conjugate variable of φ .

Finally, under the two level special case, the mapping Hamiltonian (Eq. 91) with $\{\Theta, \varphi\}$ as the natural variables is expressed as

$$\begin{aligned} H_s &= \frac{P^2}{2M} + U_0(R) \\ &+ \left(\Theta + \frac{1}{2} \right) \cdot V_{11}(R) + \left(-\Theta + \frac{1}{2} \right) \cdot V_{22}(R) \\ &+ 2V_{12}(R) \sqrt{\left(\Theta + \frac{r_s}{2} \right) \left(-\Theta + \frac{r_s}{2} \right)} \cdot \cos \varphi. \end{aligned} \quad (\text{F12})$$

It is interesting to note that this classical Hamiltonian was introduced by Miller and McCurdy (Eq. 3.20 in Ref. 34) for the case of $r_s = 1$, and was later introduced by Meyer and Miller (Eq. 2.10 in Ref. 7) using spin mapping for the case of $r_s = 2$ (with the “Langer correction”).

Using the conjugate variables Θ and φ , the corresponding EOMs in Eq. C8 becomes

$$\dot{\Theta}_n = - \frac{\partial H_s}{\partial \varphi_n} \quad (\text{F13a})$$

$$= 2V_{12}(R) \sqrt{\left(\Theta + \frac{r_s}{2} \right) \left(-\Theta + \frac{r_s}{2} \right)} \cdot \sin \varphi,$$

$$\dot{\varphi} = \frac{\partial H_s}{\partial \Theta} = V_{11}(R) - V_{22}(R) \quad (\text{F13b})$$

$$+ V_{12}(R) \left[\sqrt{\frac{-\Theta + \frac{r_s}{N}}{\Theta + \frac{r_s}{N}}} - \sqrt{\frac{\Theta + \frac{r_s}{N}}{-\Theta + \frac{r_s}{N}}} \right] \cos \varphi.$$

¹J. C. Tully, J. Chem. Phys. **137**, 22A301 (2012).

²J. C. Tully and R. K. Preston, J. Chem. Phys. **55**, 562 (1971).

³J. C. Tully, J. Chem. Phys. **93**, 1061 (1990).

Comment: Klimov's works were cited several times in WIREs. Comput. Mol. Sci. e1619 (2022):

109. Klimov AB, Espinoza P. Moyal-like form of the star product for generalized SU(2) Stratonovich-Weyl symbols. *J Phys A Math Gen.* 2002;35:8435–47. <https://doi.org/10.1088/0305-4470/35/40/305>
110. Klimov AB, Romero JL. A generalized Wigner function for quantum systems with the SU(2) dynamical symmetry group. *J Phys A Math Theor.* 2008;41:055303. <https://doi.org/10.1088/1751-8113/41/5/055303>
111. Klimov AB, Romero JL, de Guise H. Generalized SU(2) covariant Wigner functions and some of their applications. *J Phys A Math Theor.* 2017;50:323001. <https://doi.org/10.1088/1751-8121/50/32/323001>
127. Valtierra IF, Romero JL, Klimov AB. TWA versus semiclassical unitary approximation for spin-like systems. *Ann Phys.* 2017;383:620–34. <https://doi.org/10.1016/j.aop.2017.06.006>
128. Valtierra IF, Klimov AB, Leuchs G, Sánchez-Soto LL. Quasiprobability currents on the sphere. *Phys Rev A.* 2020;101:033803. <https://doi.org/10.1103/PhysRevA.101.033803>
130. Morales-Hernández GE, Castellanos JC, Romero JL, Klimov AB. Semi-classical discretization and long-time evolution of variable spin systems. *Entropy.* 2021;23:684. <https://doi.org/10.3390/e23060684>
302. Klimov AB. Exact evolution equations for SU(2) quasidistribution functions. *J Math Phys.* 2002;43:2202–13. <https://doi.org/10.1063/1.1463711>

but were totally ignored in Version 1 and made up in current Version.

This citation disappeared in the first version of this manuscript (online on May 20, 2022), however was added in the second version (online May 27, 2022) and this accepted version (online on July 29, 2022) AFTER our WIREs. Comput. Mol. Sci. e1619 (2022) (submitted on February 5, 2022, released on arXiv on May 8, 2022 and officially published on May 13, 2022). This was just copying citation in others' work without mentioning.

- 4 J. E. Subotnik, A. Jain, B. Landry, A. Petit, W. Ouyang, and N. Bellonzi, *Annu. Rev. Phys. Chem.* **67**, 387 (2016).
- 5 L. Wang, A. Akimov, and O. V. Prezhdo, *J. Phys. Chem. Lett.* **7**, 2100 (2016).
- 6 R. Crespo-Otero and M. Barbatti, *Chem. Rev.* **118**, 7026 (2018).
- 7 H.-D. Meyer and W. H. Miller, *J. Chem. Phys.* **71**, 2156 (1979).
- 8 G. Stock and M. Thoss, *Phys. Rev. Lett.* **78**, 578 (1997).
- 9 H.-D. Meyer and W. H. Miller, *J. Chem. Phys.* **70**, 3214 (1979).
- 10 M. Thoss and G. Stock, *Phys. Rev. A* **59**, 64 (1999).
- 11 X. Sun and W. H. Miller, *J. Chem. Phys.* **106**, 916 (1997).
- 12 E. A. Coronado, J. Xing, and W. H. Miller, *Chem. Phys. Lett.* **349**, 521 (2001).
- 13 S. Bonella and D. F. Coker, *J. Chem. Phys.* **114**, 7778 (2001).
- 14 H. Kim, A. Nassimi, and R. Kapral, *J. Chem. Phys.* **129**, 084102 (2008).
- 15 P. Huo and D. F. Coker, *J. Chem. Phys.* **135**, 201101 (2011).
- 16 P. Huo and D. F. Coker, *J. Chem. Phys.* **137**, 22A535 (2012).
- 17 W. H. Miller and S. J. Cotton, *Faraday Discuss.* **195**, 9 (2016).
- 18 J. O. Richardson, P. Meyer, M.-O. Pleinert, and M. Thoss, *Chem. Phys.* **482**, 124 (2017).
- 19 J. O. Richardson and M. Thoss, *J. Chem. Phys.* **139**, 031102 (2013).
- 20 N. Ananth and T. F. Miller, *J. Chem. Phys.* **133**, 234103 (2010).
- 21 A. Kelly, R. van Zon, J. Schofield, and R. Kapral, *J. Chem. Phys.* **136**, 084101 (2012).
- 22 M. A. C. Saller, A. Kelly, and J. O. Richardson, *J. Chem. Phys.* **150**, 071101 (2019).
- 23 S. J. Cotton and W. H. Miller, *J. Chem. Phys.* **139**, 234112 (2013).
- 24 J. Liu, *J. Chem. Phys.* **145**, 204105 (2016).
- 25 X. He, B. Wu, Z. Gong, and J. Liu, *J. Phys. Chem. A* **125**, 6845 (2021).
- 26 Y. Gu, *Phys. Rev. A* **32**, 1310 (1985).
- 27 C. Brif and A. Mann, *Phys. Rev. A* **59**, 971 (1999).
- 28 A. B. Klimov and S. M. Chumakov, *A Group-Theoretical Approach to Quantum Optics: Models of Atom-Field Interactions* (John Wiley & Sons, 2009).
- 29 B. C. Hall, *GTM222: Lie Groups, Lie Algebras, and Representations, An Elementary Introduction*, 2nd Ed. (Springer, Switzerland, 2015).
- 30 See Page 71 corollary 3.47 of Ref. 29.
- 31 H. Georgi, *Lie Algebras In Particle Physics: from Isospin To Unified Theories* (CRC Press, 2000).
- 32 C. Cohen-Tannoudji, B. Diu, and F. Laloe, *Quantum Mechanics, Volume 1* (Wiley, 1997).
- 33 R. P. Feynman, F. L. Vernon, and R. W. Hellwarth, *J. App. Phys.* **28**, 49 (1957).
- 34 W. H. Miller and C. W. McCurdy, *J. Chem. Phys.* **69**, 5163 (1978).
- 35 J. E. Runeson and J. O. Richardson, *J. Chem. Phys.* **151**, 044119 (2019).
- 36 D. Bossion, S. N. Chowdhury, and P. Huo, *J. Chem. Phys.* **154**, 184106 (2021).
- 37 F. T. Hioe and J. H. Eberly, *Phys. Rev. Lett.* **47**, 838 (1981).
- 38 M. A. Marchiolli and D. Galetti, *J. Phys. A: Math. Theor.* **52**, 405305 (2019).
- 39 G. Kimura, *Phys. Lett. A* (2003) **314**, 339 (2003).
- 40 R. A. Bertlmann and P. Krammer, *J. Phys. A: Math. Theor.* **41**, 235303 (2008).
- 41 C. W. McCurdy, H. D. Meyer, and W. H. Miller, *J. Chem. Phys.* **70**, 3177 (1979).
- 42 H. Meyer and W. H. Miller, *J. Chem. Phys.* **72**, 2272 (1980).
- 43 See Appendix C of Ref. 46 for a detailed discussion.
- 44 S. J. Cotton and W. H. Miller, *J. Phys. Chem. A* **119**, 12138 (2015).
- 45 It turns out that this mapping approach does not generate the exact results for an isolated quantum system, see discussions in Sec VI of Ref. 24.
- 46 J. E. Runeson and J. O. Richardson, *J. Chem. Phys.* **152**, 084110 (2020).

- ⁴⁷R. L. Stratonovich, Sov. Phys. JETP **4** (1957).
- ⁴⁸J. C. Várilly and J. M. Gracia-Bondía, Ann. Phys. **190**, 107 (1989).
- ⁴⁹J. M. Radcliffe, J. Phys. A: Gen. Phys. **4**, 313 (1971).
- ⁵⁰K. Nemoto, J. Phys. A: Math. Gen. **33**, 3493 (2000).
- ⁵¹T. Tilma and E. C. G. Sudarshan, J. Phys. A: Math. Gen. **35**, 10467 (2002).
- ⁵²T. Tilma and E. Sudarshan, J. Geom. Phys. **52**, 263 (2004).
- ⁵³T. Tilma and K. Nemoto, J. Phys. A: Math. Theor. **45**, 015302 (2011).
- ⁵⁴H. Lang, O. Vendrell, and P. Hauke, J. Chem. Phys. **155**, 024111 (2021).
- ⁵⁵F. Halzen and A. Martin, *Quarks and Leptons: An Introductory Course in Modern Particle Physics* (Wiley, 1984).
- ⁵⁶W. Pfeifer, *The Lie Algebras SU(N): An Introduction* (Springer, 2003).
- ⁵⁷M. Gell-Mann, Phys. Rev. **125**, 1067 (1962).
- ⁵⁸More generally, for a given n -dimensional Lie algebra \mathfrak{g} , there is an associated simply connected n -dimensional Lie group G (which is also a manifold) whose Lie algebra is isomorphic to \mathfrak{g} . This is referred to as the Lie's third theorem. See Ref. 29 or 59.
- ⁵⁹D. Bump, *GTM225: Lie Groups*, 2nd Ed. (Springer, Switzerland, 2013).
- ⁶⁰Note that in the work of Tilma and Nemoto⁵³, the main focus is to get the correct integrated value over all the Euler angles, which is not sensitive to the peak of the distribution. However, to make a consistent phase space volume with the choice of the coherence state we used in Eq. 18 that gives the correct peak position along θ_n (see Fig. 1), we need to make this specific choice of $d\Omega$ in Eq. 21.
- ⁶¹C. Brif and A. Mann, J. Phys. A: Math. Gen. **31**, L9 (1998).
- ⁶²F. Bloch, Phys. Rev. **70**, 460 (1946).
- ⁶³R. K. Wangness and F. Bloch, Phys. Rev. **89**, 728 (1953).
- ⁶⁴I. I. Rabi, N. F. Ramsey, and J. Schwinger, Rev. Mod. Phys. **26**, 167 (1954).
- ⁶⁵To the best of our knowledge, we do not see this expression in the previous literature. We also made an incorrect statement in our previous work in Ref. 36 by suggesting that for $s \neq Q$, there is no simple relation between \hat{w}_s and $|\Omega^{\Gamma} E. Wigner, Phys. Rev. 40$, 749(1932).
- ⁶⁶J. E. Moyal, Math. Proc. Camb. Philos. Soc. **45**, 99–124 (1949).
- ⁶⁸M. A. C. Saller, A. Kelly, and J. O. Richardson, Faraday Discuss. **221**, 150 (2020).
- ⁶⁹A. Heslot, Phys. Rev. D **31**, 1341 (1985).
- ⁷⁰X. Sun, H. Wang, and W. H. Miller, J. Chem. Phys. **109**, 7064 (1998).
- ⁷¹J. A. Poulsen, G. Nyman, and P. J. Rossky, J. Chem. Phys. **119**, 12179 (2003).
- ⁷²Q. Shi and E. Geva, J. Chem. Phys. **118**, 8173 (2003).
- ⁷³T. J. H. Hele, M. J. Willatt, A. Muolo, and S. C. Althorpe, J. Chem. Phys. **142**, 134103 (2015).
- ⁷⁴S. N. Chowdhury and P. Huo, J. Chem. Phys. **154**, 124124 (2021).
- ⁷⁵M. Hillery, R. O'Connell, M. Scully, and E. Wigner, Phys. Rep. **106**, 121 (1984).
- ⁷⁶W. B. Case, American Journal of Physics **76**, 937 (2008).
- ⁷⁷S. Bonella and D. Coker, J. Chem. Phys. **118**, 4370 (2003).
- ⁷⁸One can in principle derive the Liouvillian in terms of the MMST variables (defined in Eq. D1), using the kernel expressed in the MMST variables and diabatic basis (Eq. D7). However, this leads to a complicated expression of $[\hat{A}\hat{B}]_s$, as opposed to the simple expression in Eq. 42.
- ⁷⁹H. Groenewold, Physica **12**, 405 (1946).
- ⁸⁰K. Imre, E. Özizmir, M. Rosenbaum, and P. F. Zweifel, J. Math. Phys. **8**, 1097 (1967).
- ⁸¹T. J. H. Hele and N. Ananth, Faraday Discuss. **195**, 269 (2016).
- ⁸²A. N. S. Bonella and R. Kapral, J. Chem. Phys. **133**, 134115 (2010).
- ⁸³H. W. Kim and Y. M. Rhee, J. Chem. Phys. **140**, 184106 (2014).
- ⁸⁴Q. Shi and E. Geva, J. Phys. Chem. A **108**, 6109 (2004).

The expression of mapping kernel in eq 27 had already been proposed in Appendix 3 of WIREs. Comput. Mol. Sci. e1619 (2022)(submitted on February 5, 2022, released on arXiv on May 8, 2022 and officially published on May 13, 2022), which could be traced back to the expression using Meyer-Miller mapping variables in J. Phys. Chem. Lett. **12**, 2496 (2021) (which submitted on January 22, 2021 and published online on March 5, 2021). The form of mapping kernel in previous work of Huo group, Ref. 36 (submitted on March 25, 2021), however, originated from Refs. 35, 46 and was never generalized except Q, W and P versions, while the mapping kernel in J. Phys. Chem. Lett. **12**, 2496 (2021) had already involved the full continuous parameter range. The corresponding original statement in Ref. 36 of Huo and his coworkers reads,

We further introduce three functions for the Stratonovich-Weyl (SW) transformation of any operator in the SM representation, named the Q-, P-, and W-functions. These functions depend on the kernel \hat{w}_s and the spin radius r_s as follows.⁵³

$$\hat{w}_s(\mathbf{u}) = \frac{1}{2}\hat{\mathcal{T}} + r_s \mathbf{u} \cdot \hat{\boldsymbol{\sigma}}, \quad s \in \{Q, P, W\}, \quad (8a)$$

$$r_Q = \frac{1}{2}, \quad r_P = \frac{3}{2}, \quad r_W = \frac{\sqrt{3}}{2}, \quad (8b)$$

where $\mathbf{u} \cdot \hat{\boldsymbol{\sigma}} = u_x \cdot \hat{\sigma}_x + u_y \cdot \hat{\sigma}_y + u_z \cdot \hat{\sigma}_z$.

The SCS projection operator is $|\mathbf{u}\rangle\langle\mathbf{u}| = \cos^2 \frac{\theta}{2} |1\rangle\langle 1| + \cos \frac{\theta}{2} \sin \frac{\theta}{2} e^{-i\varphi} |1\rangle\langle 2| + \cos \frac{\theta}{2} \sin \frac{\theta}{2} e^{i\varphi} |2\rangle\langle 1| + \sin^2 \frac{\theta}{2} |2\rangle\langle 2|$. Note that

$$\hat{w}_Q = |\mathbf{u}\rangle\langle\mathbf{u}|, \quad (9)$$

which can be easily verified using elementary trigonometric identities. On the other hand, \hat{w}_P and \hat{w}_W do not have a simple relation with $|\mathbf{u}\rangle\langle\mathbf{u}|$.

It is clear that they did not know about the continuous parameter range at all in the reference. However, the correct citations of our works were obviously absent.

- ⁸⁵H. Wang, X. Sun, and W. H. Miller, *J. Chem. Phys.* **108**, 9726 (1998).
- ⁸⁶X. Sun, H. Wang, and W. H. Miller, *J. Chem. Phys.* **109**, 7064 (1998).
- ⁸⁷J. R. Klauder, *Phys. Rev. D* **19**, 2349 (1979).
- ⁸⁸One can, in principle, directly derive Eq. 95 from Eq. 86c using the transformation in Eq. D4 and the expressions of the structure constant f_{ijk} in Eq. A1, through a rather tedious process.
- ⁸⁹M. S. Church, T. J. H. Hele, G. S. Ezra, and N. Ananth, *J. Chem. Phys.* **148**, 102326 (2018).
- ⁹⁰P. Ehrenfest, *Z. Phys.* **45**, 455 (1927).
- ⁹¹A. D. McLachlan, *Mol. Phys.* **8**, 39 (1964).
- ⁹²R. Grunwald, A. Kelly, and R. Kapral, Quantum dynamics in almost classical environments, in *Energy Transfer Dynamics in Biomaterial Systems*, edited by I. Burghardt, V. May, D. A. Micha, and E. R. Bittner (Springer Berlin Heidelberg, Berlin, Heidelberg, 2009) pp. 383–413.
- ⁹³S. N. Chowdhury and P. Huo, *J. Chem. Phys.* **150**, 244102 (2019).
- ⁹⁴J. Liu and W. H. Miller, *J. Chem. Phys.* **134**, 104101 (2011).
- ⁹⁵S. Habershon and D. E. Manolopoulos, *J. Chem. Phys.* **131**, 244518 (2009).
- ⁹⁶W. H. Miller, *J. Phys. Chem. A* **113**, 1405 (2009).
- ⁹⁷U. Müller and G. Stock, *J. Chem. Phys.* **111**, 77 (1999).
- ⁹⁸G. Stock and M. Thoss, Mixed quantum-classical description of the dynamics at conical intersections, in *Conical Intersections* (World Scientific Publishing, 2004) pp. 619–695.
- ⁹⁹R. Schneider and W. Domcke, *Chem. Phys. Lett.* **150**, 235 (1988).
- ¹⁰⁰H. Köppel, L. S. Cederbaum, and W. Domcke, *J. Chem. Phys.* **89**, 2023 (1988).
- ¹⁰¹H. Köppel, *Chem. Phys. Lett.* **205**, 361 (1993).
- ¹⁰²S. J. Cotton and W. H. Miller, *J. Chem. Phys.* **150**, 194110 (2019).
- ¹⁰³The less accurate FSSH results can be potentially improved using new diabatic population estimators in Ref. 116 or applying the decoherence corrections.¹¹⁷
- ¹⁰⁴On page 106 of Ref. 56 (Chapter 6), the author suggested that “In order to determine the structure constants of $\mathfrak{su}(N)$, no closed formulas are known, they have to be calculated by means of performing matrix multiplications (Eq. 9 in this paper).”.
- ¹⁰⁵The original definitions of $\{q_n, p_n\}$ in Eq. 27–28 of Ref. 46 are missing this phase $e^{i\Phi}$.
- ¹⁰⁶S. J. Cotton and W. H. Miller, *J. Chem. Phys.* **145**, 144108 (2016).
- ¹⁰⁷X. He, Z. Gong, B. Wu, and J. Liu, *J. Phys. Chem. Lett.* **12**, 2496 (2021).
- ¹⁰⁸W.-M. Zhang and D. H. Feng, *Phys. Rep.* **252**, 1 (1995).
- ¹⁰⁹H. Kim, *Chem. Phys. Lett.* **436**, 111 (2007).
- ¹¹⁰S. Bonella and D. F. Coker, *Chem. Phys.* **268**, 189 (2001).
- ¹¹¹C. Hsieh and R. Kapral, *J. Chem. Phys.* **137**, 22A507 (2012).
- ¹¹²C. Hsieh and R. Kapral, *J. Chem. Phys.* **138**, 134110 (2013).
- ¹¹³D. T. Pegg and S. M. Barnett, *Phys. Rev. A*, **39**, 1665 (1989).
- ¹¹⁴J. Liu, X. He, and B. Wu, *Acc. Chem. Res.* **54**, 4215 (2021).
- ¹¹⁵One can use the conjugate relationship between φ_n and Θ_n to get $\dot{\varphi}_n = \frac{\partial H_s}{\partial \Theta_n} = \sum_{j=1}^n \frac{\partial H_s}{\partial \theta_j} \frac{\partial \theta_j}{\partial \Theta_n} = \sum_{j=1}^n \frac{\partial H_s}{\partial \theta_j} \left(\frac{\partial \Theta_n}{\partial \theta_j} \right)^{-1}$, but the detailed expression obtained from the above equation is long and tedious to use.
- ¹¹⁶B. R. Landry, M. J. Falk, and J. E. Subotnik, *J. Chem. Phys.* **139**, 211101 (2013).
- ¹¹⁷J. E. Subotnik, A. Jain, B. Landry, A. Petit, W. Ouyang, and N. Bellonzi, *Annu. Rev. Phys. Chem.* **67**, 387 (2016).

This note only appeared in this updated version (second version online on May 27, 2022, and accepted version on July 29, 2022), after our work WIREs. Comput. Mol. Sci. e1619 (2022) (submitted on February 5, 2022, published on arXiv on May 8, 2022 and officially published on May 13, 2022), however not in their first version (online on May 20, 2022). It was not a careless missing at all but a correction taken from our work WIREs. Comput. Mol. Sci. e1619 (2022)!